

https://dspace.org/

An Introduction to the Role of Molybdenum and Tungsten in Biology

Helder Marques

https://hdl.handle.net/10539/45748
WOS

Downloaded from a DSpace repository. https://dspace.org/

inorganics

MDPI

Review

An Introduction to the Role of Molybdenum and Tungsten in Biology

Helder M. Marques

Molecular Sciences Institute, School of Chemistry, University of the Witwatersrand, Johannesburg P.O. Box 2050, South Africa; helder.marques@wits.ac.za

Abstract

This short review provides an overview of the bioinorganic chemistry of molybdenum and tungsten, offering insights into current research perspectives and fundamental concepts in the field, as well as gaps in our knowledge. It is designed to highlight areas where future research is needed to fully elucidate the mechanisms of molybdenum- and tungsten-dependent enzymes and their broader significance in biochemistry and bioinorganic chemistry. It also provides an accessible introduction for senior undergraduate students and novice postgraduate researchers who are new to the field of bioinorganic chemistry. Towards this end, illustrative examples are presented, showcasing the essential roles these metals play in biological systems, their coordination chemistry, and their catalytic functions in metalloenzymes.

Keywords: bioinorganic chemistry; metals in biology; d-block metal ions; molybdenum; tungsten; catalysis

1. Introduction

The latter elements of the first row of the d-block of the periodic table play a crucial role in biological systems: manganese, iron, cobalt, nickel, copper, and zinc are all essential elements, while vanadium plays a minor role [1]. Their absence has deleterious effects on many life forms [1–11]. By contrast, elements from the second and third rows of the d-block are far less common in biological systems; only molybdenum and tungsten are currently known to be essential [12–16] although tungsten's biological role appears to be restricted to specific microorganisms. Nevertheless, molybdenum and tungsten feature prominently in nature's armoury of enzymes that process gases such as N_2, CO_2 and CO [17].

Molybdenum is found across many organisms, including animals, plants, bacteria, and fungi. It constitutes an important component of several enzymes, including nitrate reductase [18–20], which catalyses the first step, the reduction of nitrate to nitrite, in the nitrogen assimilation pathway of plants, fungi, algae, and some bacteria, and xanthine oxidase, found in a wide range of organisms, which is central to purine metabolism [21–25]. Molybdenum is also part of an iron–molybdenum cofactor in nitrogenase, found in bacteria and archaea, and involved in nitrogen fixation [26–34]—thus critically important to the global nitrogen cycle, and agricultural productivity [35], in which molybdenum plays a more indirect role during the catalytic cycle. Redox active under physiological conditions, molybdenum typically cycles between the +4 and +6 oxidation states [25,36].

It has been speculated that once the oceans became sufficiently oxygenated, the availability of molybdenum (as MO_4^{2-}) was a crucial factor in the evolution of life with the

check for updates

Academic Editor: Bernhard Spingler

Received: 20 May 2025
Revised: 27 June 2025
Accepted: 28 June 2025
Published: 1 July 2025

Citation: Marques, H.M. An Introduction to the Role of Molybdenum and Tungsten in Biology. *Inorganics* **2025**, *13*, 219. https://doi.org/10.3390/inorganics13070219

Copyright: © 2025 by the author. Licensee MDPI, Basel, Switzerland. This article is an open access article distributed under the terms and conditions of the Creative Commons Attribution (CC BY) license (https://creativecommons.org/licenses/by/4.0/).

appearance of nitrogenase [37,38] and the ability of organisms to fix nitrogen. Molybdenum on its own is biologically inactive [39].

Tungsten, by contrast, and as far as is known, is found only in prokaryotic enzymes [40] and is essential for some extremophilic organisms, including several species of bacteria and archaea that inhabit extreme environments, such as hydrothermal vents and hypersaline lakes [13,41–47]. Tungsten-containing enzymes generally display greater thermal stability than their molybdenum counterparts [48]. For instance, bacteria of the genus *Moorella*, which are adapted to anaerobic and high-temperature environments, incorporate tungsten into their enzymes, enabling catalytic activity under conditions that would be detrimental to most life forms [49,50]. Tungsten is essential for enzymes such as aldehyde oxidoreductase, which is crucial for the oxidation of aldehydes to carboxylic acids [42,47,51,52]. With accessible +4 and +6 oxidation states, tungsten can also substitute for molybdenum in several enzymes under conditions of molybdenum scarcity, or where molybdenum-dependent enzymes are unable to function effectively due to environmental extremes [42].

It has been suggested that tungsten biochemistry predates molybdenum biochemistry, reflecting the more reduced atmosphere of the early Earth [53,54]. Tungsten may have been more readily available and utilised by primitive life forms before the emergence of molybdenum-dependent enzymes, which are more prevalent in contemporary organisms. The transition from tungsten to molybdenum utilisation likely reflects broader shifts in environmental conditions and elemental availability over geological timescales. This evolutionary trajectory could have implications for astrobiology; the study of tungsten-utilising organisms may provide insights into the potential for life in extraterrestrial environments characterised by similar conditions [55].

Compounds of molybdenum, vanadium and tungsten exhibit a diverse range of biomedical activities, including anti-diabetic properties, the normalisation of blood lipid levels, anti-obesity effects, and the regulation of blood pressure [56–59]. Additionally, several molybdenum compounds have demonstrable anti-neoplastic activity [59–61], as do some tungsten compounds [61].

Among the second- and third-row d-block elements, only molybdenum and tungsten are currently known to play significant biological roles. However, cadmium, usually regarded as toxic, can substitute for zinc in carbonic anhydrase in certain marine diatoms, catalysing the reversible hydration of CO_2 to facilitate inorganic carbon acquisition for photosynthesis [62]. Although other heavier d-block elements are not biologically essential, they have important medical applications. For instance, ^{99m}Tc is widely used in diagnostic imaging [63–65]; platinum compounds, such as cisplatin, carboplatin, and oxaliplatin, act as anti-cancer agents [66,67]; and ruthenium complexes are being explored as less toxic alternatives [68,69]. Ag^+ possesses antimicrobial properties [70], while complexes of gold [71,72], silver [73], palladium [74], osmium [75] and rhenium [76] also show anti-cancer activity. Clearly, Mo and W have been chosen by nature to conduct rather specific reactions, and reactions for which metal ions from the first row of the d block might not be suitable.

The reasons underlying the preferential use of lighter d-block elements over their heavier congeners in biological systems remain a matter of conjecture. The availability of these elements during the early stages of life's evolution was undoubtedly a critical factor [77]. The heavier d-block elements are significantly less abundant in the Earth's crust—for example, in ppm: Fe 56.3 $\times$ 10^3; Cu 60; Co 25; Zn 70; but Mo 1.2 and W 1.25 [78]. However, the form of molybdenum commonly available to organisms, the molybdate ion (MoO_4^{2-}), is highly water soluble compared to many Fe^{2+} and Fe^{3+} compounds [79] and is the most abundant transition metal in seawater [80]. Early bioavailability, therefore, might have played a role in shaping the trajectory of life.

Additionally, ligand exchange rates generally decrease down a group in the d-block [81]. Consequently, first-row transition metals tend to have faster ligand exchange kinetics [82], an important feature in dynamic biological processes requiring rapid molecular interactions [83–85], but a property that is not desirable if there is to be tight control over reaction intermediates. For these reasons, and undoubtedly others, the first-row elements were preferentially incorporated into living systems during evolution; however, Mo and W are also important.

Mo and W enzymes are oxidoreductases; they transfer an oxygen atom, derived from or incorporated into water, to or from a substrate in a two-electron redox reaction as the metal cycles between M^{4+} and M^{6+} [86]. These enzymes are typically involved in anaerobic and aerobic metabolism, and are especially important in carbon, nitrogen, and sulfur cycling.

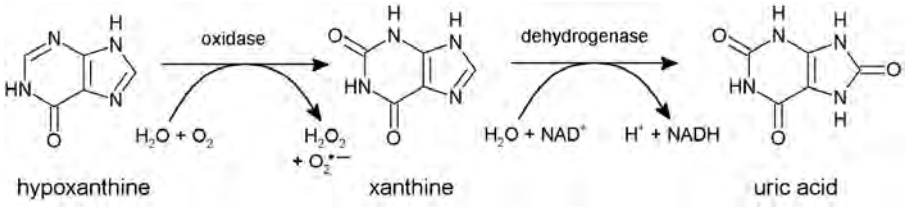
Mo (and W) is the active site in three broad enzyme families: the sulfite oxidase (SO) family (Equation (1)), the dimethylsulfoxide reductase (DMSOR) family (Equation (2)), and the xanthine oxidase (XO) family of enzymes (Equation (3)). The cycling of the metal between its oxidation states is coordinated by a pyranopterin via two dithiolene sulfurs (Figure 1). The ligand is electronically flexible and, by changing its redox or tautomeric state, exerts control over the metal's redox potential [87]. Other enzymes, for example, aldehyde oxidase (Equation (4)), are considered to belong to one of these families (the XO family in this case). The electron transfer is linked to proton transfer in these reactions, examples of which are given in Equations (1)–(4).

$$\text{Sulfite oxidase: } SO_3^{2-} + H_2O \rightarrow SO_4^{2-} + 2H^+ + 2e \quad (1)$$

$$\text{DMSO reductase: } Me_2S = O + 2H^+ + 2e \rightarrow Me_2S + H_2O \quad (2)$$

$$\text{Aldehyde oxidase: } RCHO + H_2O \rightarrow RCOOH + 2H^+ + 2e \quad (3)$$

Xanthine oxidase:



(4)

Another important class of Mo-containing enzymes, the nitrogenases, catalyse the reduction of N_2 to NH_4^+, nature's version of the Haber–Bosch process [88], but carry out the process at ambient temperature and pressure. Mo is part of the FeMo cofactor, FeMoco (Figure 1), where it plays a more indirect role during catalysis.

A key feature of the biological chemistry of Mo and W is the availability of higher and stable oxidation states, which is essential in enzymes that catalyse oxygen atom transfer, hydroxylation, or nitrate reduction [14,36]. Cycling between the +6 and +4 oxidation states (sometimes via the +5 oxidation state), Mo and W enzymes catalyse oxygen transferase reactions coupled (for example, Equations (1)–(4)) with fast and reversible two-electron redox chemistry [36]. The thermodynamically favourable profile for acquiring and losing an oxygen atom makes them outstanding oxygen atom exchangers [14]. Mo and W are better suited for this role than the lighter metals of the first row of the d block. High-valent states are less accessible and more difficult to maintain for 3d metals than their heavier congeners (see [89] and references therein). Consequently, natural systems—and synthetic catalysts for that matter—rely on 4d and 5d metals (such as Mo and W) to achieve stable, high-oxidation-state processes. Furthermore, complexes of first-row transition metals tend

to undergo significant structural changes during redox events, which slow electron transfer rates. By contrast, second- and third-row metals, and Mo and W in particular, exhibit more controlled redox processes.

As will be shown in Sections 4 and 5, a key feature of the bioinorganic chemistry of Mo and W is the occurrence of strong σ and π bonding in M=O bonds, arising from d–p overlap, creating stable multiple bonds essential for catalysis by their enzymes [90]. As shown by Zhang et al. [91], because 3d orbitals are more contracted, metal ions from the first row of the d block have less stable M–oxo species. This was probably an important factor in nature's choice of heavier metal ions to effect reactions such as those shown in Equations (1)–(4). Moreover, redox cycling in 1st-row d block metal complexes often results in large structural reorganisation, higher overpotentials, and deactivation, unlike in the case of the 4d and 5d metal complexes [92].

The pyranopterin dithiolene ligands in Moco provide sulfur-rich coordination. Their HOMO orbitals align closely with Mo/W d orbitals, stabilising multiple oxidation states via covalent bonding [93]. There is spectroscopic evidence (EPR, resonance Raman, XAS) of substantial Mo–S covalency; Mo^{5+} in particular delocalises unpaired spin onto the ligand sulfurs, confirming strong orbital mixing [94]. DFT calculations show that the frontier molecular orbitals of the complex involve metal d and sulfur p orbitals, which underscores the energy and symmetry matching of the metal and its ligands, essential for redox catalysis [95]. The use of a pyranopterin ligand requires a 4d or 5d metal ion; the more contracted 3d orbitals of the first row metals would result in poorer overlap with ligand orbitals and consequently weaker bonding. This, in turn, would likely result in reduced π-backbonding and electron donation in catalytic intermediates. 3d metals in place of Mo or W would diminish catalysis efficiency in molybdopterin-dependent enzymes.

Another important point to consider is that first-row transition metals, and especially Fe and Cu [1], react readily with O_2 through redox processes that generate reactive oxygen species (ROS, such as $O_2^{\bullet -}$, H_2O_2, and $OH^{\bullet}$). Whilst reactive oxygen species such as $O_2^{\bullet -}$ are important for increasing a cell's tolerance to oxidative stress [96], for inter- and intracellular signalling [97], and in defence against infections [98–101], they can cause protein and DNA fragmentation [102,103] and damage to sensitive enzyme structures such as Fe–S clusters [104]. By contrast, reduced Mo- and W-enzymes are rapidly reoxidised by O_2, instead of generating ROS [105,106]. The two-electron cycling between the +4 and +6 oxidation states in Mo and W enzymes militates against ROS formation.

The greater kinetic lability of the first row metal ions compared to their heavier congeners may be deleterious in situations that require a tight control of the lifetimes of reaction intermediates [83]. Factors such as difficulty in managing oxidation states due to competing one- and two-electron processes, reduced ligand field stabilisation, and faster ligand exchange, factors largely absent in 4d and 5d chemistry (see [107] are references therein), mitigate against first row d block metal ions catalysing the sort of reactions catalysed by Mo and W enzymes. The comparative electrochemistry in identical ligand scaffolds shows clear trends; Fe, Co, Mn complexes have less favourable, more variable redox potentials compared to their heavier congeners, indicating less controlled redox behaviour [108].

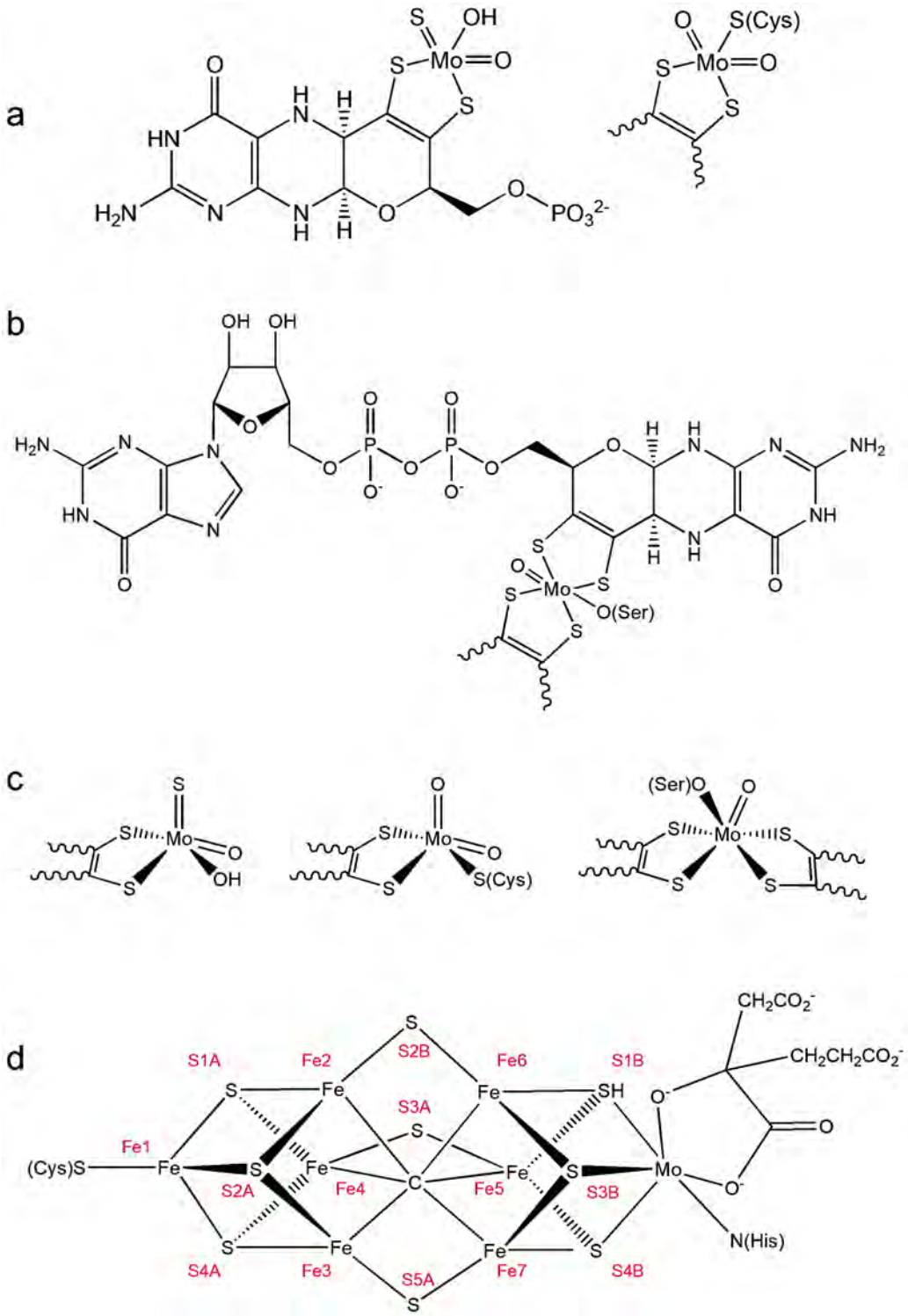


Figure 1. (**a**): The molybdenum cofactor, Moco, with the metal coordinated by a pyranopterin (also referred to as molybdopterin (MPT) via two dithiolene sulfurs. If the metal was tungsten, the cofactor would be referred to as tungstopterin, WPT. Alternatively, MPT has been used generically to refer to a metal-binding pterin. There are three families of mononuclear molybdenum enzymes: the xanthine oxidase family, the sulfite oxidase family, and the DMSO reductase family [109]. Shown on the left is Mo^{6+} in the xanthine oxidases; on the right, Mo^{6+} in the sulfite oxidases. (**b**): Mo^{6+} bis-coordinated to the molybdenum pterin guanine dinucleotide cofactor (MGD) as found in the DMSO reductases. The tungsten equivalent would be WDG. The sixth ligand, shown here as Ser,

can be Ser, Cys, selecocysteine, or H_2O/OH^-. This variability in molybdopterin derivatives is one way of fine-tuning enzyme function [110]. (**c**): Structure of the Mo centre in the xanthine oxidases, the sulfite oxidases, and the DMSO reductases, respectively. (**d**): The [Fe_7MoCS_9] FeMo-cofactor (FeMoco) of the nitrogenases. S2A, S3A and S5A are referred to as the "belt sulfurs"; they are labile and S2A can be displaced by CO, and by Se [111].

2. Molybdenum in Biology: An Overview

Molybdenum enzymes are involved in biochemical processes related to nitrogen, sulfur, and carbon metabolism. Except for the nitrogenase enzymes found in some bacteria and archaea, critical for nitrogen fixation—the process that converts atmospheric N_2 into NH_4^+, making it available to plants, and, consequently, to most life forms [26–28,30,31]—molybdenum is primarily found as a molybdopterin complex, referred to as the molybdenum cofactor (Moco), or a molybdopterin guanine dinucleotide (MGD), Figure 1 [112,113]. In nitrogenases, it is a constituent of the FeMoco factor (FeMoco, Figure 1d). The term tungstopterin guanine dinucleotide (WGD) is often applied to the equivalent tungsten complex.

FeMoco is the largest metallocluster in enzymology [114]. In its ground state, E_0, with $S = {}^3/_2$ [115], it features Mo^{3+} [116] and (assuming a formal −2 charge for each sulfide and a −4 charge on the central carbide), seven Fe ions with charges between +2 and +3, for an overall charge of either −3 (i.e., ($Mo^{3+}5Fe^{2+}2Fe^{3+}$) [117] or −1 ($Mo^{3+}3Fe^{2+}4Fe^{3+}$) [116]. DFT calculations favour the latter (see [118] and references therein). Of course, the assignment of oxidation states in clusters is a moot point, but there is evidence that Fe1, Fe3 and Fe5 (numbering in Figure 1d) are more reduced than the other Fe ions in the cluster. TD-DFT calculations show that the unpaired spin is predominantly on Mo^{3+} (66–74%) and delocalised on neighbouring Fe ions [116]. Mo^{3+} is octahedrally coordinated by *R*-homocysteine, a His residue, and three sulfides, while each Fe^{2+} or Fe^{3+} has an approximately tetrahedral coordination geometry.

The molybdopterin ligand is clearly important in the biological chemistry of Mo and W, given its prominence in their metalloenzymes. The ligand, with its dithiolene moiety, coordinates the metal strongly. Electron delocalisation between the ligand and the metal ion enables the +4 and +6 oxidation states of the metal to be attained, as required for their reactions [119]. Moreover, the ability of the ligand to undergo chelate ring distortions controls the metal–ligand covalency and fine tunes the reduction potential of these metalloenzymes [94].

Many molybdenum enzymes are found in bacteria (nitrate reductase, DMSO reductase, and formate dehydrogenase, among others). They are less common in eukaryotes but nevertheless perform important functions. Humans have four Moco-dependent enzymes: aldehyde oxidase, sulfite oxidase, xanthine oxidase, and mitochondrial amidoxime-reducing component (mARC) [10,120].

Aldehyde oxidase [121–125], found in animals, birds, some reptiles, and some invertebrates, is involved in the detoxifying oxidation of aldehydes to carboxylic acids and in the metabolism of some drugs and xenobiotics. In humans, the enzyme is found primarily in the liver.

Sulfite oxidase [25,126–130], which catalyses the oxidation of sulfite to sulfate, a crucial step in the metabolism of cysteine and methionine, is found in mammals, located in the mitochondrial intermembrane space of liver and kidney cells. The enzyme has also been identified in some bacteria and fungi [126,131], emphasising the important role it plays in sulfur metabolism across a wide range of life forms.

Xanthine oxidase [21–25] is primarily found in mammals, particularly in the liver and intestines, and is important for the breakdown of purines. It catalyses the oxidation of hypoxanthine to xanthine and then from xanthine to uric acid; this is then excreted

in the urine. An elevated level of xanthine oxidase activity is associated with conditions such as gout, where excess uric acid crystallises in the joints, leading to inflammation and pain [132]. Xanthine oxidase is also present in some species of fish and amphibians [133,134], suggesting a conserved role in purine metabolism across different vertebrate lineages. The mechanism of these reactions will be discussed below.

Other molybdenum-requiring enzymes, the mechanism of which will not be discussed in this article, include the mitochondrial amidoxime reducing component (mARC) [120,135,136] found in animals, including humans, and involved in detoxification processes by reducing N-hydroxylated compounds; the DMSO reductase family of enzymes found in bacteria and archaea and involved in reduction of dimethyl sulfoxide to dimethyl sulfide [137]; formate dehydrogenase, found in bacteria, archaea and some eukaryotes, which catalyses the oxidation of one-carbon compounds such as formate to CO_2, and is involved in energy production under anaerobic conditions [138,139]; prokaryotic nitrate reductase [140–142], which catalyses the reduction of NO_3^- to NO_2^- and is part of the nitrogen cycle; eukaryotic nitrate reductase catalyses the same reaction [143,144]; and carbon monoxide dehydrogenase [17,145], found in bacteria and archaea, which catalyses the oxidation to CO to CO_2, part of the metabolic pathway in microorganisms that use CO as a source of carbon.

The way molybdenum is taken up into cells, and how the cofactor is synthesised in nature, is now well understood [39,146–151]. Prokaryotes absorb molybdate through specific transport systems, including the high-affinity ATP-binding cassette (ABC) transporters, such as ModABC, which enable efficient uptake even at low environmental concentrations. Molybdenum enters plant roots primarily through phosphate transporters thanks to the structural similarity of phosphate and molybdate. Active transport mechanisms are also involved to ensure sufficient uptake. Animals obtain molybdenum indirectly by consuming plants or other organisms. It is absorbed in the digestive tract, primarily in the small intestine, in its soluble molybdate form. Once absorbed, molybdenum is transported in plants through the xylem by transpiration; redistribution occurs through the phloem to metabolically active tissues, and it accumulates in leaves and seeds. In animals, molybdenum is distributed to the tissues via the bloodstream, bound to carrier proteins such as blood serum albumin. The biosynthesis of Moco involves a multi-step pathway [152,153]; Moco is then incorporated into molybdoenzymes, enabling their catalytic activity.

Molybdenum is essential for human health. The daily requirement is small (45 μg day^{-1} for adults [154]) and dietary sources include milk and milk products, dried legumes, organ meats, cereals, and baked goods [155]. While very rare, molybdenum deficiency, or genetic disorders that lead to molybdenum enzymes with impaired function, can lead to conditions such as sulfite oxidase deficiency, which causes, for example, neurological damage [156], and xanthinuria [157–159], where low levels of xanthine oxidase lead to the accumulation of xanthine. This is implicated in the development of kidney stones and other effects of the compromised metabolism of purines.

Overconsumption of molybdenum leads to conditions such as gout, neurological symptoms, and reduced copper absorption [160]. The inter-relationship between molybdenum and copper can be exploited for the treatment of Wilson's disease, a congenital inability to excrete copper, which results in its accumulation in the body [161,162]. Molybdenum compounds have also shown promise as antitumor, antibacterial, antiviral, and antioxidant agents in medical applications [163,164].

3. Tungsten in Biology: An Overview

As mentioned in the Introduction, tungsten is a relatively rare element in biological systems and plays a role in the metabolism of various microorganisms, particularly

those that thrive in extreme environments, such as hyperthermophilic bacteria and archaea [13,165]. Tungsten is transported into some prokaryotes by very specific transport proteins, such as the WO_4^{2-}-specific ABC transporter TupABC in archaea and in *Eubacterium acidaminophilum* [166], and the transporter WtpA in the hyperthermophilic archaeon *Pyrococcus furiosus* [167], facilitating its use in very particular biological processes [168–170]. The transporters bind it with a high affinity (K_D < 1 nM) [168].

There is no established biological function for tungsten in higher organisms, and its accumulation can be toxic, as it interferes with the activity of molybdenum-dependent enzymes [171].

In tungsten-dependent enzymes, the metal typically (but not always) participates in redox reactions. Notable examples include (i) formate dehydrogenase (FDH), which plays a key role in the energy metabolism of various anaerobic microorganisms by oxidising formate to carbon dioxide [14,42,138,172]; (ii) aldehyde oxidoreductase (AOR), also integral to anaerobic energy metabolism, which oxidises aldehydes to carboxylic acids while reducing ferredoxin [14,42,173,174]; and (iii) formylmethanofuran dehydrogenase, which catalyses the reversible conversion of CO_2 and methanofuran to formylmethanofuran, contributing to the methanogenesis pathway and producing methane as a metabolic byproduct [175–177]. In acetylene hydratase, which catalyses the hydration of acetylene to acetaldehyde, a crucial step in the anaerobic degradation of acetylene, tungsten catalyses a non-redox reaction [178–180]. The mechanism of some of these reactions will be discussed later in this article.

Tungsten is typically coordinated by a metal-binding pterin in the tungsten-dependent enzymes. The presence of tungsten in the active site, with its various oxidation states, enables these enzymes to catalyse redox reactions, often under extreme environmental conditions. Tungsten enzymes have a more negative redox potential (by −200 to −300 mV) than molybdenum enzymes, which allows them to function efficiently in high-temperature, reducing anaerobic environments [181].

Moreover, tungsten's more temperature-sensitive redox potential compared to molybdenum likely provides an advantage for organisms operating in extreme environments with fluctuating temperatures [40,182], as is their greater thermal stability [183,184]. As a result, tungsten-dependent enzymes are of considerable interest in biotechnology for their robustness and activity under harsh conditions, with potential applications in industrial processes that require resilient catalysts, such as biofuel production and the biodegradation of environmental pollutants [185–187].

4. Examples of Molybdenum-Dependent Enzymes

4.1. Nitrogenase

The nitrogenases are vital enzymes for life on Earth, as they catalyse the conversion of atmospheric nitrogen into NH_4^+ [30,31,35,188–192]. This makes nitrogen, an essential element, available to plants, and subsequently to animals that feed on the plants. The nitrogenases are found primarily in bacteria and archaea (for example, *Rhizobium* in legumes and *Azotobacter* in soils). There are a variety of nitrogenases, but all are from a common evolutionary origin [193]. They include a molybdenum-dependent form, a vanadium-dependent form (usually referred to as V-Nase) and an iron-only form [194].

The nitrogenases have a [Fe_8S_7] P-cluster, and a [MFe_7S_xC] cluster (M = Mo, x = 9 in the molybdenum-dependent enzymes, Figure 2; M = V, x = 8 in the vanadium-dependent nitrogenases, with CO_3^{2-} bridging two of the iron centres; and M = Fe, x = 9 in the iron-only enzymes) [195]. They are reduced by a dinitrogenase reductase (NifH) with an [Fe_4S_4] active site. The [Fe_4S_4] cluster of the reductase protein can access three oxidation states: oxidised [Fe_4S_4]$^{2+}$ with S = 0, reduced [Fe_4S_4]$^+$, an admixture of S = ½ and $^3/_2$ states, and

the super-reduced, all ferrous state, $[Fe_4S_4]^0$ [196–198]. The reductase is itself reduced by a ferredoxin or a flavodoxin. The $[MFe_7S_xC]$ cluster has inspired a great deal of work on synthetic clusters and an exploration of their chemistry [199].

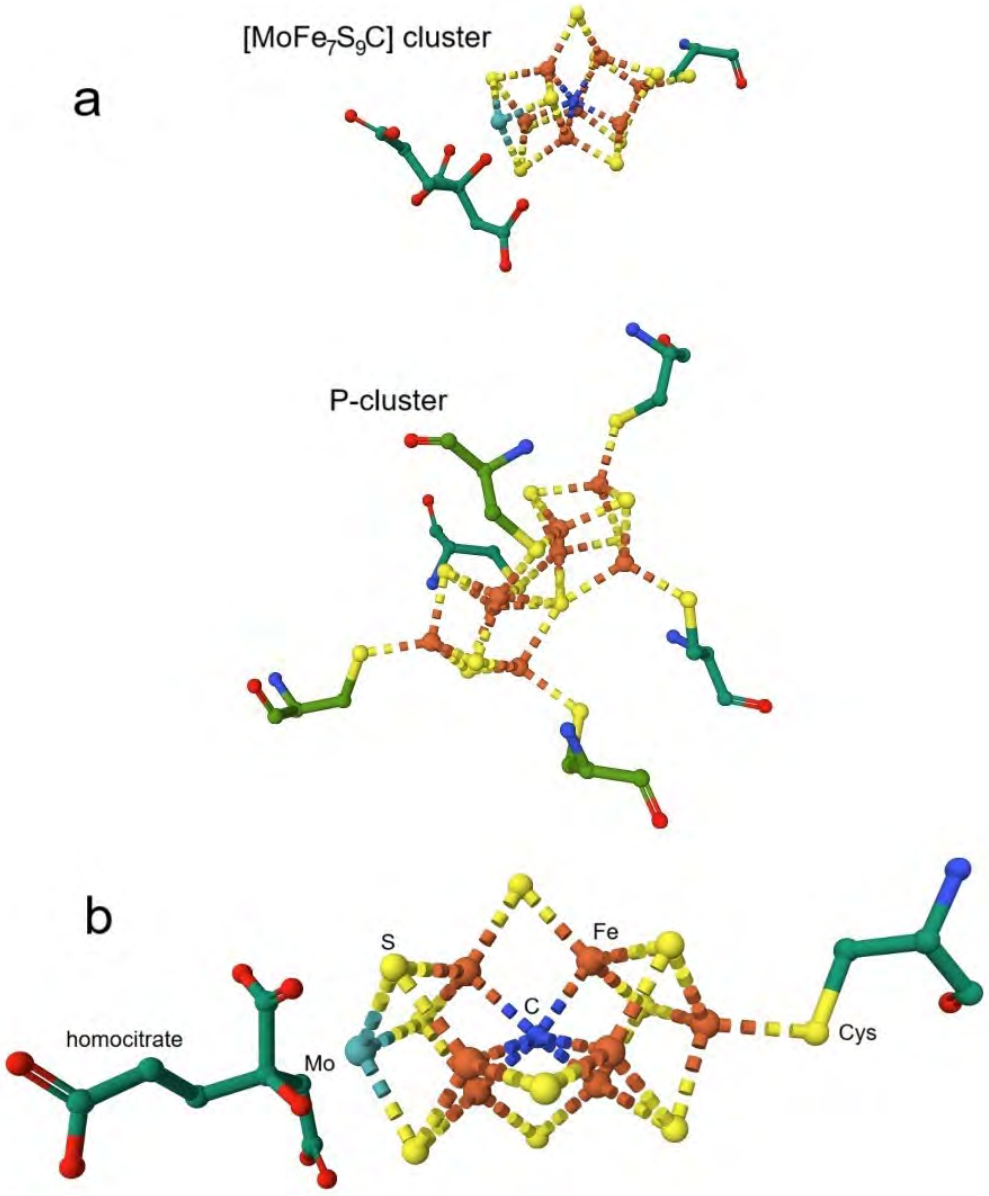


Figure 2. (**a**): The active site $[MoFe_7S_9C]$ cluster and the P-cluster of nitrogenase from *Azotobacter vinelandii* (Protein Data Bank PDB 1M1N [200]). (**b**): The $[MoFe_7S_9C]$ cluster. Mo in light green, Fe in red, S in yellow. (For side chains, C in green, O in red, N in blue, S in yellow).

The V-Nases are only expressed under molybdenum-deficient conditions; the iron-only nitrogenases are less active than the Mo-Nases and V-Nases and are only expressed under V and Mo-deficient conditions [201–204].

The fixation of N_2 is a challenging problem. The N_2 triple bond has a bond dissociation enthalpy of -945 kJ mol^{-1}, so an overpotential of -1.6 V would be required to split the bond, well outside nature's "electrochemical window" (in an aqueous environment, potentials between the oxidation of H_2O with evolution of O_2 and the reduction of H^+ to

produce H_2; under standard conditions at pH 7, this is +817 mV and −413 mV, respectively). Nitrogenases perform this reaction, using ATP, under ambient conditions (Equation (5)).

$$N_2 + 8e + 10H^+ + 16ATP \rightarrow 2\ NH_4^+ + H_2 + 16ADP + 16P_i \quad (5)$$

In addition, nitrogenases can reduce other substrates, including CO, CN^- and acetylene [196,205,206].

The mechanism of these enzymes is still a matter of conjecture despite many experimental and computational investigations (see [32] and references therein); what is generally accepted has been summarised recently [190], but many questions remain [30].

The reductase protein utilises the +1 | +2 couple to receive an electron from a ferredoxin or a flavodoxin; it then binds 2 ATP and forms a complex with the catalytic enzyme, which places its $[Fe_4S_4]$ centre within outer sphere electron transfer distance of the P-cluster. Hydrolysis of ATP leads to electron transfer from the reductase via the P-cluster to the catalytic site (Figure 2) (see [195,207] and references therein). Whether $[Fe_4S_4]$ is first reduced by ATP hydrolysis or the P-cluster first passes an electron to the $[MoFe_7S_xC]$ cluster to initiate the electron transfer from the reductase is unclear [208,209]. It is the hydrolysis of ATP that lowers the redox potential for the transfer of the electron from the P-cluster to the cofactor. After the hydrolysis of ATP and the transfer of an electron, the complex between the reductase and the nitrogenase dissociates with the release of phosphate; this is the rate-limiting step of the reaction. The entire eight-electron reduction process is slow and takes about 1 s. It involves eight intermediate steps (E_0 through E_7), the eight one-electron transfer steps from the reductase to the catalytic cycle.

Based upon extensive kinetic studies, Lowe and Thorneley introduced a model that is still largely accepted [210]. The basic scheme is outlined in Figure 3 and involves eight states, representing the successive electron transfer steps from the reductase protein. In addition to the FeMoco active site, surrounding amino acids (a Gln, His, Val, Ser, Cys, Arg and Tyr) and, connected to *R*-homocitrate, a hydrogen bonded network of water molecules, which extend from the active site to the protein surface and that serves as the proton supply chain to effect the required proton transfer on conversion of N_2 to NH_3 (see [32] and references therein) are also important for enzyme turnover.

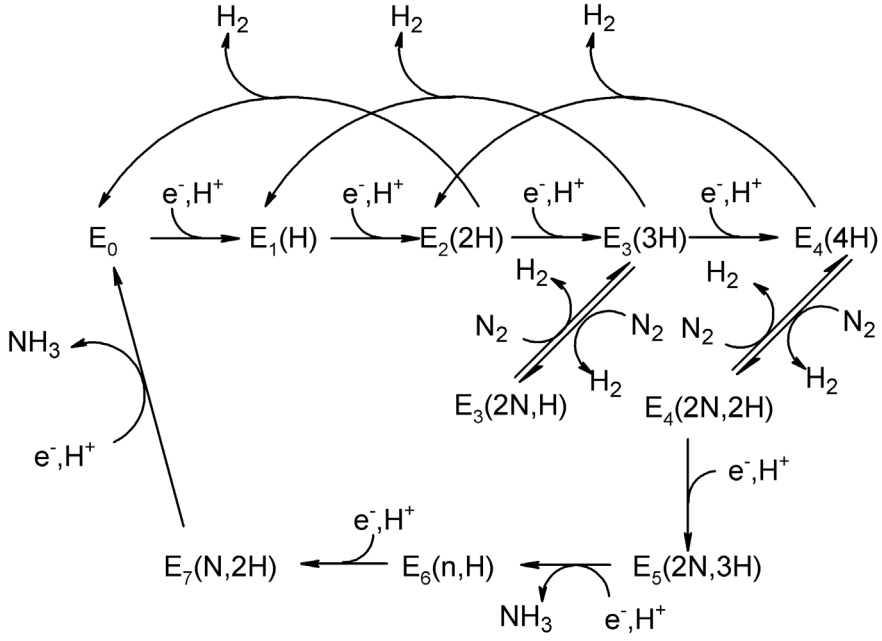


Figure 3. The Lowe–Thorneley mechanism of nitrogenase (adapted from [30,118,190]).

Nitrogen binding occurs after three or four electron transfer steps and is accompanied by the release of H_2. N_2 undergoes a two-electron reduction to a diazene-type intermediate, which then undergoes further reduction to produce NH_4^+. Unproductive loss of H_2 from $E_4(4H)$, $E_3(3H)$ and $E_2(2H)$ sets the reaction back by two equivalents in each case.

The electrons transferred to the FeMo catalytic cluster are stored either by reducing the iron atoms of the cluster, or as hydrides attached to the cluster [211–214]. If H^- is indeed present, it will only be formed after two electrons are transferred, and each odd E state would presumably feature a reduced cluster. The loss of H_2 leaves the FeMo cofactor in a super-reduced state, which then acts as the reductant of N_2 to form a diazene-type intermediate.

It is known from EPR and IR studies (see [190] and references therein) that FeMoco of nitrogenase (Figure 1d) contains two sites that bind CO: in one, CO bridges two Fe ions (the μ-site), and in the other CO binds terminally to Fe (the t-site). A similar binding of two equivalents of CO to the FeV cofactor of V-Nase has been crystallographically demonstrated [215]. This then suggests a possible sequence for the binding of H^+, its reduction to H^-, elimination of H_2 to form the super-reduced FeMoco, and the binding and reduction of N_2 (Figure 4). (DFT calculations favour bridging hydrides over terminal hydrides, however [214,216–218].) There is no experimental evidence in favour of, or against, the accumulation of more than two hydrides by FeMoco. This remains an open question.

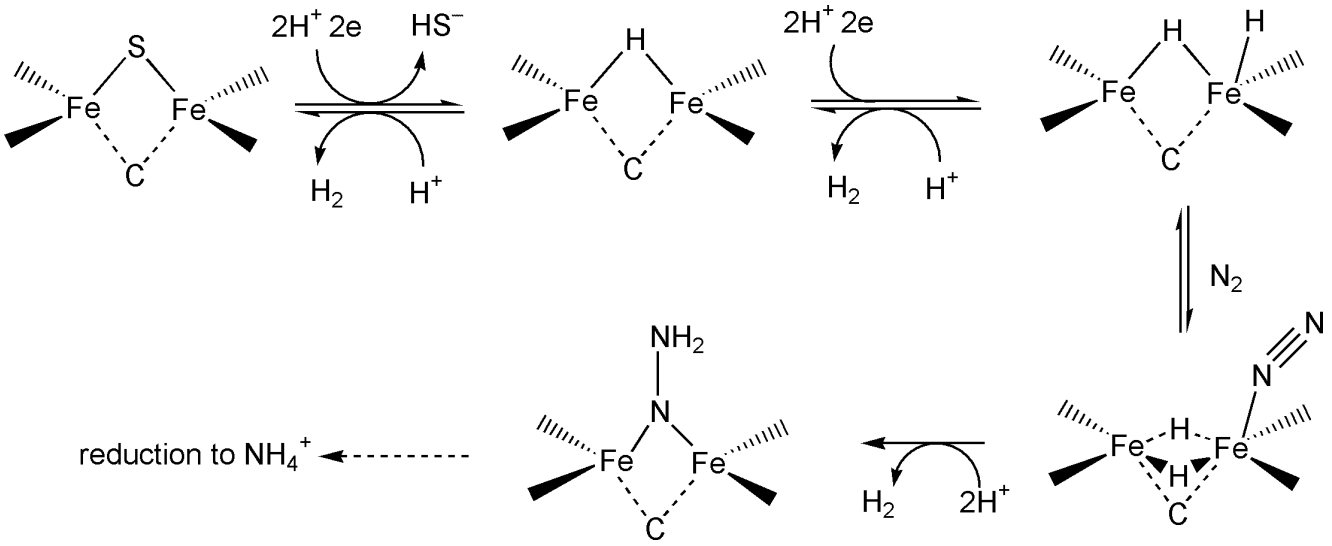


Figure 4. Possible sequence of events from the binding of H^+ as a hydride, to the reduction of N_2 to ammonia at the FeMo cofactor of nitrogenase. Adapted from [215]. See [214,216–218] for DFT structures showing the positions of the bridging hydrides in the FeMo cluster. The lability of the belt sulfurs is important to allow for substrate binding [111,219].

Sequential transfer of H^+ and an electron through diazene (HNNH) and hydrazine (H_2NNH_2) intermediates, with final release of NH_4^+, would be a feasible mechanism for the remainder of the reaction [220,221].

While the outline of the Lowe–Thorneley mechanism is widely accepted, several more detailed proposals have been put forward to describe the intimate mechanism of the reaction. Many are based on DFT or QM/MM calculations (for example, [32,118,222–226]). Still, the mechanism is yet to be resolved. For illustrative purposes, one of these proposals [222] (somewhat simplified) is shown in Figure 5. The iron atoms involved are Fe3 and Fe7, and bridging sulfide S5A (see Figure 1d). The protonation of sulfides, as demonstated by a spectroelectrochemical study [34], is important for catalytic function. Another very

detailed proposed mechanism that is worthy of consideration and is based on extensive DFT calculations using a >485 atom model, is given in [32].

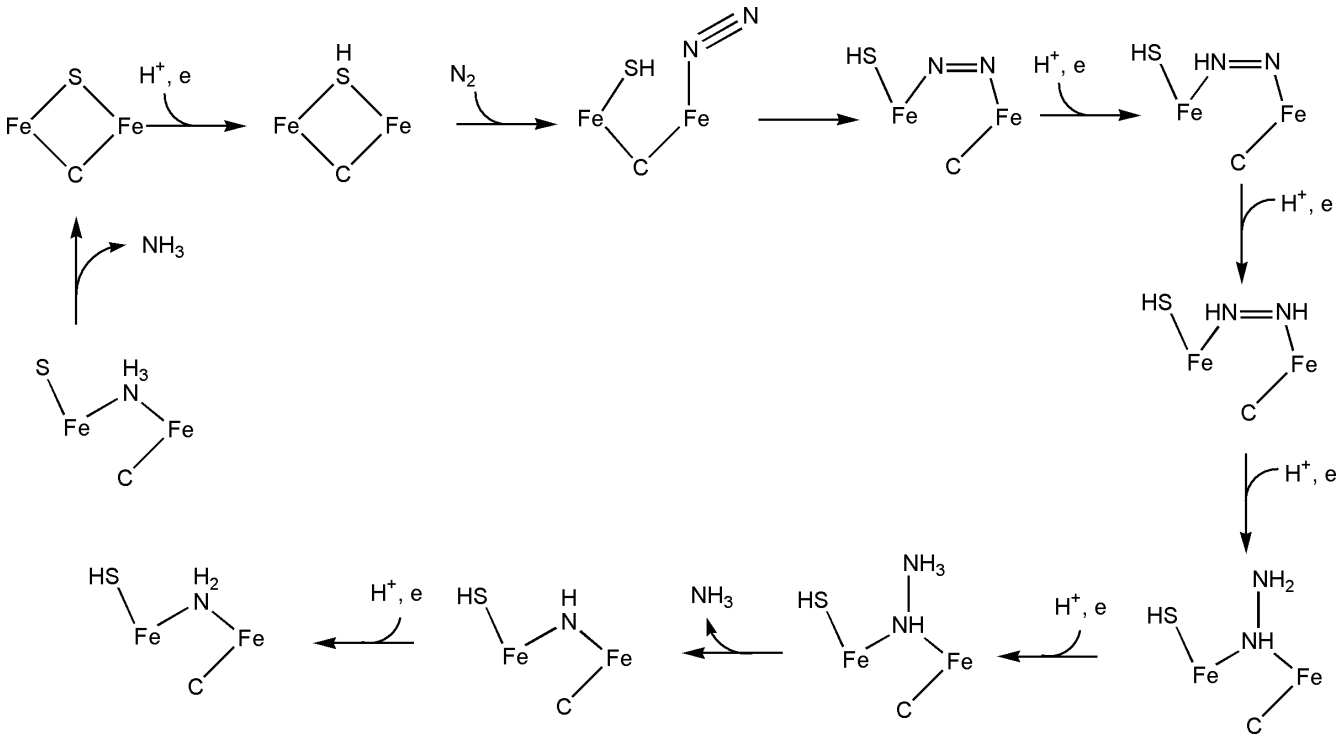


Figure 5. A possible reaction mechanism for the reduction of N_2 to NH_3 by FeMo nitrogenase [222].

The reader will appreciate that in the proposed mechanisms shown in Figures 4 and 5, there is no direct interaction between N_2 and Mo^{3+}—the substrate binds to the central Fe ions (Fe2 and Fe6) of the FeMoco cluster [213,219]. What then is Mos's function?

The role Mo plays during enzyme turnover is indirect yet essential, as it undoubtedly contributes to the structural configuration of the active site, thereby facilitating N_2 capture and its proton-coupled reduction between Fe2 and Fe6 [32,227], a process enabled by the protonation and lability of the belt sulfurs [111]. Upon substrate binding, the Mo–hydroxy bond to homocitrate is elongated from 2.2 Å to 2.7 Å [219], effectively altering the coordination of homocitrate from bidentate to monodentate, a coordination that is subsequently restored following turnover [219]. This transient change in coordination may promote proton transfer from the proton delivery pathway during N_2 reduction [219]. The presence of homocitrate is critical for catalytic activity; in a *nifV* mutant of *Klebsiella pneumoniae*, where homocitrate is replaced by citrate, nitrogenase activity is reduced to only 7% of that observed in the wild-type enzyme [228].

Nitrogenases are sensitive to, and inhibited by, O_2, and nitrogen-fixing microbes have developed strategies to shield themselves from O_2 [10,229–234]. Indeed, it is speculated that this sensitivity may have been one of the reasons for the relatively slow evolution of land-based life forms after the onset of oxygenic photosynthesis (perhaps as early as 3.5 b.y.a. [235]) and the Great Oxidation Event (2.4 to 2.1 b.y.a.) that heralded early life, the Proterozoic eon. Recent cryo-EM reports [236–238] show that in *Azotobacter vinelandii* a small protein, FeSII, is oxidised and forms a protective complex with two MoFe nitrogenases when O_2 levels increase. This can grow into extended filaments. The nitrogenase is inactive under these conditions. Once O_2 levels drop, FeSII is reduced, the complex dissociates, and nitrogenase activity is restored.

4.2. Xanthine Oxidoreductase

Xanthine oxidoreductase (XO, also referred to as xanthine oxidase) is widespread in nature, as all organisms must metabolise purines [239–241]. This is an ancient enzyme that has been traced back to the Last Universal Common Ancestor (LUCA) [242]. The enzyme features in the later stages of purine catabolism and catalyses the oxidation of hypoxanthine to xanthine, and then xanthine to uric acid (Equation (4)). For a fascinating account of the history of research into xanthine oxidase, see [24].

Elevated levels of uric acid can lead to conditions such as gout, inflammatory arthritis characterised by sudden and severe pain, redness, and swelling in the joints. Inhibiting XO using compounds such as allopurinol and febuxostat can be beneficial in treating hyperuricemia and its associated disorders [243,244]. Whilst an essential enzyme, elevated XO activity is associated with a variety of conditions, including liver pathologies, hepatocellular carcinoma [25,245], and, due to its involvement in oxidative stress pathways, various cardiovascular diseases, such as hypertension and atherosclerosis [246–248]. Therefore, targeting this enzyme has therapeutic implications beyond gout management.

There are two forms of the enzyme (refer to Equation (4)): the dehydrogenase uses NAD^+ as the electron acceptor and does not generate superoxide, $O_2^{\bullet -}$; the oxidase uses O_2 as the electron acceptor and generates $O_2^{\bullet -}$ in the process. The crystal structure of homodimeric bovine xanthine oxidase is shown in Figure 6, as are the redox-active centres—a flavin adenine dinucleotide (FAD), two $[Fe_2S_2]$ centres, and Moco.

As mentioned before, whilst reactive oxygen species such as $O_2^{\bullet -}$ can have deleterious effects through protein and DNA fragmentation [102,103], they are important for defence against infections [98–101], in increasing a cell's tolerance to oxidative stress [96], and in inter- and intracellular signalling [97].

It is known that a Glu residue and an Arg residue near the Moco site are important for catalytic activity [245]. At least three possible mechanisms have been proposed [245,249,250]. That by Cerqueira et al. [250], based on QM/MM methods, is shown in Figure 7. In this mechanism, Glu and Arg, as well as a water molecule near the Moco site, are involved in the reaction, which occurs in four steps. In the first step, a Gly residue deprotonates the hydroxyl ligand of $Mo^{6+,}$ and the activated hydroxyl group initiates a nucleophilic attack on xanthine. A hydride is transferred to the Moco sulfur, in the process reducing Mo^{6+} to Mo^{4+}. This is the rate-determining step of the reaction (with $\Delta G^{\ddagger}$ = 70.7 kJ mol^{-1}; experimentally, 65.7 kJ mol^{-1} [245]). In the third step, proton transfer from Arg, via a water molecule, produces uric acid. Two one-electron transfers to $[Fe_2S_2]$ oxidise Mo^{4+} to Mo^{6+}, and the cycle is completed by the reaction of H_2O with Moco.

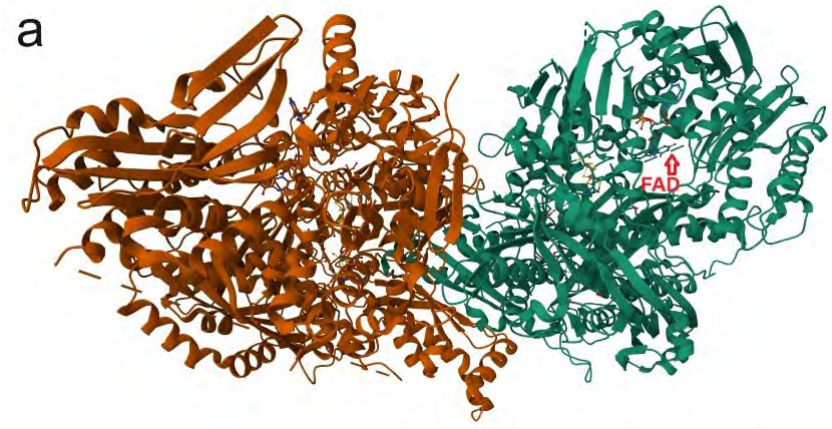


Figure 6. *Cont.*

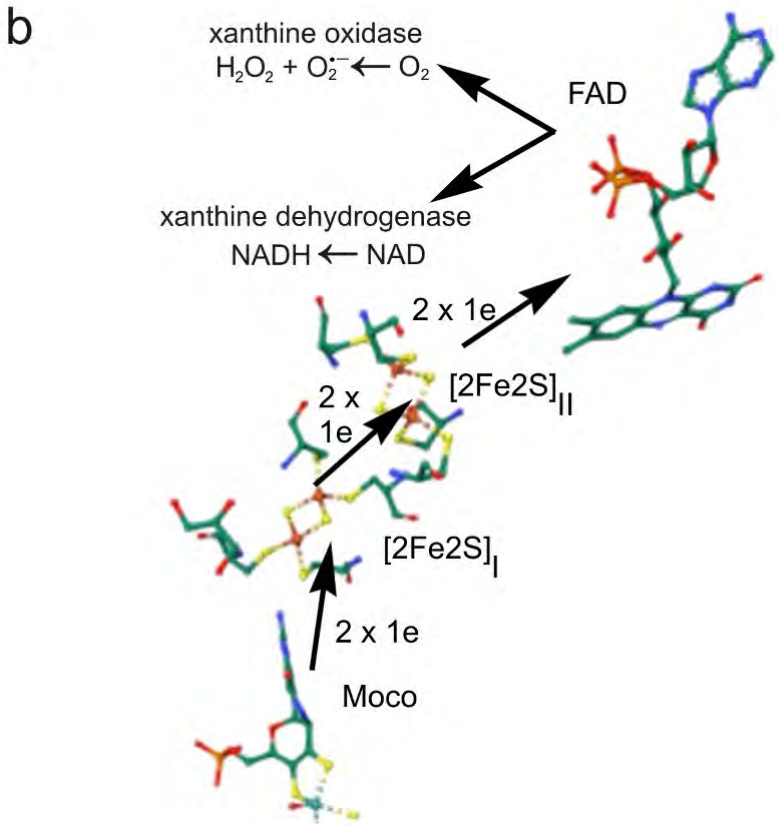


Figure 6. (**a**): Bovine xanthine oxidase (PDB 3AX7 [251]). The enzyme is a homodimer. (**b**): The redox-active sites of one of the monomers and the flow of electrons to the oxidants (the orientation is preserved; FAD in the top picture is labelled).

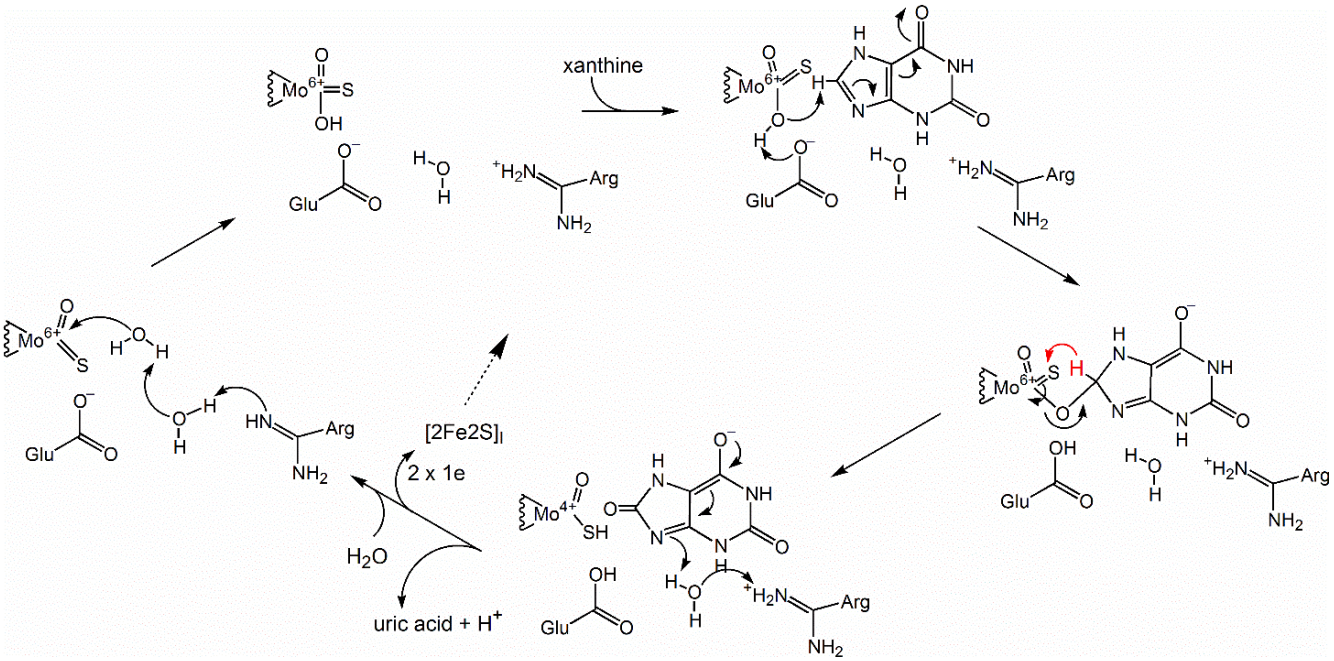


Figure 7. A possible mechanism of the reaction catalysed by xanthine oxidase (adapted and modified from [250]).

4.3. Aldehyde Oxidase

Aldehyde oxidase (AO) is found in a range of organisms, particularly in animals, but also in plants, some invertebrates and some bacteria [121,252]. It is involved in the

metabolic pathway of many drugs [253,254]. The enzyme is a homodimer homologous to xanthine oxidase, with a similar primary amino acid sequence and the same cofactors. The enzyme is capable of catalysing both oxidation and reduction reactions (examples are shown in Figure 8). O_2 acts as the electron acceptor in the oxidation of a wide range of substances containing, for example, an aldehyde or an N-heterocyclic group.

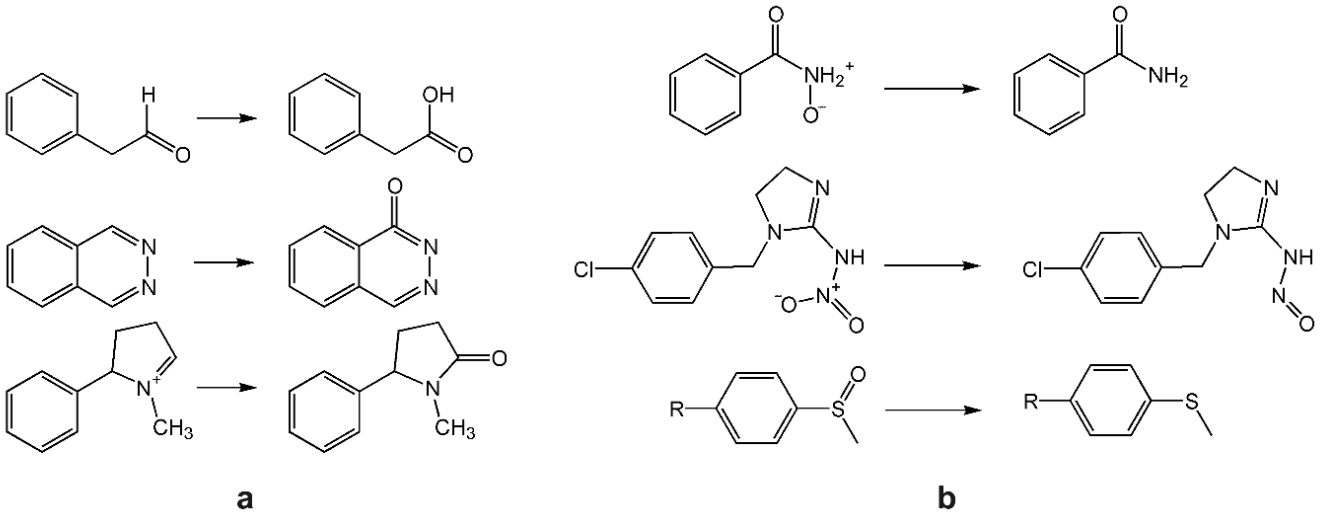


Figure 8. Examples of (**a**), oxidation reactions and (**b**), reduction reactions catalysed by aldehyde oxidase.

The mechanism of the oxidation of phthalazine, a N-heterocyclic compound, to phthalazine-1(2*H*)-one by AO has been studied by QM/MM methods [255] and is similar to the mechanism of oxidations catalysed by xanthine oxidase. See also [256]. An outline is shown in Figure 9. A Glu and a Lys residue near Moco play a crucial role in the reaction.

The first step is protonation of the substrate by the Lys residue. This increases the carbocation character at the adjacent carbon, rendering it susceptible to nucleophilic attack. The transfer of a proton from Moco–OH to Glu enables Moco–O^- to attack the (formally) cationic carbon of the substrate. The third and rate-limiting step ($\Delta G^{\ddagger} \approx 60$ kJ mol^{-1}) is a hydride shift from the substrate carbon to the sulfur ligand of the Moco, reducing Mo^{6+} to Mo^{4+}. The availability of these two oxidation states of the metal assists in overcoming this energy barrier. Mo^{4+} is then oxidised back to Mo^{6+} by two one-electron transfer steps via the iron–sulfur clusters (see Figure 9a) to the FAD cofactor, regenerating the catalyst. The critical steps are the protonation of the substrate by a Lys residue and the deprotonation of the hydroxyl ligand on Mo^{6+}, which generates the nucleophile that attacks the substrate.

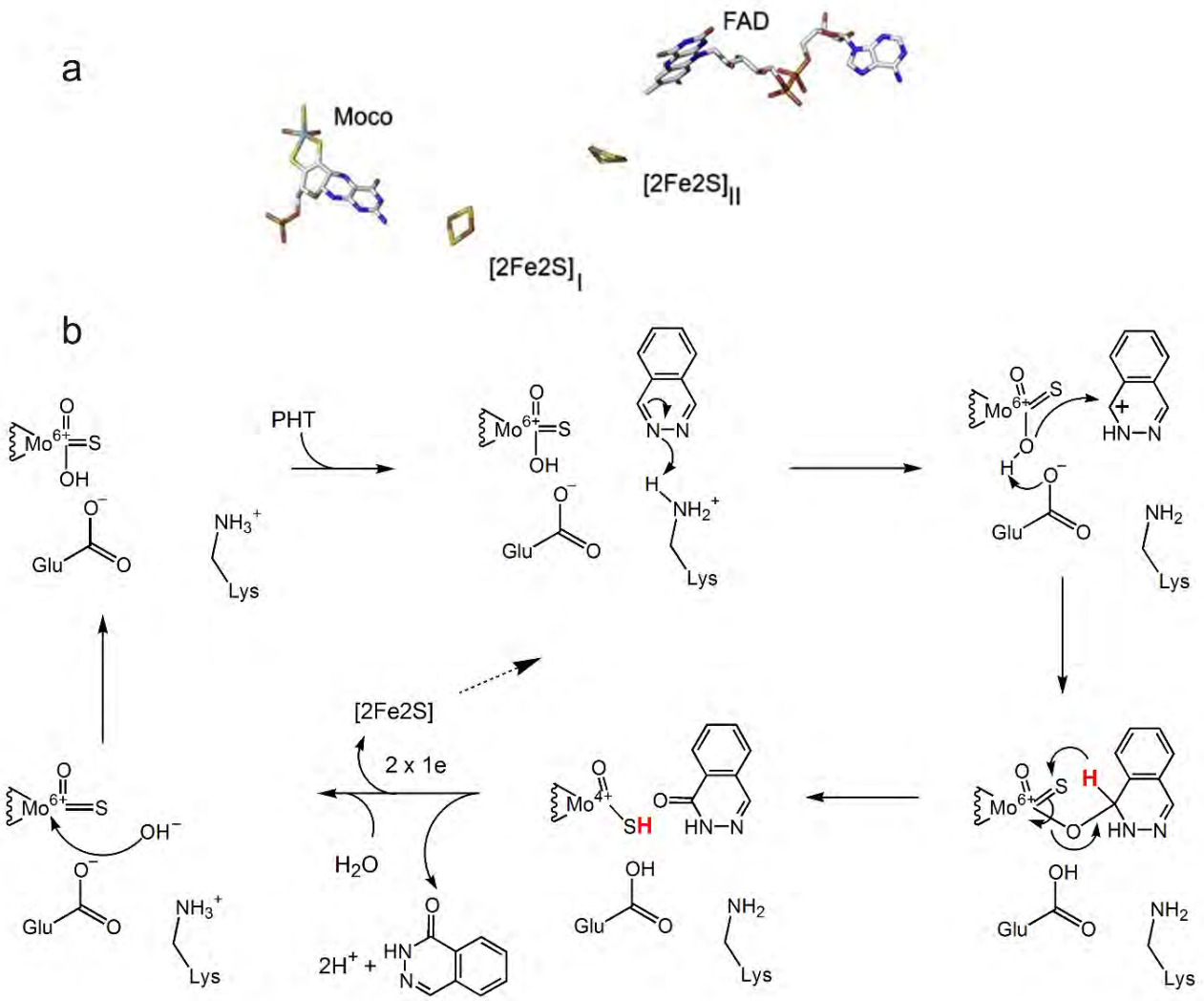


Figure 9. Top (**a**): The cofactors of mouse liver AO (PDB 4UHX [257]). Bottom (**b**): The oxidation of an N-heterocycle by AO (from [255], simplified).

4.4. Sulfite Oxidase

Sulfite oxidase (SOX) catalyses the final stage in the oxidative degradation of sulfur-containing amino acids and lipids. SOX is widespread in nature and is found in animals, plants, and many microorganisms [126,258]. It is crucial for human health [25,259], and SOX deficiency leads to severe neurological damage and early childhood death [260,261].

The enzyme is found in the intermembrane space of mitochondria and transfers the electrons from sulfite oxidation (Equation (6)) to cytochrome *c*.

$$SO_3^{2-} + H_2O \rightarrow SO_4^{2-} + 2H^+ + 2e \quad (6)$$

One of the pathways of cysteine metabolism that generates SO_3^{2-} is shown in Figure 10 [262].

In vertebrates, the mechanism of SOX involves two one-electron transfer steps from Moco to a b_5-type haem and, thence, to cytochrome *c* [263]; in plants, the electron transfer is directly to O_2 [264]. The Moco and haem from the crystal structure of the sulfite oxidase from chicken liver (PDB 1SOX [265]) is shown in Figure 11. The oxidation changes that occur at the Mo and Fe centres of vertebrate SOX turnover during the oxidation, together with the reduction of cyt *c*, are shown in Figure 12 [264].

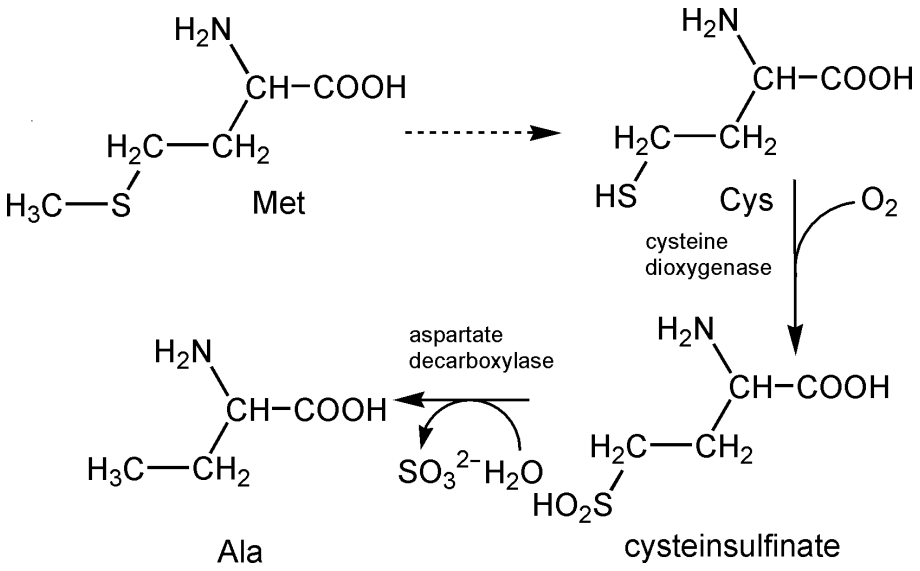


Figure 10. Pathway of the metabolism of Cys that leads to formation of sulfite.

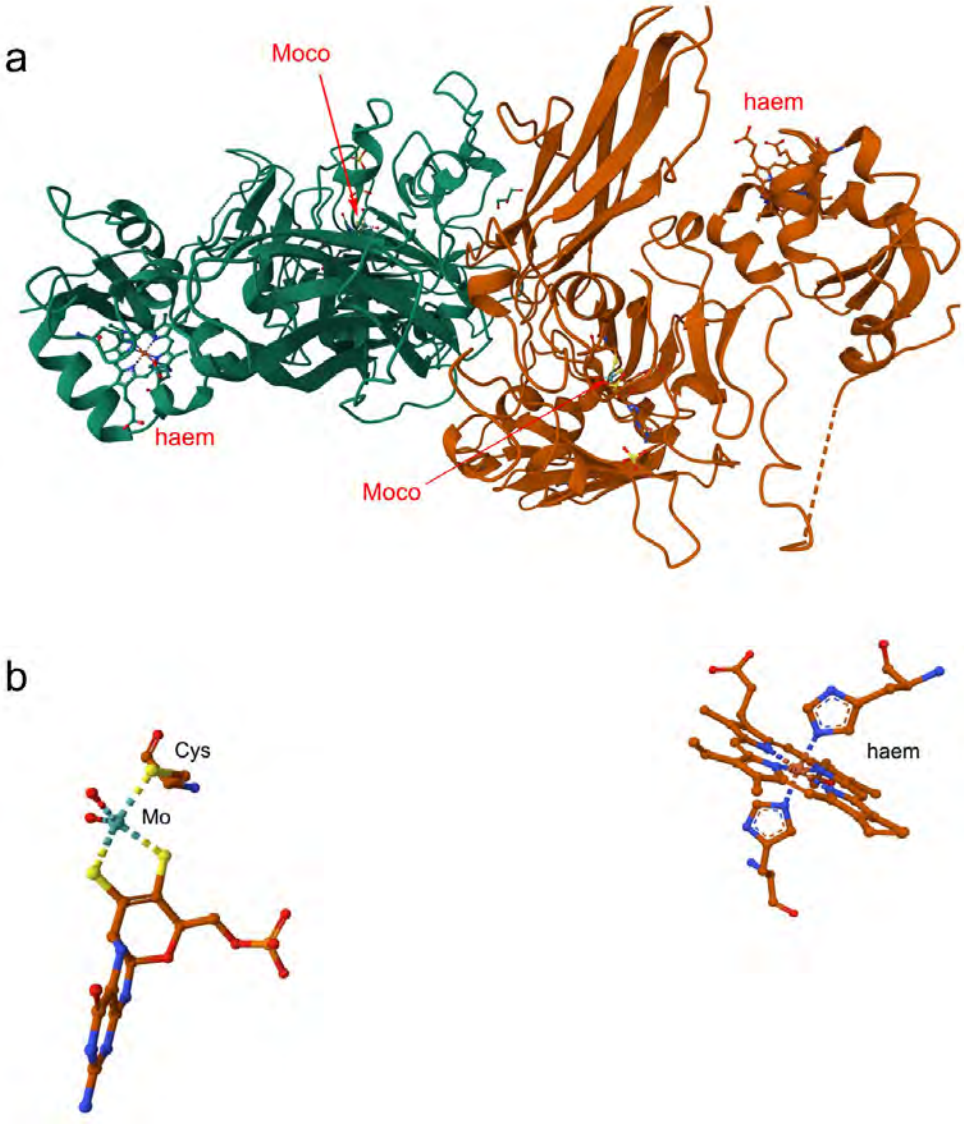


Figure 11. (**a**): The crystal structure of homodimeric SOX from chicken liver (PDB 1SOX [265]). (**b**): The Moco and haem prosthetic groups from one of the dimers of SOX.

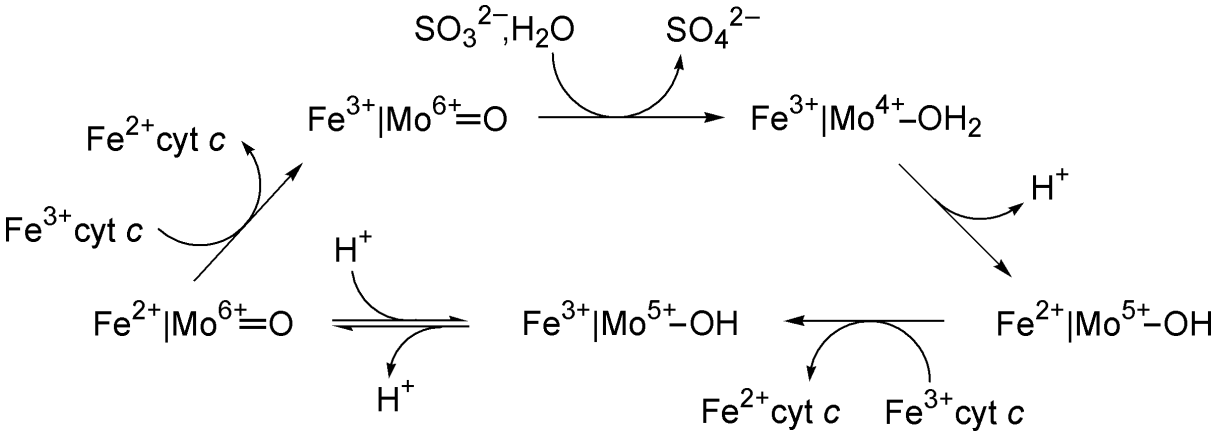


Figure 12. Changes in the oxidation state of Mo in Moco and Fe in the b_5-type haem in SOX during enzyme turnover on the oxidation of sulfite [263,264].

The resting state of the enzyme contains Fe^{3+} in the b_5-type haem and a Mo^{6+}=O species. The Mo centre oxidises SO_3^{2-} to SO_4^{2-}, and Mo^{6+} is reduced to Mo^{4+}. There is an intramolecular electron transfer from Mo^{4+} to haem Fe^{3+}, producing a Fe^{2+} | Mo^{5+} state. (A $4d^1$ Mo^{5+} centre has been observed by EPR ([266] and references therein)). The b_5 Fe^{2+} transfers an electron to the physiological electron acceptor, Fe^{3+} cytochrome *c*, forming the Fe^{3+} | Mo^{5+} state. This then undergoes a second intramolecular electron transfer, followed by the transfer of the electron to Fe^{3+} cytochrome *c*, regenerating the resting enzyme.

4.5. Nitrate Reductase

Nitrate reductase is an important enzyme in the global nitrogen cycle, reducing NO_3^- to NO_2^- (Equation (7)) [18–20].

$$NO_3^- + 2H^+ + 2e \rightarrow NO_2^- + H_2O \quad (7)$$

Assimilatory nitrate reductases (NAS) are found in plants, fungi, and bacteria, where they play a crucial role in incorporating (assimilating) nitrogen into biomass. The enzyme in plants and fungi is a soluble, monomeric protein with three domains, whereas in bacteria, it exists as a multi-subunit complex bound to the cytoplasmic membrane [144,267]. Dissimilatory nitrate reductases are enzymes used by bacteria and archaea for anaerobic respiration. Respiratory nitrate reductases (NAR), which are membrane-bound, and periplasmic nitrate reductases (NAP), located in the periplasm, are essential for energy production. These enzymes contribute to denitrification and other nitrogen cycling processes [268–273].

In NAS, electrons are typically supplied by NADH or NADPH, which serve as essential cofactors in reductive biosynthetic reactions, including the reduction of nitrate to nitrite by assimilatory nitrate reductases [274–277]. By contrast, electron donors for NAR and NAP vary considerably among different prokaryotic organisms and are often dependent on environmental conditions and the organism's metabolic capabilities [270,277,278].

In many facultative anaerobic bacteria, NADH-derived electrons are channelled through components of an electron transport chain to drive nitrate reduction. For instance, in *Paracoccus denitrificans*, electrons from NADH enter the respiratory chain via NADH dehydrogenase and are passed through cytochrome complexes to the membrane-bound NAR system [279]. In *Escherichia coli*, formate frequently serves as the primary electron donor under anaerobic conditions, with formate dehydrogenase transferring electrons to the menaquinone pool, which subsequently donates them to NAR or NAP reductases [277]. In addition, a wide range of inorganic compounds can serve as electron donors in specific taxa. H_2 is used by some hydrogenotrophic bacteria and archaea; their

hydrogenases couple H_2 oxidation to nitrate reduction [280–282]. Fe^{2+} acts as an electron donor in some chemolithoautotrophic bacteria, such as *Acidithiobacillus ferrooxidans*, where electrons derived from its oxidation can be channelled into nitrate reduction pathways [283]. H_2S and $S_2O_3^{2-}$ are used by some sulfur-oxidising bacteria; in species such as *Beggiatoa* and *Thiobacillus denitrificans*, these reduced sulfur species are oxidised to sulfate while concomitantly reducing nitrate to nitrite or further to gaseous nitrogen compounds [284].

Nitrate is a major source of nitrogen in soils. In plants, nitrate reductase is essential for converting nitrate into forms that can be used for the synthesis of amino acids, proteins, and nucleotides, which are vital for plant growth and development [285]. Some bacteria, such as *Rhizobium* species, use nitrate reductase as a component of the denitrification process, converting nitrate into N_2 or other nitrogen-containing compounds. Treatment of water streams for nitrate pollution can be achieved by encouraging the growth of denitrifying bacteria, such as *Paracoccus denitrificans* and *Thiobacillus denitrificans* [140,286,287]. Nitrate reductase is also involved in gut microbiota function and affects nitrate metabolism in humans and other animals [288].

The bacterial nitrate reductase from *E.coli* will be used as an example [289]. The structure of the Mo-bis(MGD) group, and a chain of iron–sulfur clusters linking it to two haem *b* moieties, as determined by crystallographic methods [290], is shown in Figure 13. It is likely that one or more H_2O (perhaps OH^-) or sulfido ligands and/or a Cys, are coordinated to Mo^{6+} in the resting state of the enzyme.

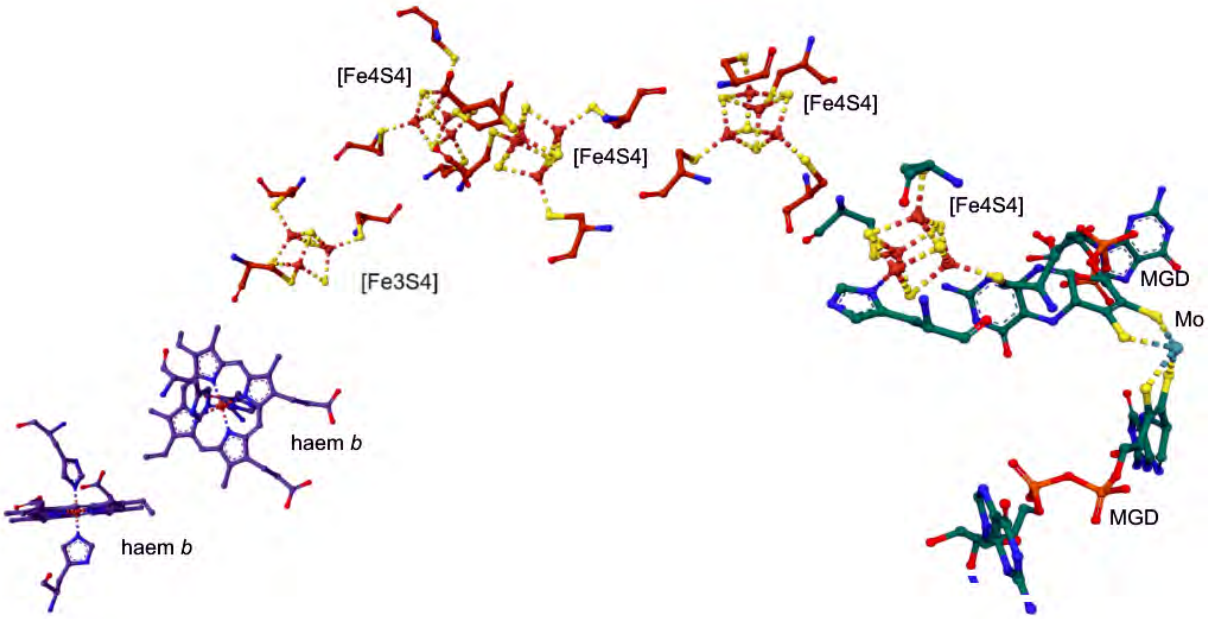


Figure 13. The Moco active site, and the chain of iron–sulfur clusters linking it to two haem groups, in the nitrate reductase from *E. coli* [290].

Electrons are transferred from the quinol pool (menaquinol) through the two haem groups and the iron–sulfur cluster chain to Moco, reducing Mo^{6+} to Mo^{4+}, releasing the H_2O (OH^-) or sulfide ligands and creating a substrate-binding site for NO_3^-. This binds to Mo^{4+} (or possibly to Mo^{5+}, followed by a further one electron reduction [267,291]). NO_2^- is released from the Mo^{4+}–ONO_2^- complex, leaving a Mo^{6+}=O complex. Protonation of the oxo ligand releases H_2O, regenerating the resting enzyme. There is an alternative mechanism, based on DFT modelling, that envisages NO_3^- initially binding to a sulfide ligand on Mo^{6+}, displacing the sulfide, which is relocated to form a Mo^{6+}–S–S(Cys) complex. NO_2^- departs, leaving a O=Mo^{6+}–S–S(Cys) intermediate, which then undergoes two one-electron reductions with the uptake of two protons, releasing H_2O [292].

5. Examples of Tungsten-Dependent Enzymes

5.1. Formate Dehydrogenase

Formate dehydrogenase enzymes (FDHs) oxidise formate to CO_2 using, for example, NAD^+ (Equation (8)) [293–296]. Formate is important for the growth of many bacteria and archaea. The CO_2 produced is fixed in the Calvin–Benson cycle in many autotrophic organisms. Other electron acceptors or mediators include ferrodoxins, coenzyme F_{420}, quinols and haems.

$$HCO_2^- + NAD^+ \rightleftharpoons CO_2 + NADH \quad (8)$$

There are both metal-dependent and metal-independent enzymes [293]. Hence, a metal ion is not absolutely essential to catalyse this reaction. The metal-dependent FDH's, found in bacteria and archaea, contain either molybdenum or tungsten in the active site [297]. Mo^{6+} or W^{6+} is bis-coordinated by pterins (Figure 1b), a sulfide ligand, and the sixth ligand is provided by a protein cysteine or selenocysteine; there is usually one (or multiple) $[Fe_4S_4]$ cluster near the active site, and there are also additional cofactors (iron–sulfur clusters, FMN, haems [298]) either in the same or in a neighbouring subunit. For a useful schematic representation, see [17].

Under a variety of physiological conditions, the enzymes will catalyse the reverse reaction, serving as CO_2 reductases. This has potential industrial application since formic acid is a promising source of hydrogen energy [299], and there is an ever-increasing need for CO_2 remediation [300]

Because (i) Mo and W have similar chemical properties; (ii) the Mo- and W-containing enzymes have a very similar active site; and (iii) W can replace Mo in some enzymes, it is generally accepted that the Mo- and W-enzymes have a common reaction mechanism [172,294]. However, the W^{4+} enzymes are more reducing than the Mo^{4+} enzymes [301] and are, therefore, preferentially used for the conversion of CO_2 to formate [302]. W is usually preferred to Mo in low-potential redox catalysis (for example, −430 mV in FDHs and −560 to −610 mV in the aldehyde ferredoxin oxidoreductase (AOR) families [36,168,303,304]).

In effect, W centres in enzymes are better electron acceptors and exhibit lower redox potentials than Mo centres, probably a consequence of relativistic effects that become important in the heavier transition metals [305]. DFT and sulfur K-edge X-ray absorption studies of W^{5+}=O vs. Mo^{5+}=O in bis(dithiolene) complexes show that relativistic effects destabilise the redox-active $d(x^2–y^2)$ orbital of W, lowering its reduction potential and accelerating oxygen-atom transfer rates [306,307]. DFT calculations comparing the ionisation potentials of Mo^{4+} | Mo^{5+} and W^{4+} | W^{5+} complexes show a c. 160 mV difference. The radial expansion of the 5d orbitals of W and the contraction of its s and p orbitals due to relativistic effects bring the 5d and 6s orbital energies closer together, enhancing the stability of higher oxidation states when compared to Mo [306,308].

The sulfide ligand likely acts as a hydride acceptor from formate when this is oxidised [309]. Two possible mechanisms for the reaction are shown in Figure 14, although details are still not clear and clearly merit further investigation. For a comprehensive discussion, see [17]. Many FDHs are inactivated by O_2, probably by substitution of the sulfide ligand by an oxo ligand [310], which will not act as a hydride acceptor.

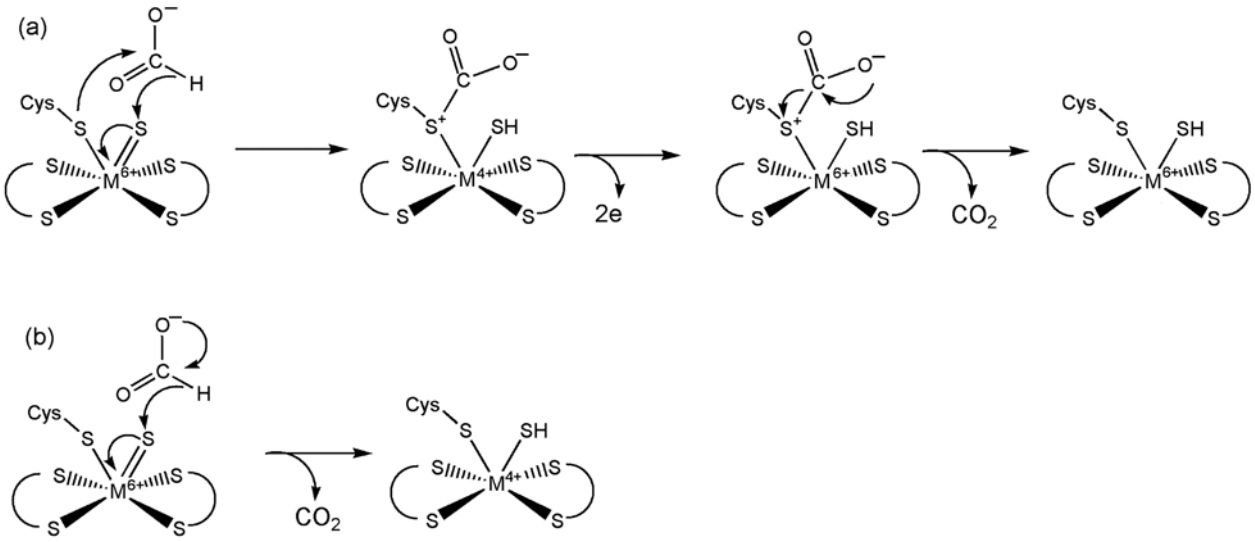


Figure 14. Outline of two possible mechanisms of the oxidation of formate to CO_2 by the FDHs. M = Mo or W. (**a**) [311]; (**b**) [312]. Seleocysteine is a better nucleophile than Cys, rationalising why enzymes with this amino acid exhibit increased catalytic activity [313]. This would tend to favour (but not prove) mechanisms such as that shown in (**a**), which involve the (Se)Cys ligand and hydride transfer from formate [314]. Another proposed mechanism, involving the initial displacement of Cys by a solvent-derived hydroxide, which then acts as a nucleophile to attack the substrate resulting in the formation of a bicarbonate attached to the metal [315], has been discounted [314].

The $[Fe_4S_4]$ cluster, cycling between 2+ | 1+, within 6 Å of the pterin in the Mo or W active site is likely to be the entry point for electron transfer needed for formate oxidation or CO_2 reduction. The bis-WGD cofactors are non-innocent and participate in the electron transfer process [316,317].

5.2. Aldehyde Oxidoreductase

The aldehyde oxidoreductases (AORs) catalyse the oxidation of aldehydes to carboxylic acids (Equation (9)) with the reduction of an electron acceptor, such as an oxidised ferredoxin.

$$RCHO + H_2O + Fd_{ox} \rightarrow RCOOH + Fd_{red} \quad (9)$$

The enzymes are involved in the pathway for the degradation of glucose [318] (and perhaps in the oxidation of the aldehyde side products from amino acid metabolism [319]) and found in hyperthermophillic archaea, such as *Pyrococcus furiosus*, which functions at elevated temperatures (80–100 °C) and optimally at pH 8–9 [320,321]. Some strains of *Thermococcus*, for example, use amino acids as their source of carbon and use AORs to metabolise them [303]. Tungsten AORs are also found in some bacteria [322–324]. The use of tungsten-dependent oxidoreductase to detoxify aldehydes by the human gut microbiome is perhaps an underappreciated aspect of human health [52,325]. Replacement of tungsten by molybdenum in AORs results in an inactive enzyme [326].

An AOR from the mesophilic bacterium *Aromatoleum aromaticum* has been immobilised on a glassy carbon working electrode and used to oxidise a wide range of aliphatic and aromatic aldehydes using benzyl viologen, methylene blue or dichlorophenol as electron transfer mediator [327], opening up the possibility of an energy-efficient catalytic system. This enzyme is also capable of reducing organic acids to aldehydes with H_2 as an electron donor [328]. Using AORs for the microbially catalysed production of alcohols from organic acids is potentially another useful industrial process [173,329].

The active site consists of W^{6+} coordinated by two MPTs in a distorted square pyramidal fashion and a $[Fe_4S_4]$ cluster 10 Å from the active site (PDB 1AOR [330], Figure 15). No protein residues are coordinated to $W^{6+,}$ but two water molecules, or oxo ligands (not resolved in the structure shown in Figure 15), are coordinated to it, resulting in an overall trigonal prismatic arrangement. A recent cryo-EM structure of the AOR from *Aromatoleum aromaticum* shows that the two oxygen atoms coordinated to tungsten are probably oxo ligands [322].

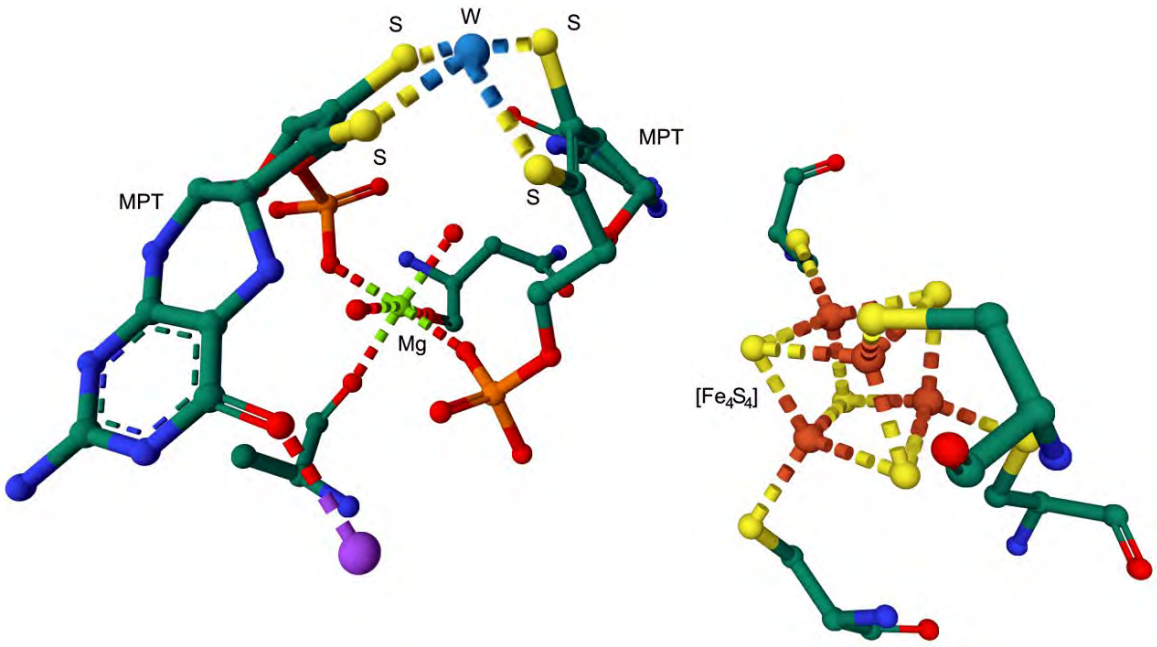


Figure 15. The active site of *P. furiosus* aldehyde ferredoxin oxidoreductase PDB 1AOR [330].

The AOR from *A. aromaticum* has a similar active site $[W(MTP)_2(O)_2]$ but is more complex (Figure 16) (see [331] and PDB 8C0Z for the structure determined by cryo-EM [322]). It uses NAD^+ as an electron acceptor for the oxidation of a wide variety of aldehydes. The site of substrate oxidation is some 55 Å from a FAD moiety near which NAD^+ binds. A mechanism for the reaction has been proposed (Figure 17) [322].

5.3. Acetylene Hydratase

Acetylene hydratase, a member of the DMSOR family of enzymes, is a hydrolase that catalyses the oxidation of acetylene to acetaldehyde (Equation (10)) [178–180,332] in anaerobic bacteria such as *Pelobacter acetylenicus* [178]. It is the only known enzyme to catalyse this reaction.

$$C_2H_2 + H_2O \rightarrow CH_3CHO \quad (10)$$

Acetylene is very water soluble (0.12 g mL^{-1} [333]) and is, therefore, a suitable substrate for many microorganisms [334]. While the concentration of acetylene on Earth from non-anthropogenic sources is low (0.02–0.08 ppbv [335]), it is speculated that Earth's primordial atmosphere may have been much richer in acetylene and that it could have served as a source of carbon and energy [336,337]. The acetaldehyde produced is converted into acetate and ethanol in the fermentation pathway of anaerobes such *P. acetylenicus.* Sulfate-reducing bacteria further oxidise acetate and ethanol to CO_2 [337]. The only other known enzymatic reaction involving acetylene is its reduction to ethylene by nitrogenase [335,338].

This is an example of a W enzyme in which the metal is not redox active. W^{4+} is bound by two pyranopterins (WDG), a Cys residue and a water molecule as seen in a

high-resolution crystal structure (PDB ref. 2E7Z)—Figure 18 [339]. The presence of a $[Fe_4S_4]$ cluster near the active site of a non-redox enzyme is surprising. Perhaps the primordial ancestor of the enzyme was a redox-active metalloenzyme that underwent a mutation that converted it into its present form. Indeed, as has been noted [180,339], access from the surface of the protein towards the active site is unusual, and the substrate migrates there in a unique manner when compared to other enzymes of the DMSOR family. There is a small pocket formed by six hydrophobic residues at the end of the access tunnel, another notable difference to the other members of the DMSOR family [339,340]. An Asp residue near the active site is essential for catalytic activity. W^{4+} can be replaced by Mo^{4+} to yield a much less active enzyme (1.9 vs. 14.8 μmol min^{-1} mg^{-1}) [338].

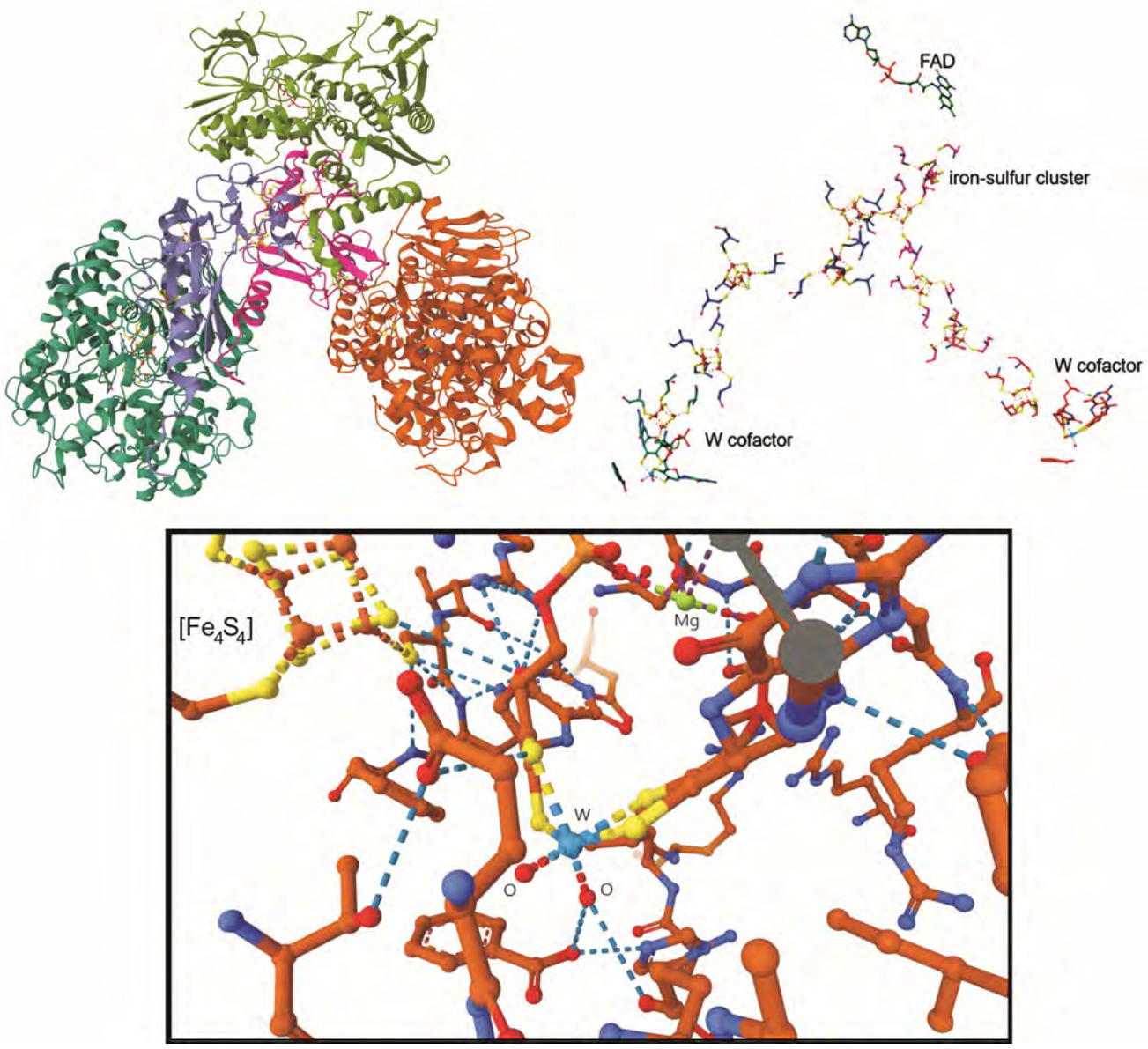


Figure 16. The structure of AOR from *A. aromaticum* (PDB 8C0Z [322]), top left. Top right: the two tungsten active sites and the chain of iron–sulfur clusters, with the orientation of the top left structure preserved. Bottom: Details of one of the active sites.

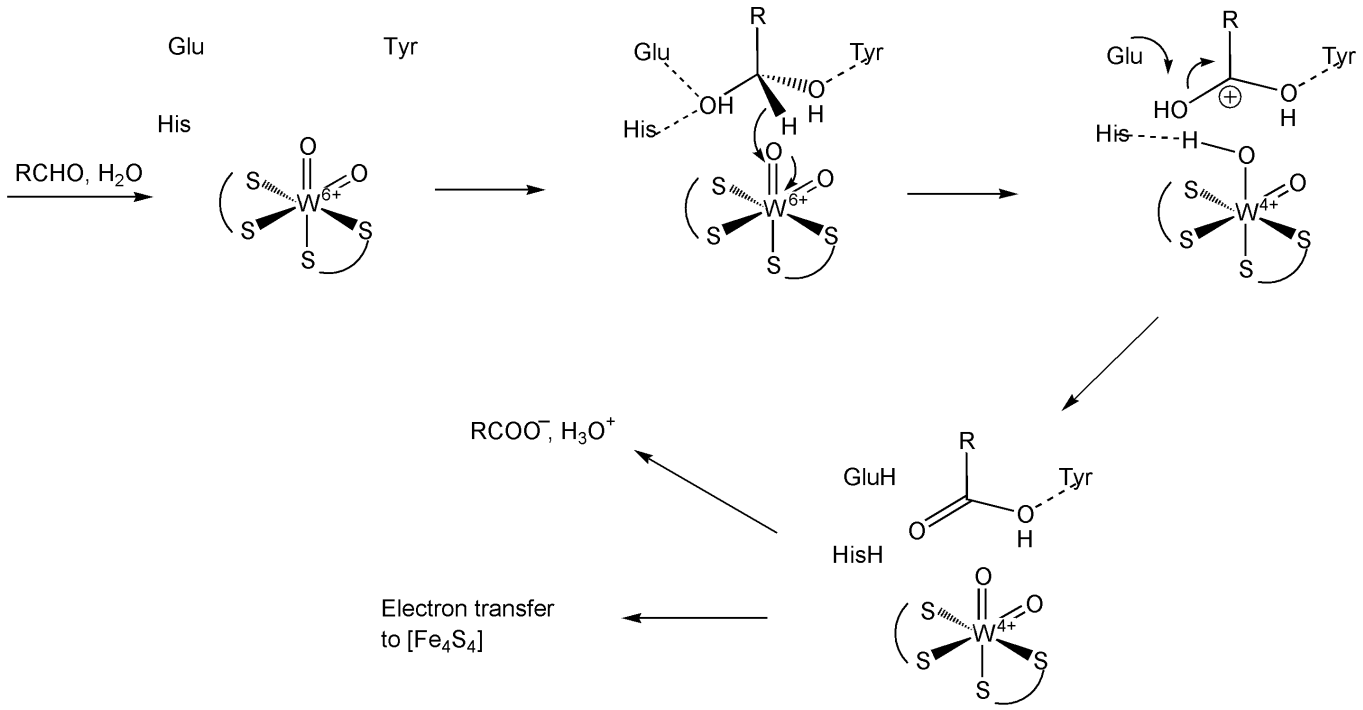


Figure 17. Proposed mechanism for the oxidation of an aldehyde by an AOR [322]. The spontaneous addition of H_2O to the aldehyde produces a gem-diol. Glu, His and Tyr bond the gem-diol, positioning it to hydrogen bond to an oxo ligand on W^{6+}. Hydride abstraction and proton transfer to Glu produce the carboxylic acid. W^{4+} then passes electrons to an electron acceptor, such as Fd_{ox}, in two one-electron transfer steps via a $[Fe_4S_4]$ cluster.

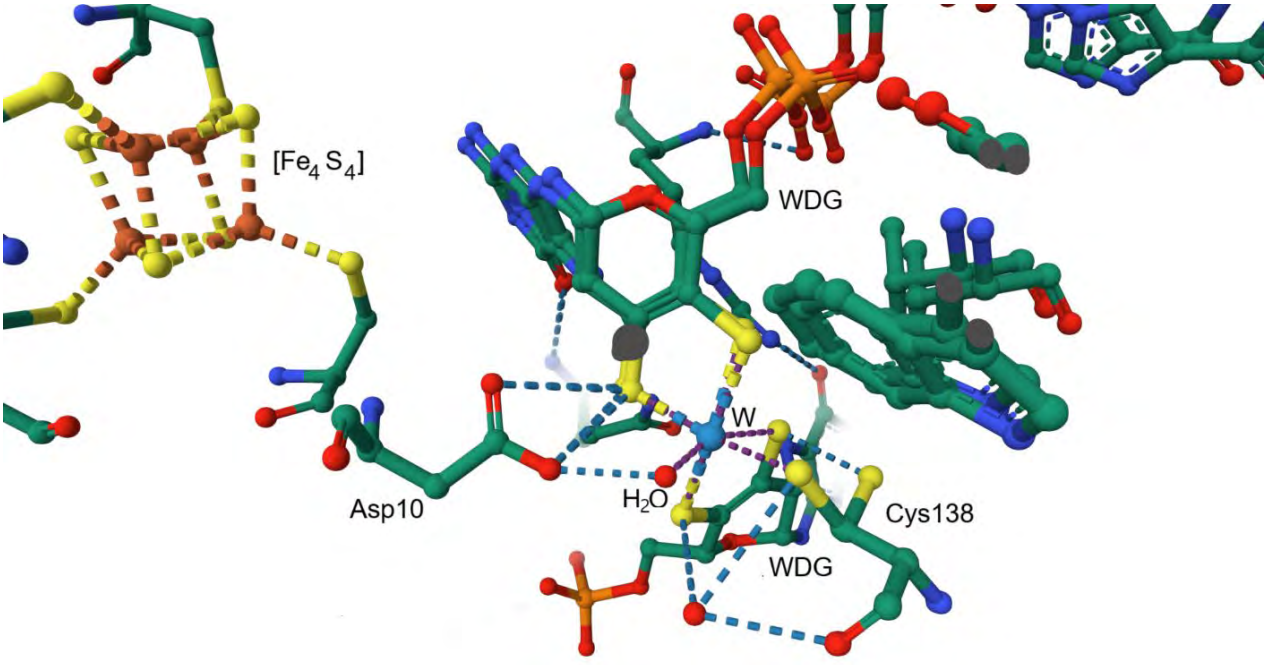


Figure 18. Active site of acetylene hydratase from *P. acetylenicus* [339]. One of the WDG ligands is disordered and was refined over two positions. W in light blue, S in yellow, O in red.

The mechanism of the reaction involves the conserved Asp residue near the active site, and both an outer shell and an inner shell mechanism have been proposed (Figure 19) [341]. The outer shell mechanism sees the substrate accommodated within a hydrophobic pocket

above the active site. Hydrogen bonding of coordinated H_2O to the Asp residue confers on it some electrophilic character, which enables its reaction with C_2H_2.

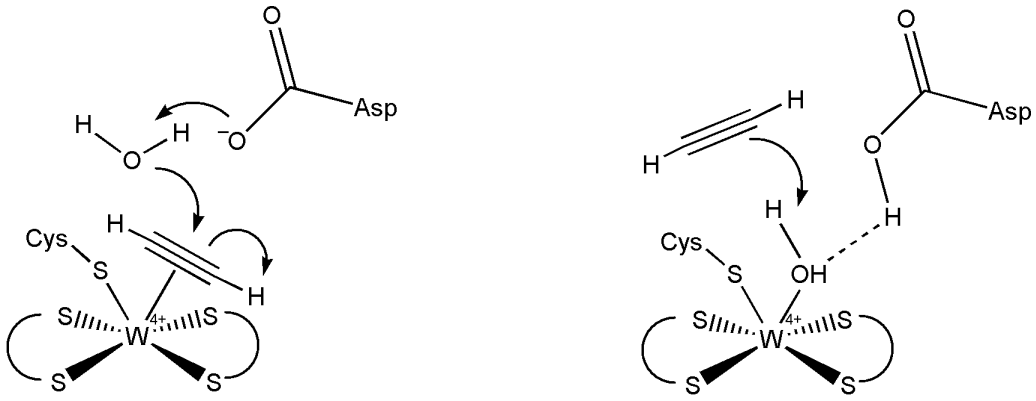


Figure 19. Two possible modes of the binding of the substrate to the active site of acetylene hydratase: the inner shell mode (left) and the outer shell mode (right).

Computational studies favour an inner shell mechanism where η^2 complexation of C_2H_2 with W^{4+} forms a vinyl anion, which is then attacked by the displaced H_2O molecule [179,342,343]. Such a mechanism is outlined in Figure 20 (adapted from [179]). For other possible mechanisms, see the summary in [332].

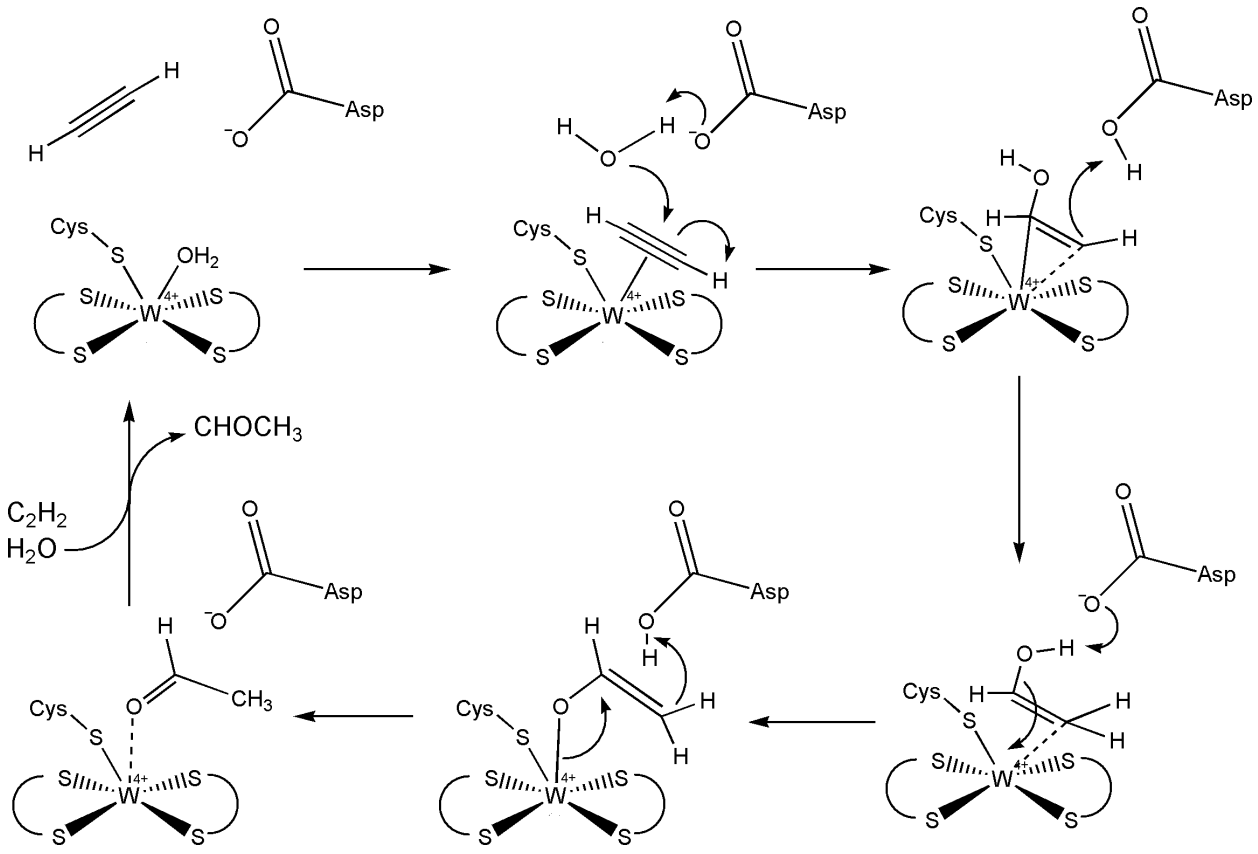


Figure 20. Oxidation of acetylene to acetaldehyde on η^2 complexation by W^{4+} [179].

5.4. Formylmethanofuran Dehydrogenase

Formylmethanofuran dehydrogenase (FMD) is an important oxygen-sensitive enzyme in methanogenic archaea and is responsible for the reversible reduction of CO_2 to formylmethanofuran (formyl-MFR) (Equation (11), Figure 21) [297]. The methanogenesis

pathway is used to generate energy, particularly in anaerobic environments, such as wetlands, deep-sea sediments, and the guts of ruminants. The reaction fixes CO_2, enabling its eventual conversion to methane. CO_2 rather than HCO_3^- is the active species utilised by the enzyme [344].

$$MFR^+ + CO_2 + 2[H] \rightleftharpoons \text{formyl-MFR} + H_2O + H^+ \quad (11)$$

The enzyme is notable for containing either Mo or W within its active site, with the specific metal variant often depending on the organism and environmental conditions. Part of the interest in this system is the possibility of mimicking its chemistry to fix CO_2 and create one-unit carbon feedstocks for the chemical industry [345,346].

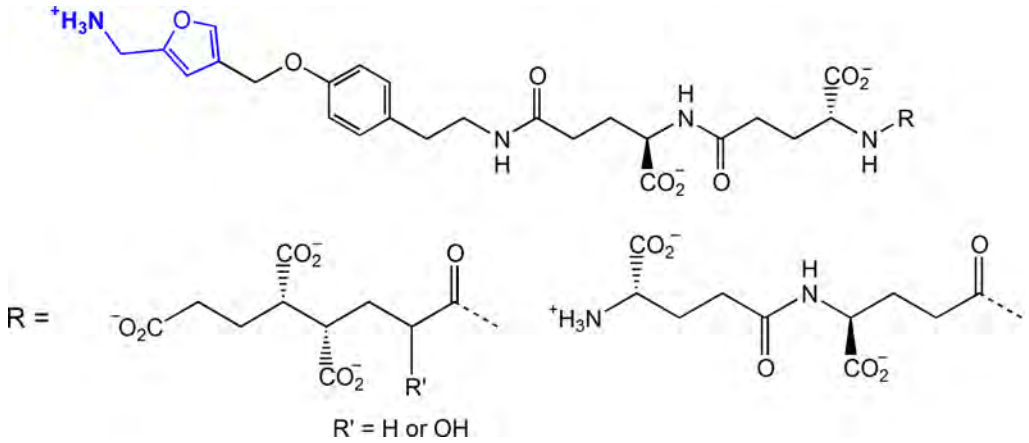


Figure 21. The structure of methanofurans. The furfurylamine (in blue) acts as the formyl-accepting group.

The crystal structure of the enzyme from *Methanothermobacter wolfei* (PDB 5Y5M [345]) shows that the enzyme is composed of several subunits that are bound together. There is an electron transport unit comprising a chain of iron–sulfur clusters that delivers electrons from, for example, reduced ferredoxin or NADH [347], to the tungsten bispterin CO_2-reducing module, with CO_2 delivered through a hydrophobic channel to the site; the formate produced is delivered through a hydrophilic channel to a binuclear [Zn,Zn] centre. This catalyses the condensation of formate and the amino moiety of a methanofuran, generating H_2O and formyl-MFR. The chain of iron–sulfur groups leading to the tungsten–bispterin complex of *M. wolfei* is shown in Figure 22.

Since the condensation of formate and MFR is thermodynamically unfavourable ($\Delta G \approx 21$ kJ mol^{-1}) it has been suggested [345] that the accumulation of formate in the hydrophilic channel provides the driving force for the condensation reaction. This accumulation is driven by the enzyme structure, which reduces the E^o of the CO_2 | formate couple from its standard value of -400 mV to -530 mV.

There is still uncertainty about the actual mechanism of the reduction of CO_2 to formate at the tungsten centre. Either the Cys and/or S^{2-} ligands are displaced by CO_2 and the reduction occurs through an inner-sphere mechanism, or CO_2 reduction occurs in the second coordination sphere of the metal by an outer-sphere electron transfer (see, for example [106,317,348]). Clearly this merits further investigation.

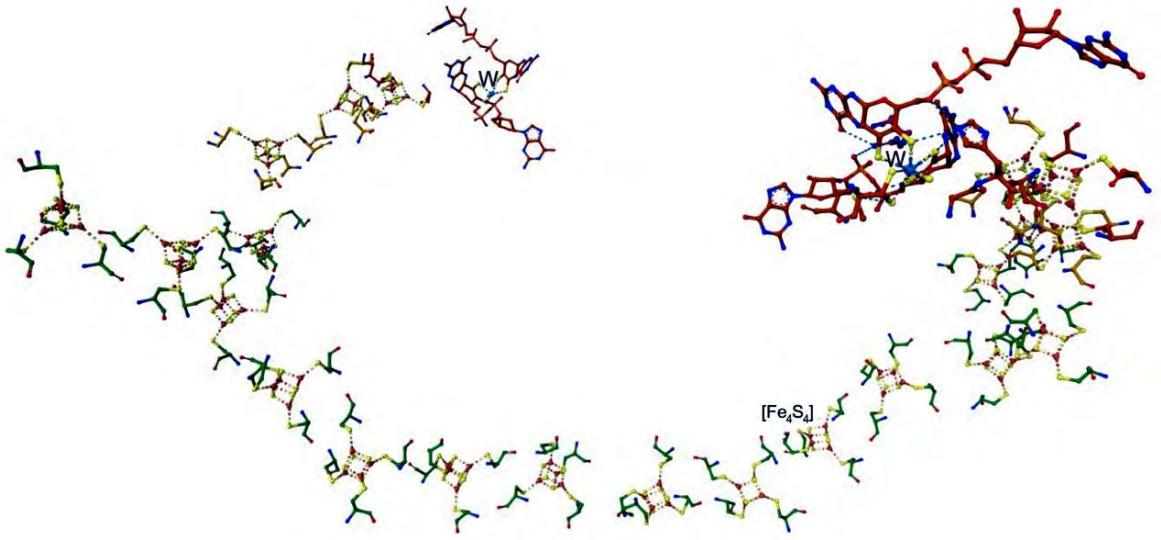


Figure 22. The iron–sulfur clusters leading to the tungsten–bispterin site in the FMD from *M. wolfei* (PDB 5Y5M [345]). W is also coordinated by S^{2-} (or HS^-) and a Cys residue.

6. Concluding Remarks

Given their relatively low geological abundance and typical kinetic inertness, it may seem surprising that second- and third-row d-block metal ions play any role in biology. As far as is known at present, only molybdenum and tungsten do so. While cadmium is generally toxic to living systems, it is found in a cadmium-containing carbonic anhydrase (CdCA) in the phytoplankton *Thalassiosira weissflogii*, where it replaces the usual metal, Zn^{2+}, in zinc-scarce marine environments [349–351]. Relative kinetic inertness is probably an advantage when tight control of intermediates—as in the reduction of N_2 to NH_3 by nitrogenase—is important.

Though the biological roles of Mo and W are limited, they are crucial. They are not mere substitutes for more abundant metals but serve as essential catalysts for specific, often challenging reactions that no other elements can perform as effectively. Both metals form complexes with a pyranopterin cofactor, a ligand capable of fine-tuning redox properties, enabling their participation in diverse oxygen transfer and redox reactions [36].

Mo and W are incorporated into enzymes because their unique redox flexibility, bonding characteristics, and stability under physiological conditions allow them to catalyse demanding redox and oxygen atom transfer reactions. First-row transition metals lack the required redox stability, orbital size compatibility, and ligand binding properties, making them less suitable for these enzymatic functions

Molybdenum is indispensable for processes such as nitrogen fixation and nitrate reduction, key steps in the global nitrogen cycle. Nitrogenases catalyse the conversion of atmospheric N_2 into NH_4^+ in diverse diazotrophic prokaryotes, including free-living, symbiotic, and associative bacteria. Free-living *Azospirillum* species, such as *Azotobacter*, not only fix N_2 but also produce extracellular polysaccharides that enhance soil structure and moisture retention, as well as phytohormones, such as indole-3-acetic acid and gibberellins, which promote plant growth [352,353].

Symbiotic nitrogen-fixing bacteria, such as *Rhizobium* species, establish relationships with leguminous plants, forming root nodules where nitrogen fixation occurs. In exchange for this fixed nitrogen, host plants supply the bacteria with carbon sources [354].

Nitrogenase is highly O_2-sensitive, and organisms have devised various strategies to shield this crucial enzyme. Filamentous cyanobacteria, such as *Anabaena* and *Nostoc*, play a similar role in aquatic and terrestrial environments. They possess specialised heterocysts,

differentiated cells that create the low-oxygen conditions required for nitrogenase activity [355]. These cyanobacteria contribute significantly to nitrogen inputs in rice paddies, wetlands, and marine ecosystems [354]. The role of nitrogen-fixing bacteria is crucial, therefore, in sustainable agriculture [352,353].

Beyond nitrogen fixation, Mo functions as a cofactor in enzymes such as sulfite oxidase, xanthine oxidase, and aldehyde oxidase. These enzymes facilitate key biochemical reactions, including the oxidation of sulfite to sulfate, the degradation of xanthine to uric acid, and the detoxification of aldehydes. Mo also influences the metabolism of sulfur-containing amino acids and plays a regulatory role in protein synthesis, as well as in the metabolism of trace elements, such as phosphorus and copper, underscoring its broader metabolic significance [356,357].

Tungsten, though less common than molybdenum in biology, substitutes for Mo in certain enzymes, particularly in bacteria and archaea adapted to extreme environments [358]. This highlights the versatility of these metals, as tungstopterin-containing enzymes resemble their Mo-dependent counterparts but function more effectively at high temperatures or under strongly reducing conditions. Tungsten's lower and more temperature-sensitive redox potential compared to Mo, a consequence of relativistic effects, particularly in the $+4 \rightleftharpoons +5$ and $+5 \rightleftharpoons +6$ transitions, is likely advantageous to organisms operating in fluctuating thermal environments [40,182].

The ability of Mo and W to adopt high oxidation states (+4 and +6), which are generally inaccessible to first-row d-block metals under normal environmental conditions, is likely a key factor in their biological incorporation. Additionally, their capacity to coordinate a wide range of ligands with S-, N-, and O-donors makes them particularly well suited for catalytic roles [146]. Unlike many iron- and copper-based enzymes, which pose oxidative risks due to the formation of reactive oxygen species (ROS) in side reactions, Mo- and W-containing enzymes operate within tightly controlled redox environments with minimal ROS generation.

Extensive experimental and (more recently) computational investigations have revealed much about the chemistry of the Mo and W enzymes. But much remains to be learned. The mechanisms, for example, of nitrogenase, formate dehydrogenase, and formylmethanofuran dehydrogenase are by no means settled. The transient nature of the intermediates makes direct experimental observations challenging. Perhaps time-resolved cryo-electron microscopy [359] will, in the not-too-distant future, provide greater insights.

The structural similarities between Mo and W enzymes, such as the shared pyranopterin cofactor, suggest a common evolutionary origin. However, their functional diversity is testament to nature's ability to adapt to specific metabolic needs and environmental conditions. Their roles in nitrogen fixation, metabolic redox reactions, and survival in extreme environments underscore the adaptability of life and the selective pressures that have shaped metal utilisation in biological systems.

Funding: This research received no external funding.

Institutional Review Board Statement: Not applicable.

Informed Consent Statement: Not applicable.

Data Availability Statement: No new data were created in this study.

Conflicts of Interest: The author declares no conflicts of interest.

References

1. Marques, H.M. The Bioinorganic Chemistry of the First Row d-Block Metal Ions—An Introduction. *Inorganics* **2025**, *13*, 137. [CrossRef]

2. Soetan, K.O.; Olaiya, C.O.; Oyewole, O.E. The importance of mineral elements for humans, domestic animals and plants: A review. *Afr. J. Food Sci.* **2010**, *4*, 200–222.
3. Yatoo, M.I.; Saxena, A.; Deepa, P.M.; Habeab, B.P.; Devi, S.; Jatav, R.S.; Dimri, U. Role of trace elements in animals: A review. *Vet. World* **2013**, *6*, 963–967. [CrossRef]
4. Andresen, E.; Peiter, E.; Küpper, H. Trace metal metabolism in plants. *J. Exp. Biol.* **2018**, *69*, 909–954. [CrossRef]
5. Moustakas, M. The Role of Metal Ions in Biology, Biochemistry and Medicine. *Materials* **2021**, *14*, 549. [CrossRef]
6. Pajarillo, E.A.B.; Lee, E.; Kang, D.-K. Trace metals and animal health: Interplay of the gut microbiota with iron, manganese, zinc, and copper. *Anim. Nutr.* **2021**, *7*, 750–761. [CrossRef]
7. Wong, C.P.; Magnusson, K.R.; Sharpton, T.J.; Ho, E. Effects of zinc status on age-related T cell dysfunction and chronic inflammation. *BioMetals* **2021**, *34*, 291–301. [CrossRef]
8. Jomova, K.; Makova, M.; Alomar, S.Y.; Alwasel, S.H.; Nepovimova, E.; Kuca, K.; Rhodes, C.J.; Valko, M. Essential metals in health and disease. *Chem.-Biol. Interact.* **2022**, *367*, 110173. [CrossRef]
9. Rozenberg, J.M.; Kamynina, M.; Sorokin, M.; Zolotovskaia, M.; Koroleva, E.; Kremenchutckaya, K.; Gudkov, A.; Buzdin, A.; Borisov, N. The Role of the Metabolism of Zinc and Manganese Ions in Human Cancerogenesis. *Biomedicines* **2022**, *10*, 1072. [CrossRef]
10. Remick, K.A.; Helmann, J.D. The elements of life: A biocentric tour of the periodic table. *Adv. Microb. Physiol.* **2023**, *82*, 1–127. [CrossRef]
11. Verma, S.; Kumar, S.; Sharma, S. Exploring the Importance of Trace Elements in Nutrition: Understanding Their Vital Role in Health and Well-being. *E3S Web Conf.* **2024**, *509*, 03016. [CrossRef]
12. Hille, R. Molybdenum and tungsten in biology. *Trends Biochem. Sci.* **2002**, *27*, 360–367. [CrossRef] [PubMed]
13. Bevers, L.E.; Hagedoorn, P.-L.; Hagen, W.R. The bioinorganic chemistry of tungsten. *Coord. Chem. Rev.* **2009**, *253*, 269–290. [CrossRef]
14. Maia, L.B.; Moura, I.; Moura, J.J.G. Molybdenum and Tungsten-Containing Enzymes: An Overview. In *Molybdenum and Tungsten Enzymes: Biochemistry*; Hille, R., Schulzke, C., Kirk, M.L., Kirk, M.L., Hille, R., Schulzke, C., Eds.; The Royal Society of Chemistry: London, UK, 2016; pp. 1–80.
15. Huang, X.-Y.; Hu, D.-W.; Zhao, F.-J. Molybdenum: More than an essential element. *J. Exp. Biol.* **2021**, *73*, 1766–1774. [CrossRef]
16. Bursakov, S.A.; Kroupin, P.Y.; Karlov, G.I.; Divashuk, M.G. Tracing the Element: The Molecular Bases of Molybdenum Homeostasis in Legumes. *Agronomy* **2023**, *13*, 2300. [CrossRef]
17. Stripp, S.T.; Duffus, B.R.; Fourmond, V.; Léger, C.; Leimkühler, S.; Hirota, S.; Hu, Y.; Jasniewski, A.; Ogata, H.; Ribbe, M.W. Second and Outer Coordination Sphere Effects in Nitrogenase, Hydrogenase, Formate Dehydrogenase, and CO Dehydrogenase. *Chem. Rev.* **2022**, *122*, 11900–11973. [CrossRef]
18. McGarry, J.; Mintmier, B.; Metzger, M.C.; Giri, N.C.; Britt, N.; Basu, P.; Wilcoxen, J. Insights into periplasmic nitrate reductase function under single turnover. *J. Biol. Inorg. Chem.* **2024**, *29*, 811–819. [CrossRef]
19. Zhang, Y.; Sun, H.; Lu, C.; Li, H.; Guo, J. Role of molybdenum compounds in enhancing denitrification: Structure-activity relationship and the regulatory mechanisms. *Chemosphere* **2024**, *367*, 143433. [CrossRef]
20. Giri, N.C.; Mintmier, B.; Radhakrishnan, M.; Mielke, J.W.; Wilcoxen, J.; Basu, P. The critical role of a conserved lysine residue in periplasmic nitrate reductase catalyzed reactions. *J. Biol. Inorg. Chem.* **2024**, *29*, 395–405. [CrossRef]
21. Dash, S.; Pattanayak, S.; Jena, B.; Panda, K.M.; Singh, D.Y. Xanthine Oxidase Perspective in Human Health. *Curr. Biotechnol.* **2020**, *9*, 255–262. [CrossRef]
22. Iksat, N.N.; Zhangazin, S.B.; Madirov, A.A.; Omarov, R.T. Effect of Molybdenum on The Activity of Molybdoenzymes. *Eurasian J. Appl. Biotechnol.* **2020**, 2. [CrossRef]
23. Kirk, M.L.; Hille, R. Spectroscopic Studies of Mononuclear Molybdenum Enzyme Centers. *Molecules* **2022**, *27*, 4802. [CrossRef] [PubMed]
24. Hille, R. Xanthine Oxidase—A Personal History. *Molecules* **2023**, *28*, 1921. [CrossRef] [PubMed]
25. Adamus, J.P.; Ruszczyńska, A.; Wyczałkowska-Tomasik, A. Molybdenum's Role as an Essential Element in Enzymes Catabolizing Redox Reactions: A Review. *Biomolecules* **2024**, *14*, 869. [CrossRef]
26. Garcia, A.K.; McShea, H.; Kolaczkowski, B.; Kaçar, B. Reconstructing the evolutionary history of nitrogenases: Evidence for ancestral molybdenum-cofactor utilization. *Geobiology* **2020**, *18*, 394–411. [CrossRef]
27. Burén, S.; Jiménez-Vicente, E.; Echavarri-Erasun, C.; Rubio, L.M. Biosynthesis of Nitrogenase Cofactors. *Chem. Rev.* **2020**, *120*, 4921–4968. [CrossRef]
28. Watanabe, T.; Horiike, T. The Evolution of Molybdenum Dependent Nitrogenase in Cyanobacteria. *Biology* **2021**, *10*, 329. [CrossRef]
29. Dance, I. The binding of reducible N_2 in the reaction domain of nitrogenase. *Dalton Trans.* **2023**, *52*, 2013–2026. [CrossRef]
30. Threatt, S.D.; Rees, D.C. Biological nitrogen fixation in theory, practice, and reality: A perspective on the molybdenum nitrogenase system. *FEBS Lett.* **2023**, *597*, 45–58. [CrossRef]

31. Einsle, O. On the Shoulders of Giants—Reaching for Nitrogenase. *Molecules* **2023**, *28*, 7959. [CrossRef]
32. Dance, I. The mechanism of Mo-nitrogenase: From N_2 capture to first release of NH_3. *Dalton Trans.* **2024**, *53*, 19360–19377. [CrossRef] [PubMed]
33. Dance, I. What triggers the coupling of proton transfer and electron transfer at the active site of nitrogenase? *Dalton Trans.* **2024**, *53*, 7996–8004. [CrossRef] [PubMed]
34. Sengupta, K.; Joyce, J.P.; Decamps, L.; Kang, L.; Bjornsson, R.; Rüdiger, O.; DeBeer, S. Investigating the Molybdenum Nitrogenase Mechanistic Cycle Using Spectroelectrochemistry. *J. Am. Chem. Soc.* **2025**, *147*, 2099–2114. [CrossRef]
35. Riyaz, Z.; Khan, S.T. Nitrogen fixation by methanogenic Archaea, literature review and DNA database-based analysis; significance in face of climate change. *Arch. Microbiol.* **2024**, *207*, 6. [CrossRef] [PubMed]
36. Pushie, M.J.; Cotelesage, J.J.; George, G.N. Molybdenum and tungsten oxygen transferases- structural and functional diversity within a common active site motif. *Metallomics* **2014**, *6*, 15–24. [CrossRef]
37. Scott, C.; Lyons, T.W.; Bekker, A.; Shen, Y.; Poulton, S.W.; Chu, X.; Anbar, A.D. Tracing the stepwise oxygenation of the Proterozoic ocean. *Nature* **2008**, *452*, 456–459. [CrossRef]
38. Rayner-Canham, G.; Grandy, J. Did molybdenum control evolution on Earth? *Educ. Chem.* **2011**, 144–147. Available online: https://edu.rsc.org/feature/molybdenum-and-evolution/2020196.article (accessed on 19 May 2025).
39. Mendel, R.R.; Bittner, F. Cell biology of molybdenum. *Biochim. Biophys. Acta* **2006**, *1763*, 621–635. [CrossRef]
40. Kletzin, A.; Adams, M.W.W. Tungsten in biological systems. *FEMS Microbiol. Rev.* **1996**, *18*, 5–63. [CrossRef]
41. Tse, C.; Ma, K. Growth and Metabolism of Extremophilic Microorganisms. In *Biotechnology of Extremophiles: Advances and Challenges*; Rampelotto, P.H., Ed.; Springer: Cham, Switzerland, 2016; pp. 1–46.
42. Seelmann, C.S.; Willistein, M.; Heider, J.; Boll, M. Tungstoenzymes: Occurrence, Catalytic Diversity and Cofactor Synthesis. *Inorganics* **2020**, *8*, 44. [CrossRef]
43. Buessecker, S.; Palmer, M.; Lai, D.; Dimapilis, J.; Mayali, X.; Mosier, D.; Jiao, J.-Y.; Colman, D.R.; Keller, L.M.; St. John, E.; et al. An essential role for tungsten in the ecology and evolution of a previously uncultivated lineage of anaerobic, thermophilic Archaea. *Nat. Commun.* **2022**, *13*, 3773. [CrossRef]
44. Gutiérrez-Preciado, A.; Dede, B.; Baker, B.A.; Eme, L.; Moreira, D.; López-García, P. Extremely acidic proteomes and metabolic flexibility in bacteria and highly diversified archaea thriving in geothermal chaotropic brines. *Nat. Ecol. Evol.* **2024**, *8*, 1856–1869. [CrossRef] [PubMed]
45. Valdez, S.; de la Vega, F.V.; Pairazaman, O.; Castellanos, R.; Esparza, M. Hyperthermophile diversity microbes in the Calientes geothermal field, Tacna, Peru. *Braz. J. Microbiol.* **2023**, *54*, 2927–2937. [CrossRef]
46. Das, U.; Das, A.; Das, A.K. Relativistic effect behind the molybdenum vs. tungsten selectivity in enzymes. *Dalton Trans.* **2025**, *54*, 8728–8744. [CrossRef] [PubMed]
47. Hagen, W.R. The Development of Tungsten Biochemistry—A Personal Recollection. *Molecules* **2023**, *28*, 4017. [CrossRef] [PubMed]
48. Das, U.; Das, A.; Das, A.K. Exploring the nature's discriminating factors behind the selection of molybdoenzymes and tungstoenzymes depending on the biological environment. *Coord. Chem. Rev.* **2025**, *523*, 216290. [CrossRef]
49. Laukel, M.; Chistoserdova, L.; Lidstrom, M.E.; Vorholt, J.A. The tungsten-containing formate dehydrogenase from *Methylobacterium extorquens AM1*: Purification and properties. *Eur. J. Biochem.* **2003**, *270*, 325–333. [CrossRef]
50. Rosenbaum, F.P.; Müller, V. *Moorella thermoacetica*: A promising cytochrome- and quinone-containing acetogenic bacterium as platform for a CO_2-based bioeconomy. *Green Carbon* **2023**, *1*, 2–13. [CrossRef]
51. Boes, D.M.; Schmitz, R.A.; Hagedoorn, P.L. Tungsten containing aldehyde oxidoreductase (AOR)-family enzymes; past, present and future production strategies. *Methods Enzymol.* **2025**, *714*, 313–336. [CrossRef]
52. Putumbaka, S.; Schut, G.J.; Thorgersen, M.P.; Poole, F.L.; Shao, N.; Rodionov, D.A.; Adams, M.W.W. Tungsten is utilized for lactate consumption and SCFA production by a dominant human gut microbe Eubacterium limosum. *Proc. Natl. Acad. Sci. USA* **2025**, *122*, e2411809121. [CrossRef]
53. Williams, R.J.P.; Fraústo da Silva, J.J.R. The Involvement of Molybdenum in Life. *Biochem. Biophys. Res. Commun.* **2002**, *292*, 293–299. [CrossRef]
54. Reimink, J.R.; Mundl-Petermeier, A.; Carlson, R.W.; Shirey, S.B.; Walker, R.J.; Pearson, D.G. Tungsten Isotope Composition of Archean Crustal Reservoirs and Implications for Terrestrial μ182W Evolution. *Geochem. Geophys. Geosys.* **2020**, *21*, e2020GC009155. [CrossRef]
55. Kleine, T.; Walker, R.J. Tungsten Isotopes in Planets. *Ann. Rev. Earth Planet. Sci.* **2017**, *45*, 389–417. [CrossRef]
56. Jelikić-Stankov, M.; Uskoković-Marković, S.; Holclajtner-Antunović, I.; Todorović, M.; Djurdjević, P. Compounds of Mo, V and W in biochemistry and their biomedical activity. *J. Trace Elem. Med. Biol.* **2007**, *21*, 8–16. [CrossRef]
57. Amaral, L.M.P.F.; Moniz, T.; Silva, A.M.N.; Rangel, M. Vanadium Compounds with Antidiabetic Potential. *Int. J. Molec. Sci.* **2023**, *24*, 15675. [CrossRef]
58. Dayanand, Y.; Pather, R.; Xulu, N.; Booysen, I.; Sibiya, N.; Khathi, A.; Ngubane, P. Exploring the Biological Effects of Anti-Diabetic Vanadium Compounds in the Liver, Heart and Brain. *Diabetes Metab. Syndr. Obes.* **2024**, *17*, 3267–3278. [CrossRef]

59. Fuchs, V.; Cseh, K.; Hejl, M.; Vician, P.; Neuditschko, B.; Meier-Menches, S.M.; Janker, L.; Bileck, A.; Gajic, N.; Kronberger, J.; et al. Highly Cytotoxic Molybdenocenes with Strong Metabolic Effects Inhibit Tumour Growth in Mice. *Chem. Eur. J.* **2023**, *29*, e202202648. [CrossRef]
60. Yamase, T. Polyoxometalates for Molecular Devices: Antitumor Activity and Luminescence. In *Polyoxometalates: From Platonic Solids to Anti-Retroviral Activity*; Pope, M.T., Müller, A., Eds.; Springer: Dordrecht, The Netherlands, 1994; pp. 337–358.
61. Kostova, I. Anticancer Metallocenes and Metal Complexes of Transition Elements from Groups 4 to 7. *Molecules* **2024**, *29*, 824. [CrossRef]
62. Alterio, V.; Langella, E.; De Simone, G.; Monti, S.M. Cadmium-Containing Carbonic Anhydrase CDCA1 in Marine Diatom Thalassiosira weissflogii. *Mar. Drugs* **2015**, *13*, 1688–1697. [CrossRef]
63. Boschi, A.; Uccelli, L.; Marvelli, L.; Cittanti, C.; Giganti, M.; Martini, P. Technetium-99m Radiopharmaceuticals for Ideal Myocardial Perfusion Imaging: Lost and Found Opportunities. *Molecules* **2022**, *27*, 1188. [CrossRef]
64. Tahara, N.; Lairez, O.; Endo, J.; Okada, A.; Ueda, M.; Ishii, T.; Kitano, Y.; Lee, H.E.; Russo, E.; Kubo, T. (99m) Technetium-pyrophosphate scintigraphy: A practical guide for early diagnosis of transthyretin amyloid cardiomyopathy. *ESC Heart Fail.* **2022**, *9*, 251–262. [CrossRef] [PubMed]
65. Papagiannopoulou, D. Technetium-99m radiochemistry for pharmaceutical applications. *J. Label. Comp. Radiopharm.* **2017**, *60*, 502–520. [CrossRef] [PubMed]
66. Zhang, C.; Xu, C.; Gao, X.; Yao, Q. Platinum-based drugs for cancer therapy and anti-tumor strategies. *Theranostics* **2022**, *12*, 2115–2132. [CrossRef]
67. Dasari, S.; Tchounwou, P.B. Cisplatin in cancer therapy: Molecular mechanisms of action. *Eur. J. Pharmacol.* **2014**, *740*, 364–378. [CrossRef]
68. Lee, S.Y.; Kim, C.Y.; Nam, T.G. Ruthenium Complexes as Anticancer Agents: A Brief History and Perspectives. *Drug Des. Dev. Ther.* **2020**, *14*, 5375–5392. [CrossRef]
69. Gama Justi, F.V.; Araújo Matos, G.; de Sá Roriz Caminha, J.; Rodrigues Roque, C.; Muniz Carvalho, E.; Soares Campelo, M.W.; Belayev, L.; Gonzaga de França Lopes, L.; Barreto Oriá, R. The Role of Ruthenium Compounds in Neurologic Diseases: A Minireview. *J. Pharm. Exp. Ther.* **2022**, *380*, 47–53. [CrossRef]
70. Aguilar-Garay, R.; Lara-Ortiz, L.F.; Campos-López, M.; Gonzalez-Rodriguez, D.E.; Gamboa-Lugo, M.M.; Mendoza-Pérez, J.A.; Anzueto-Ríos, Á.; Nicolás-Álvarez, D.E. A Comprehensive Review of Silver and Gold Nanoparticles as Effective Antibacterial Agents. *Pharmaceuticals* **2024**, *17*, 1134. [CrossRef]
71. Malik, M.A.; Hashmi, A.A.; Al-Bogami, A.S.; Wani, M.Y. Harnessing the power of gold: Advancements in anticancer gold complexes and their functionalized nanoparticles. *J. Mater. Chem. B* **2024**, *12*, 552–576. [CrossRef]
72. van der Westhuizen, D.; Bezuidenhout, D.I.; Munro, O.Q. Cancer molecular biology and strategies for the design of cytotoxic gold(i) and gold(iii) complexes: A tutorial review. *Dalton Trans.* **2021**, *50*, 17413–17437. [CrossRef]
73. Shukla, S.; Mishra, A.P. Synthesis, Structure, and Anticancerous Properties of Silver Complexes. *J. Chem.* **2013**, *2013*, 527123. [CrossRef]
74. Czarnomysy, R.; Radomska, D.; Szewczyk, O.K.; Roszczenko, P.; Bielawski, K. Platinum and Palladium Complexes as Promising Sources for Antitumor Treatments. *Int. J. Mol. Sci.* **2021**, *22*, 8271. [CrossRef] [PubMed]
75. Nabiyeva, T.; Marschner, C.; Blom, B. Synthesis, structure and anti-cancer activity of osmium complexes bearing π-bound arene substituents and phosphane Co-Ligands: A review. *Eur. J. Med. Chem.* **2020**, *201*, 112483. [CrossRef] [PubMed]
76. Matlou, M.L.; Louis, H.; Charlie, D.E.; Agwamba, E.C.; Amodu, I.O.; Tembu, V.J.; Manicum, A.-L.E. Anticancer Activities of Re(I) Tricarbonyl and Its Imidazole-Based Ligands: Insight from a Theoretical Approach. *ACS Omega* **2023**, *8*, 10242–10252. [CrossRef] [PubMed]
77. Hong Enriquez, R.P.; Do, T.N. Bioavailability of Metal Ions and Evolutionary Adaptation. *Life* **2012**, *2*, 274–285. [CrossRef]
78. Haynes, W.M. (Ed.) *CRC Handbook of Chemistry and Physics*, 97th ed.; CRC Press: Boca Raton, FL, USA, 2016.
79. Burgmayer, S.J.N.; Stiefel, E.I. Molybdenum enzymes, cofactors, and systems: The chemical uniqueness of molybdenum. *J. Chem. Ed.* **1985**, *62*, 943. [CrossRef]
80. Leimkühler, S. Molybdenum and Ions in Living Systems. In *Encyclopedia of Metalloproteins*; Kretsinger, R.H., Uversky, V.N., Permyakov, E.A., Eds.; Springer: New York, NY, USA, 2013; pp. 1420–1429.
81. Basolo, F.; Pearson, R.G. *Mechanisms of Inorganic Reactions*; Wiley: New York, NY, USA, 1967.
82. Bohme, D.K. Toward ICP-SIFT mass spectrometry and atomic cation ligation as a probe of relativistic effects—A personal journey. *Mass Spectrom. Rev.* **2022**, *41*, 593–605. [CrossRef]
83. Helm, L.; Merbach, A.E. Inorganic and Bioinorganic Solvent Exchange Mechanisms. *Chem. Rev.* **2005**, *105*, 1923–1960. [CrossRef]
84. van Eldik, R. Introduction: Inorganic and Bioinorganic Mechanisms. *Chem. Rev.* **2005**, *105*, 1917–1922. [CrossRef]
85. Richens, D.T. Ligand Substitution Reactions at Inorganic Centers. *Chem. Rev.* **2005**, *105*, 1961–2002. [CrossRef]
86. Kisker, C.; Schindelin, H.; Rees, D.C. Molybdenium-factor-containing enzymes: Structure and Mechanism. *Ann. Rev. Biochem.* **1997**, *66*, 233–267. [CrossRef]

87. Rothery, R.A.; Stein, B.; Solomonson, M.; Kirk, M.L.; Weiner, J.H. Pyranopterin conformation defines the function of molybdenum and tungsten enzymes. *Proc. Natl. Acad. Sci. USA* **2012**, *109*, 14773–14778. [CrossRef] [PubMed]
88. Varadwaj, P.R.; Marques, H.M.; Grabowski, I. Ammonia Synthesis over Transition Metal Catalysts: Reaction Mechanisms, Rate-Determining Steps, and Challenges. *Int. J. Mol. Sci.* **2025**, *26*, 4670. [CrossRef] [PubMed]
89. Beller, M. Introduction: First Row Metals and Catalysis. *Chem. Rev.* **2019**, *119*, 2089. [CrossRef] [PubMed]
90. Kirk, M.L.; Stein, B. Molybdenum Enzymes. In *Comprehensive Inorganic Chemistry II*, 2nd ed.; Reedijk, J., Poeppelmeier, K., Eds.; Elsevier: Amsterdam, The Netherlands, 2013; pp. 263–293.
91. Zhang, L.-H.; Mathew, S.; Hessels, J.; Reek, J.N.H.; Yu, F. Homogeneous Catalysts Based on First-Row Transition-Metals for Electrochemical Water Oxidation. *ChemSusChem* **2021**, *14*, 234–250. [CrossRef]
92. Glaser, F.; Wenger, O.S. Recent progress in the development of transition-metal based photoredox catalysts. *Coord. Chem. Rev.* **2020**, *405*, 213129. [CrossRef]
93. Wiebelhaus, N.J.; Cranswick, M.A.; Klein, E.L.; Lockett, L.T.; Lichtenberger, D.L.; Enemark, J.H. Metal–Sulfur Valence Orbital Interaction Energies in Metal–Dithiolene Complexes: Determination of Charge and Overlap Interaction Energies by Comparison of Core and Valence Ionization Energy Shifts. *Inorg. Chem.* **2011**, *50*, 11021–11031. [CrossRef]
94. Yang, J.; Enemark, J.H.; Kirk, M.L. Metal–Dithiolene Bonding Contributions to Pyranopterin Molybdenum Enzyme Reactivity. *Inorganics* **2020**, *8*, 19. [CrossRef]
95. Ryde, U.; Schulzke, C.; Starke, K. Which functional groups of the molybdopterin ligand should be considered when modeling the active sites of the molybdenum and tungsten cofactors? A density functional theory study. *J. Biol. Inorg. Chem.* **2009**, *14*, 1053–1064. [CrossRef]
96. Thorpe, G.W.; Reodica, M.; Davies, M.J.; Heeren, G.; Jarolim, S.; Pillay, B.; Breitenbach, M.; Higgins, V.J.; Dawes, I.W. Superoxide radicals have a protective role during H_2O_2 stress. *Molec. Biol. Cell* **2013**, *24*, 2876–2884. [CrossRef]
97. D'Autréaux, B.; Toledano, M.B. ROS as signalling molecules: Mechanisms that generate specificity in ROS homeostasis. *Nat. Rev. Molec. Cell Biol.* **2007**, *8*, 813–824. [CrossRef]
98. Shekhova, E. Mitochondrial reactive oxygen species as major effectors of antimicrobial immunity. *PLoS Pathog.* **2020**, *16*, e1008470. [CrossRef] [PubMed]
99. Paiva, C.N.; Bozza, M.T. Are reactive oxygen species always detrimental to pathogens? *Antioxid.Redox Signal.* **2014**, *20*, 1000–1037. [CrossRef] [PubMed]
100. Li, H.; Zhou, X.; Huang, Y.; Liao, B.; Cheng, L.; Ren, B. Reactive Oxygen Species in Pathogen Clearance: The Killing Mechanisms, the Adaption Response, and the Side Effects. *Front. Microbiol.* **2021**, *11*, 622534. [CrossRef] [PubMed]
101. Hansel, C.M.; Diaz, J.M.; Plummer, S. Tight Regulation of Extracellular Superoxide Points to Its Vital Role in the Physiology of the Globally Relevant *Roseobacter* Clade. *mBio* **2019**, *10*, e02668-18. [CrossRef]
102. Marques, H.M. Electron transfer in biological systems. *J. Biol. Inorg. Chem.* **2024**, *29*, 641–683. [CrossRef]
103. Hayyan, M.; Hashim, M.A.; AlNashef, I.M. Superoxide Ion: Generation and Chemical Implications. *Chem. Rev.* **2016**, *116*, 3029–3085. [CrossRef]
104. Jang, S.; Imlay, J.A. Micromolar Intracellular Hydrogen Peroxide Disrupts Metabolism by Damaging Iron-Sulfur Enzymes. *J. Biol. Chem.* **2007**, *282*, 929–937. [CrossRef]
105. Niks, D.; Hille, R. Molybdenum-Containing Enzymes. In *Metalloproteins: Methods and Protocols*; Hu, Y., Ed.; Springer: New York, NY, USA, 2019; pp. 55–63.
106. Fernandes, H.S.; Teixeira, C.S.S.; Sousa, S.F.; Cerqueira, N.M.F.S.A. Formation of Unstable and very Reactive Chemical Species Catalyzed by Metalloenzymes: A Mechanistic Overview. *Molecules* **2019**, *24*, 2462. [CrossRef]
107. Watson, M.P.; Weix, D.J. The Once and Future Catalysts: How the Challenges of First-Row Transition-Metal Catalysis Grew to Become Strengths. *Acc. Chem. Res.* **2024**, *57*, 2451–2452. [CrossRef]
108. Boniolo, M.; Chernev, P.; Cheah, M.H.; Heizmann, P.A.; Huang, P.; Shylin, S.I.; Salhi, N.; Hossain, M.K.; Gupta, A.K.; Messinger, J.; et al. Electronic and geometric structure effects on one-electron oxidation of first-row transition metals in the same ligand framework. *Dalton Trans.* **2021**, *50*, 660–674. [CrossRef]
109. Enemark, J.H. $[Moco]^n$, (n = 0–8): A general formalism for describing the highly covalent molybdenum cofactor of sulfite oxidase and related Mo enzymes. *J. Inorg. Biochem.* **2022**, *231*, 111801. [CrossRef] [PubMed]
110. Lake, M.W.; Temple, C.A.; Rajagopalan, K.V.; Schindelin, H. The Crystal Structure of the *Escherichia coli*MobA Protein Provides Insight into Molybdopterin Guanine Dinucleotide Biosynthesis. *J. Biol. Chem.* **2000**, *275*, 40211–40217. [CrossRef] [PubMed]
111. Spatzal, T.; Perez, K.A.; Howard, J.B.; Rees, D.C. Catalysis-dependent selenium incorporation and migration in the nitrogenase active site iron-molybdenum cofactor. *eLife* **2015**, *4*, e11620. [CrossRef] [PubMed]
112. Hille, R. The Mononuclear Molybdenum Enzymes. *Chem. Rev.* **1996**, *96*, 2757–2816. [CrossRef]
113. Hille, R.; Nishino, T.; Bittner, F. Molybdenum enzymes in higher organisms. *Coord. Chem. Rev.* **2011**, *255*, 1179–1205. [CrossRef]
114. Rees, D.C. Great Metalloclusters in Enzymology. *Ann. Rev. Biochem.* **2002**, *71*, 221–246. [CrossRef]

115. Zimmermann, R.; Münck, E.; Brill, W.J.; Shah, V.K.; Henzl, M.T.; Rawlings, J.; Orme-Johnson, W.H. Nitrogenase X: Mössbauer and EPR studies on reversibly oxidized MoFe protein from Azotobacter vinelandii OP Nature of the iron centers. *Biochim. Biophs. Acta* **1978**, *537*, 185–207. [CrossRef]
116. Bjornsson, R.; Lima, F.A.; Spatzal, T.; Weyhermüller, T.; Glatzel, P.; Bill, E.; Einsle, O.; Neese, F.; DeBeer, S. Identification of a spin-coupled Mo(III) in the nitrogenase iron–molybdenum cofactor. *Chem. Sci.* **2014**, *5*, 3096–3103. [CrossRef]
117. Bjornsson, R.; Neese, F.; Schrock, R.R.; Einsle, O.; DeBeer, S. The discovery of Mo(III) in FeMoco: Reuniting enzyme and model chemistry. *J. Biol. Inorg. Chem.* **2015**, *20*, 447–460. [CrossRef]
118. Dance, I. Computational Investigations of the Chemical Mechanism of the Enzyme Nitrogenase. *ChemBioChem* **2020**, *21*, 1671–1709. [CrossRef]
119. Maiti, B.K.; Maia, L.B.; Moura, J.J.G. Sulfide and transition metals—A partnership for life. *J. Inorg. Biochem.* **2022**, *227*, 111687. [CrossRef] [PubMed]
120. Clement, B.; Struwe, M.A. The History of mARC. *Molecules* **2023**, *28*, 4713. [CrossRef] [PubMed]
121. Terao, M.; Romão, M.J.; Leimkühler, S.; Bolis, M.; Fratelli, M.; Coelho, C.; Santos-Silva, T.; Garattini, E. Structure and function of mammalian aldehyde oxidases. *Arch. Toxicol.* **2016**, *90*, 753–780. [CrossRef] [PubMed]
122. Hutzler, J.M.; Obach, R.S.; Dalvie, D.; Zientek, M.A. Strategies for a comprehensive understanding of metabolism by aldehyde oxidase. *Expert Opin. Drug Metab. Toxicol.* **2013**, *9*, 153–168. [CrossRef]
123. Garattini, E.; Fratelli, M.; Terao, M. Mammalian aldehyde oxidases: Genetics, evolution and biochemistry. *Cell Mol. Life Sci.* **2008**, *65*, 1019–1048. [CrossRef]
124. Terao, M.; Garattini, E.; Romão, M.J.; Leimkühler, S. Evolution, expression, and substrate specificities of aldehyde oxidase enzymes in eukaryotes. *J. Biol. Chem.* **2020**, *295*, 5377–5389. [CrossRef]
125. Beedham, C. Aldehyde oxidase; new approaches to old problems. *Xenobiotica* **2020**, *50*, 34–50. [CrossRef]
126. Mendel, R.R.; Schwarz, G. The History of Animal and Plant Sulfite Oxidase—A Personal View. *Molecules* **2023**, *28*, 6998. [CrossRef]
127. Feng, C.; Tollin, G.; Enemark, J.H. Sulfite oxidizing enzymes. *Biochim. Biophs. Acta* **2007**, *1774*, 527–539. [CrossRef]
128. Kappler, U.; Enemark, J.H. Sulfite-oxidizing enzymes. *J. Biol. Inorg. Chem.* **2015**, *20*, 253–264. [CrossRef]
129. Hänsch, R.; Lang, C.; Rennenberg, H.; Mendel, R.R. Significance of Plant Sulfite Oxidase. *Plant Biol.* **2007**, *9*, 589–595. [CrossRef]
130. Schwahn, B.C.; van Spronsen, F.; Misko, A.; Pavaine, J.; Holmes, V.; Spiegel, R.; Schwarz, G.; Wong, F.; Horman, A.; Pitt, J.; et al. Consensus guidelines for the diagnosis and management of isolated sulfite oxidase deficiency and molybdenum cofactor deficiencies. *J. Inherit. Metab. Dis.* **2024**, *47*, 598–623. [CrossRef] [PubMed]
131. Kappler, U. Bacterial sulfite-oxidizing enzymes. *Biochim. Biophys. Acta* **2011**, *1807*, 1–10. [CrossRef]
132. Sun, Z.; Zhang, X.; Zhao, Z.; Li, X.; Pang, J.; Chen, J. Recent Progress and Future Perspectives on Anti-Hyperuricemic Agents. *J. Med. Chem.* **2024**, *67*, 19966–19987. [CrossRef]
133. Souza, C.F.; Baldissera, M.D.; Moreira, K.L.S.; da Rocha, M.I.U.M.; da Veiga, M.L.; Santos, R.C.V.; Baldisserotto, B. Involvement of xanthine oxidase activity with oxidative and inflammatory renal damage in silver catfish experimentally infected with *Streptococcus agalactiae*: Interplay with reactive oxygen species and nitric oxide. *Micro. Patho.* **2017**, *111*, 1–5. [CrossRef]
134. Justi, L.H.Z.; Silva, J.F.; Santana, M.S.; Laureano, H.A.; Pereira, M.E.; Oliveira, C.S.; Guiloski, I.C. Non-steroidal anti-inflammatory drugs and oxidative stress biomarkers in fish: A meta-analytic review. *Toxicol. Rep.* **2025**, *14*, 101910. [CrossRef] [PubMed]
135. Klein, J.M.; Busch, J.D.; Potting, C.; Baker, M.J.; Langer, T.; Schwarz, G. The Mitochondrial Amidoxime-reducing Component (mARC1) Is a Novel Signal-anchored Protein of the Outer Mitochondrial Membrane *. *J. Biol. Chem.* **2012**, *287*, 42795–42803. [CrossRef] [PubMed]
136. Struwe, M.A.; Scheidig, A.J.; Clement, B. The mitochondrial amidoxime reducing component-from prodrug-activation mechanism to drug-metabolizing enzyme and onward to drug target. *J. Biol. Chem.* **2023**, *299*, 105306. [CrossRef]
137. Miralles-Robledillo, J.M.; Torregrosa-Crespo, J.; Martínez-Espinosa, R.M.; Pire, C. DMSO Reductase Family: Phylogenetics and Applications of Extremophiles. *Int. J. Mol. Sci.* **2019**, *20*, 3349. [CrossRef]
138. Calzadiaz-Ramirez, L.; Meyer, A.S. Formate dehydrogenases for CO_2 utilization. *Curr. Opin. Biotechnol.* **2022**, *73*, 95–100. [CrossRef]
139. Le, C.C.; Bae, M.; Kiamehr, S.; Balskus, E.P. Emerging Chemical Diversity and Potential Applications of Enzymes in the DMSO Reductase Superfamily. *Annu. Rev. Biochem.* **2022**, *91*, 475–504. [CrossRef] [PubMed]
140. Berger, A.; Boscari, A.; Puppo, A.; Brouquisse, R. Nitrate reductases and hemoglobins control nitrogen-fixing symbiosis by regulating nitric oxide accumulation. *J. Exp. Biol.* **2020**, *72*, 873–884. [CrossRef] [PubMed]
141. Liu, H.; Huang, Y.; Huang, M.; Wang, M.; Ming, Y.; Chen, W.; Chen, Y.; Tang, Z.; Jia, B. From nitrate to NO: Potential effects of nitrate-reducing bacteria on systemic health and disease. *Eur. J. Med. Res.* **2023**, *28*, 425. [CrossRef] [PubMed]
142. Besson, S.; Almeida, M.G.; Silveira, C.M. Nitrite reduction in bacteria: A comprehensive view of nitrite reductases. *Coord. Chem. Rev.* **2022**, *464*, 214560. [CrossRef]
143. Campbell, W.H. Nitrate Reductase Structure, Function and Regulation:: Bridging the Gap between Biochemistry and Physiology. *Annu. Rev. Plant Physio.L Plant Mol. Biol.* **1999**, *50*, 277–303. [CrossRef]

144. Fischer, K.; Barbier, G.G.; Hecht, H.-J.; Mendel, R.R.; Campbell, W.H.; Schwarz, G. Structural Basis of Eukaryotic Nitrate Reduction: Crystal Structures of the Nitrate Reductase Active Site. *Plant Cell* **2005**, *17*, 1167–1179. [CrossRef]
145. Jeoung, J.-H.; Martins, B.M.; Dobbek, H. Carbon Monoxide Dehydrogenases. In *Metalloproteins: Methods and Protocols*; Hu, Y., Ed.; Springer: New York, NY, USA, 2019; pp. 37–54.
146. Schwarz, G.; Mendel, R.R.; Ribbe, M.W. Molybdenum cofactors, enzymes and pathways. *Nature* **2009**, *460*, 839–847. [CrossRef]
147. Llamas, A.; Tejada-Jiménez, M.; Fernández, E.; Galván, A. Molybdenum metabolism in the alga Chlamydomonas stands at the crossroad of those in Arabidopsis and humans. *Metallomics* **2011**, *3*, 578–590. [CrossRef]
148. Mendel, R.R. Cell biology of molybdenum in plants. *Plant Cell Rep.* **2011**, *30*, 1787–1797. [CrossRef]
149. Mendel, R.R.; Schwarz, G. Molybdenum cofactor biosynthesis in plants and humans. *Coord. Chem. Rev.* **2011**, *255*, 1145–1158. [CrossRef]
150. Mendel, R.R.; Kruse, T. Cell biology of molybdenum in plants and humans. *Biochim. Biophys. Acta* **2012**, *1823*, 1568–1579. [CrossRef]
151. Weber, J.N.; Minner-Meinen, R.; Kaufholdt, D. The Mechanisms of Molybdate Distribution and Homeostasis with Special Focus on the Model Plant Arabidopsis thaliana. *Molecules* **2023**, *29*, 40. [CrossRef]
152. Mendel, R.R. The Molybdenum Cofactor. *J. Biol. Chem.* **2013**, *288*, 13165–13172. [CrossRef] [PubMed]
153. Sickerman, N.S.; Rettberg, L.A.; Lee, C.C.; Hu, Y.; Ribbe, M.W. Cluster assembly in nitrogenase. *Essays Biochem.* **2017**, *61*, 271–279. [CrossRef] [PubMed]
154. Institute of Medicine (US) Panel on Micronutrients. *Dietary Reference Intakes for Vitamin A, Vitamin K, Arsenic, Boron, Chromium, Copper, Iodine, Iron, Manganese, Molybdenum, Nickel, Silicon, Vanadium, and Zinc*; National Academic Press: Washington, DC, USA, 2001.
155. Winston, P.W. 8—Molybdenum. In *Disorders of Mineral Metabolism*; Bronner, F., Coburn, J.W., Eds.; Academic Press: New York, NY, USA, 1981; pp. 295–315.
156. Claerhout, H.; Witters, P.; Régal, L.; Jansen, K.; Van Hoestenberghe, M.-R.; Breckpot, J.; Vermeersch, P. Isolated sulfite oxidase deficiency. *J. Inherit. Metabol. Dis.* **2018**, *41*, 101–108. [CrossRef] [PubMed]
157. Lee, E.J.; Dandamudi, R.; Granadillo, J.L.; Grange, D.K.; Kakajiwala, A. Rare cause of xanthinuria: A pediatric case of molybdenum cofactor deficiency B. *CEN Case Rep.* **2021**, *10*, 378–382. [CrossRef]
158. Endres, W.; Shin, Y.S.; Günther, R.; Ibel, H.; Duran, M.; Wadman, S.K. Report on a new patient with combined deficiencies of sulphite oxidase and xanthine dehydrogenase due to molybdenum cofactor deficiency. *Eur. J. Pediatr.* **1988**, *148*, 246–249. [CrossRef]
159. Stiburkova, B.; Pavelcova, K.; Petru, L.; Krijt, J. Thiopurine-induced toxicity is associated with dysfunction variant of the human molybdenum cofactor sulfurase gene (xanthinuria type II). *Toxicol. Appl. Pharmacol.* **2018**, *353*, 102–108. [CrossRef]
160. Dror, Y.; Stern, F. Molybdenum. In *Trace Elements and Minerals in Health and Longevity*; Malavolta, M., Mocchegiani, E., Eds.; Springer: Cham, Switzerland, 2018; pp. 179–207.
161. Haywood, S.; Dincer, Z.; Holding, J.; Parry, N.M. Metal (molybdenum, copper) accumulation and retention in brain, pituitary and other organs of ammonium tetrathiomolybdate-treated sheep. *Br. J. Nutr.* **1998**, *79*, 329–331. [CrossRef]
162. Brewer, G.J.; Hedera, P.; Kluin, K.J.; Carlson, M.; Askari, F.; Dick, R.B.; Sitterly, J.; Fink, J.K. Treatment of Wilson Disease With Ammonium Tetrathiomolybdate: III. Initial Therapy in a Total of 55 Neurologically Affected Patients and Follow-up With Zinc Therapy. *Arch. Neurol.* **2003**, *60*, 379–385. [CrossRef]
163. Odularu, A.T.; Ajibade, P.A.; Mbese, J.Z. Impact of Molybdenum Compounds as Anticancer Agents. *Bioinorg. Chem. Appl.* **2019**, *2019*, 6416198. [CrossRef] [PubMed]
164. Yamase, T. Polyoxometalates Active Against Tumors, Viruses, and Bacteria. In *Biomedical Inorganic Polymers: Bioactivity and Applications of Natural and Synthetic Polymeric Inorganic Molecules*; Müller, W.E.G., Wang, X., Schröder, H.C., Eds.; Springer: Berlin/Heidelberg, Germany, 2013; pp. 65–116.
165. Amend, J.P.; Shock, E.L. Energetics of overall metabolic reactions of thermophilic and hyperthermophilic Archaea and Bacteria. *FEMS Microbiol. Rev.* **2001**, *25*, 175–243. [CrossRef] [PubMed]
166. Makdessi, K.; Andreesen, J.R.; Pich, A. Tungstate Uptake by a highly specific ABC transporter in Eubacterium acidaminophilum. *J. Biol. Chem.* **2001**, *276*, 24557–24564. [CrossRef] [PubMed]
167. Bevers, L.E.; Hagedoorn, P.L.; Krijger, G.C.; Hagen, W.R. Tungsten transport protein A (WtpA) in Pyrococcus furiosus: The first member of a new class of tungstate and molybdate transporters. *J. Bacteriol.* **2006**, *188*, 6498–6505. [CrossRef]
168. Andreesen, J.R.; Makdessi, K. Tungsten, the surprisingly positively acting heavy metal element for prokaryotes. *Ann. N. Y. Acad. Sci.* **2008**, *1125*, 215–229. [CrossRef]
169. Bevers, L.E.; Schwarz, G.; Hagen, W.R. A Molecular Basis for Tungstate Selectivity in Prokaryotic ABC Transport Systems. *J. Bacteriol.* **2011**, *193*, 4999–5001. [CrossRef]
170. Milojevic, T. Microbial Tungsten Assimilation. In *Microbial Metabolism of Metals and Metalloids*; Hurst, C.J., Ed.; Springer: Cham, Switzerland, 2022; pp. 545–561.

171. Bolt, A.M.; Mann, K.K. Tungsten: An Emerging Toxicant, Alone or in Combination. *Curr. Environ. Health Rep.* **2016**, *3*, 405–415. [CrossRef]
172. Maia, L.B.; Moura, J.J.G.; Moura, I. Molybdenum and tungsten-dependent formate dehydrogenases. *J. Biol. Inorg. Chem.* **2015**, *20*, 287–309. [CrossRef]
173. Nissen, L.S.; Basen, M. The emerging role of aldehyde:ferredoxin oxidoreductases in microbially-catalyzed alcohol production. *J. Biotechnol.* **2019**, *306*, 105–117. [CrossRef]
174. Nissen, L.S.; Moon, J.; Hitschler, L.; Basen, M. A Versatile Aldehyde: Ferredoxin Oxidoreductase from the Organic Acid Reducing Thermoanaerobacter sp. Strain X514. *Int. J. Mol. Sci.* **2024**, *25*, 1077. [CrossRef]
175. Karrasch, M.; Börner, G.; Enßle, M.; Thauer, R.K. Formylmethanofuran dehydrogenase from methanogenic bacteria, a molybdoenzyme. *FEBS Lett.* **1989**, *253*, 226–230. [CrossRef] [PubMed]
176. Bertram, P.A.; Karrasch, M.; Schmitz, R.A.; Bocher, R.; Albracht, S.P.J.; Thauer, R.K. Formylmethanofuran dehydrogenases from methanogenic Archaea Substrate specificity, EPR properties and reversible inactivation by cyanide of the molybdenum or tungsten iron-sulfur proteins. *Eur. J. Biochem.* **1994**, *220*, 477–484. [CrossRef]
177. Schwörer, B.; Thauer, R.K. Activities of formylmethanofuran dehydrogenase, methylenetetrahydromethanopterin dehydrogenase, methylenetetrahydromethanopterin reductase, and heterodisulfide reductase in methanogenic bacteria. *Arch. Microbiol.* **1991**, *155*, 459–465. [CrossRef]
178. Meckenstock, R.U.; Krieger, R.; Ensign, S.; Kroneck, P.M.H.; Schink, B. Acetylene hydratase of *Pelobacter acetylenicus*. *Eur. J. Biochem.* **1999**, *264*, 176–182. [CrossRef] [PubMed]
179. Liao, R.-Z.; Yu, J.-G.; Himo, F. Mechanism of tungsten-dependent acetylene hydratase from quantum chemical calculations. *Proc. Natl. Acad. Sci. USA* **2010**, *107*, 22523–22527. [CrossRef]
180. Kroneck, P.M.H. Acetylene hydratase: A non-redox enzyme with tungsten and iron–sulfur centers at the active site. *J. Biol. Inorg. Chem.* **2016**, *21*, 29–38. [CrossRef]
181. Cordas, C.M.; Moura, J.J.G. Molybdenum and tungsten enzymes redox properties—A brief overview. *Coord. Chem. Rev.* **2019**, *394*, 53–64. [CrossRef]
182. Döring, A.; Schulzke, C. Tungsten's redox potential is more temperature sensitive than that of molybdenum. *Dalton Trans.* **2010**, *39*, 5623–5629. [CrossRef]
183. Buc, J.; Santini, C.-L.; Giordani, R.; Czjzek, M.; Wu, L.-F.; Giordano, G. Enzymatic and physiological properties of the tungsten-substituted molybdenum TMAO reductase from Escherichia coli. *Mol. Microbiol.* **1999**, *32*, 159–168. [CrossRef]
184. Dridge, E.J.; Butler, C.S. Thermostable properties of the periplasmic selenate reductase from *Thauera selenatis*. *Biochimie* **2010**, *92*, 1268–1273. [CrossRef]
185. Mesbah, N.M. Industrial Biotechnology Based on Enzymes From Extreme Environments. *Front. Bioeng. Biotechnol.* **2022**, *10*, 870083. [CrossRef] [PubMed]
186. Barnard, D.; Casanueva, A.; Tuffin, M.; Cowan, D. Extremophiles in biofuel synthesis. *Environ. Technol.* **2010**, *31*, 871–888. [CrossRef]
187. Mukhtar, S.; Aslam, M. Biofuel Synthesis by Extremophilic Microorganisms. In *Biofuels Production—Sustainability and Advances in Microbial Bioresources*; Yadav, A.N., Rastegari, A.A., Yadav, N., Gaur, R., Eds.; Springer: Cham, Switzerland, 2020; pp. 115–138.
188. Einsle, O.; Rees, D.C. Structural Enzymology of Nitrogenase Enzymes. *Chem. Rev.* **2020**, *120*, 4969–5004. [CrossRef]
189. Warmack, R.A.; Rees, D.C. Nitrogenase beyond the Resting State: A Structural Perspective. *Molecules* **2023**, *28*, 7952. [CrossRef]
190. Einsle, O. Catalysis and structure of nitrogenases. *Curr. Opin. Struct. Biol.* **2023**, *83*, 102719. [CrossRef]
191. Rucker, H.R.; Kaçar, B. Enigmatic evolution of microbial nitrogen fixation: Insights from Earth's past. *Trends Microbiol.* **2024**, *32*, 554–564. [CrossRef]
192. Mrnjavac, N.; Degli Esposti, M.; Mizrahi, I.; Martin, W.F.; Allen, J.F. Three enzymes governed the rise of O_2 on Earth. *Biochim. Biophys. Acta* **2024**, *1865*, 149495. [CrossRef]
193. Eady, R.R. Structure−Function Relationships of Alternative Nitrogenases. *Chem. Rev.* **1996**, *96*, 3013–3030. [CrossRef]
194. Peters, J.W.; Szilagyi, R.K. Exploring new frontiers of nitrogenase structure and mechanism. *Curr. Opin. Chem. Biol.* **2006**, *10*, 101–108. [CrossRef] [PubMed]
195. Hu, Y.; Lee, C.C.; Grosch, M.; Solomon, J.B.; Weigand, W.; Ribbe, M.W. Enzymatic Fischer–Tropsch-Type Reactions. *Chem. Rev.* **2023**, *123*, 5755–5797. [CrossRef] [PubMed]
196. Burgess, B.K.; Lowe, D.J. Mechanism of Molybdenum Nitrogenase. *Chem. Rev.* **1996**, *96*, 2983–3012. [CrossRef] [PubMed]
197. Lindahl, P.A.; Day, E.P.; Kent, T.A.; Orme-Johnson, W.H.; Münck, E. Mössbauer, EPR, and magnetization studies of the Azotobacter vinelandii Fe protein. Evidence for a [4Fe-4S]1+ cluster with spin S = 3/2. *J. Biol. Chem.* **1985**, *260*, 11160–11173. [CrossRef] [PubMed]
198. Angove, H.C.; Yoo, S.J.; Münck, E.; Burgess, B.K. An All-ferrous State of the Fe Protein of Nitrogenase: Interaction with Nucleotides and Electron Transfer to the MoFe Protein. *J. Biol. Chem.* **1998**, *273*, 26330–26337. [CrossRef] [PubMed]

199. Wang, C.-H.; DeBeer, S. Structure, reactivity, and spectroscopy of nitrogenase-related synthetic and biological clusters. *Chem. Soc. Rev.* **2021**, *50*, 8743–8761. [CrossRef]
200. Einsle, O.; Tezcan, F.A.; Andrade, S.L.A.; Schmid, B.; Yoshida, M.; Howard, J.B.; Rees, D.C. Nitrogenase MoFe-Protein at 1.16 Å Resolution: A Central Ligand in the FeMo-Cofactor. *Science* **2002**, *297*, 1696–1700. [CrossRef]
201. Miller, R.W.; Eady, R.R. Molybdenum and vanadium nitrogenases of *Azotobacter chroococcum.* Low temperature favours N_2 reduction by vanadium nitrogenase. *Biochem. J.* **1988**, *256*, 429–432. [CrossRef]
202. Seefeldt, L.C.; Yang, Z.-Y.; Lukoyanov, D.A.; Harris, D.F.; Dean, D.R.; Raugei, S.; Hoffman, B.M. Reduction of Substrates by Nitrogenases. *Chem. Rev.* **2020**, *120*, 5082–5106. [CrossRef]
203. Appia-Ayme, C.; Little, R.; Chandra, G.; de Oliveira Martins, C.; Bueno Batista, M.; Dixon, R. Interactions between paralogous bacterial enhancer-binding proteins enable metal-dependent regulation of alternative nitrogenases in *Azotobacter vinelandii*. *Molec. Microbiol.* **2022**, *118*, 105–124. [CrossRef]
204. Harwood, C.S. Iron-Only and Vanadium Nitrogenases: Fail-Safe Enzymes or Something More? *Annu. Rev. Microbiol.* **2020**, *74*, 247–266. [CrossRef]
205. Rees, D.C.; Akif Tezcan, F.; Haynes, C.A.; Walton, M.Y.; Andrade, S.; Einsle, O.; Howard, J.B. Structural basis of biological nitrogen fixation. *Phil. Trans. Roy. Soc. A* **2005**, *363*, 971–984. [CrossRef]
206. Hoffman, B.M.; Lukoyanov, D.; Yang, Z.-Y.; Dean, D.R.; Seefeldt, L.C. Mechanism of Nitrogen Fixation by Nitrogenase: The Next Stage. *Chem. Rev.* **2014**, *114*, 4041–4062. [CrossRef] [PubMed]
207. Rutledge, H.L.; Tezcan, F.A. Electron Transfer in Nitrogenase. *Chem. Rev.* **2020**, *120*, 5158–5193. [CrossRef] [PubMed]
208. Duval, S.; Danyal, K.; Shaw, S.; Lytle, A.K.; Dean, D.R.; Hoffman, B.M.; Antony, E.; Seefeldt, L.C. Electron transfer precedes ATP hydrolysis during nitrogenase catalysis. *Proc. Natl. Acad. Sci. USA* **2013**, *110*, 16414–16419. [CrossRef] [PubMed]
209. Danyal, K.; Dean, D.R.; Hoffman, B.M.; Seefeldt, L.C. Electron Transfer within Nitrogenase: Evidence for a Deficit-Spending Mechanism. *Biochemistry* **2011**, *50*, 9255–9263. [CrossRef]
210. Thorneley, R.N.F.; Lowe, D.J. Kinetics and Mechanism of the Nitrogenase Enzyme System. In *Metal Ions in Biology: Molybdenum Enzymes*; Spiro, T.G., Ed.; Wiley-Interscience: New York, NY, USA, 1985; Volume 7, pp. 221–284.
211. Cao, L.; Ryde, U. Putative reaction mechanism of nitrogenase after dissociation of a sulfide ligand. *J. Catal.* **2020**, *391*, 247–259. [CrossRef]
212. Siegbahn, P.E.M. Model Calculations Suggest that the Central Carbon in the FeMo-Cofactor of Nitrogenase Becomes Protonated in the Process of Nitrogen Fixation. *J. Am. Chem. Soc.* **2016**, *138*, 10485–10495. [CrossRef]
213. Lukoyanov, D.; Dikanov, S.A.; Yang, Z.-Y.; Barney, B.M.; Samoilova, R.I.; Narasimhulu, K.V.; Dean, D.R.; Seefeldt, L.C.; Hoffman, B.M. ENDOR/HYSCORE Studies of the Common Intermediate Trapped during Nitrogenase Reduction of N_2H_2, CH_3N_2H, and N_2H_4 Support an Alternating Reaction Pathway for N_2 Reduction. *J. Am. Chem. Soc.* **2011**, *133*, 11655–11664. [CrossRef]
214. Raugei, S.; Seefeldt, L.C.; Hoffman, B.M. Critical computational analysis illuminates the reductive-elimination mechanism that activates nitrogenase for N_2 reduction. *Proc. Natl. Acad. Sci. USA* **2018**, *115*, E10521–E10530. [CrossRef]
215. Rohde, M.; Laun, K.; Zebger, I.; Stripp, S.T.; Einsle, O. Two ligand-binding sites in CO-reducing V nitrogenase reveal a general mechanistic principle. *Sci. Adv.* **2021**, *7*, eabg4474. [CrossRef]
216. Khadka, N.; Milton, R.D.; Shaw, S.; Lukoyanov, D.; Dean, D.R.; Minteer, S.D.; Raugei, S.; Hoffman, B.M.; Seefeldt, L.C. Mechanism of Nitrogenase H_2 Formation by Metal-Hydride Protonation Probed by Mediated Electrocatalysis and H/D Isotope Effects. *J. Am. Chem. Soc.* **2017**, *139*, 13518–13524. [CrossRef]
217. Cao, L.; Caldararu, O.; Ryde, U. Protonation and Reduction of the FeMo Cluster in Nitrogenase Studied by Quantum Mechanics/Molecular Mechanics (QM/MM) Calculations. *J. Chem. Theory Comput.* **2018**, *14*, 6653–6678. [CrossRef] [PubMed]
218. Dance, I. Survey of the Geometric and Electronic Structures of the Key Hydrogenated Forms of FeMo-co, the Active Site of the Enzyme Nitrogenase: Principles of the Mechanistically Significant Coordination Chemistry. *Inorganics* **2019**, *7*, 8. [CrossRef]
219. Kang, W.; Lee, C.C.; Jasniewski, A.J.; Ribbe, M.W.; Hu, Y. Structural evidence for a dynamic metallocofactor during N_2 reduction by Mo-nitrogenase. *Science* **2020**, *368*, 1381–1385. [CrossRef]
220. Jia, H.-P.; Quadrelli, E.A. Mechanistic aspects of dinitrogen cleavage and hydrogenation to produce ammonia in catalysis and organometallic chemistry: Relevance of metal hydride bonds and dihydrogen. *Chem. Soc. Rev.* **2014**, *43*, 547–564. [CrossRef] [PubMed]
221. van der Ham, C.J.M.; Koper, M.T.M.; Hetterscheid, D.G.H. Challenges in reduction of dinitrogen by proton and electron transfer. *Chem. Soc. Rev.* **2014**, *43*, 5183–5191. [CrossRef]
222. Kästner, J.; Blöchl, P.E. Ammonia Production at the FeMo Cofactor of Nitrogenase: Results from Density Functional Theory. *J. Am. Chem. Soc.* **2007**, *129*, 2998–3006. [CrossRef]
223. Dance, I. The chemical mechanism of nitrogenase: Calculated details of the intramolecular mechanism for hydrogenation of η2-N2 on FeMo-co to NH3. *Dalton Trans.* **2008**, 5977–5991. [CrossRef]
224. Varley, J.B.; Wang, Y.; Chan, K.; Studt, F.; Nørskov, J.K. Mechanistic insights into nitrogen fixation by nitrogenase enzymes. *Phys. Chem. Chem. Phys.* **2015**, *17*, 29541–29547. [CrossRef]

225. Rao, L.; Xu, X.; Adamo, C. Theoretical Investigation on the Role of the Central Carbon Atom and Close Protein Environment on the Nitrogen Reduction in Mo Nitrogenase. *ACS Catal.* **2016**, *6*, 1567–1577. [CrossRef]
226. Siegbahn, P.E.M. The mechanism for nitrogenase including all steps. *Phys. Chem. Chem. Phys.* **2019**, *21*, 15747–15759. [CrossRef]
227. Dance, I. Understanding non-reducible N_2 in the mechanism of Mo–nitrogenase. *Dalton Trans.* **2025**, *54*, 3013–3026. [CrossRef] [PubMed]
228. Mayer, S.M.; Gormal, C.A.; Smith, B.E.; Lawson, D.M. Crystallographic Analysis of the MoFe Protein of Nitrogenase from a nifV Mutant of *Klebsiella pneumoniae* Identifies Citrate as a Ligand to the Molybdenum of Iron Molybdenum Cofactor (FeMoco). *J. Biol. Chem.* **2002**, *277*, 35263–35266. [CrossRef]
229. Poole, R.K.; Hill, S. Respiratory Protection of Nitrogenase Activity in *Azotobacter vinelandii* -Roles of the Terminal Oxidases. *Biosci. Rep.* **1997**, *17*, 303–317. [CrossRef] [PubMed]
230. Saito, M.A.; Bertrand, E.M.; Dutkiewicz, S.; Bulygin, V.V.; Moran, D.M.; Monteiro, F.M.; Follows, M.J.; Valois, F.W.; Waterbury, J.B. Iron conservation by reduction of metalloenzyme inventories in the marine diazotroph *Crocosphaera watsonii*. *Proc. Natl. Acad. Sci. USA* **2011**, *108*, 2184–2189. [CrossRef] [PubMed]
231. Johnson, E.A.; Lecomte, J.T.J. The Globins of Cyanobacteria and Algae. In *Advances in Microbial Physiology*; Poole, R.K., Ed.; Academic Press: New York, NY, USA, 2013; Volume 63, pp. 195–272.
232. Rutten, P.J.; Poole, P.S. Oxygen regulatory mechanisms of nitrogen fixation in rhizobia. In *Advances in Microbial Physiology*; Poole, R.K., Ed.; Academic Press: New York, NY, USA, 2019; Volume 75, pp. 325–389.
233. Allen, J.F.; Thake, B.; Martin, W.F. Nitrogenase Inhibition Limited Oxygenation of Earth's Proterozoic Atmosphere. *Trends Plant Sci.* **2019**, *24*, 1022–1031. [CrossRef]
234. Wofford, J.D.; Bolaji, N.; Dziuba, N.; Outten, F.W.; Lindahl, P.A. Evidence that a respiratory shield in *Escherichia coli* protects a low-molecular-mass Fe^{II} pool from O_2-dependent oxidation. *J. Biol. Chem.* **2019**, *294*, 50–62. [CrossRef]
235. Cardona, T.; Sánchez-Baracaldo, P.; Rutherford, A.W.; Larkum, A.W. Early Archean origin of Photosystem II. *Geobiology* **2019**, *17*, 127–150. [CrossRef]
236. Franke, P.; Freiberger, S.; Zhang, L.; Einsle, O. Conformational protection of molybdenum nitrogenase by Shethna protein II. *Nature* **2025**, *637*, 998–1004. [CrossRef]
237. Narehood, S.M.; Cook, B.D.; Srisantitham, S.; Eng, V.H.; Shiau, A.A.; McGuire, K.L.; Britt, R.D.; Herzik, M.A.; Tezcan, F.A. Structural basis for the conformational protection of nitrogenase from O_2. *Nature* **2025**, *637*, 991–997. [CrossRef]
238. Rosenzweig, A.C. How a nitrogen-fixing enzyme avoids oxygen. *Nature* **2025**, *637*, 796–798. [CrossRef]
239. Kasahara, K.; Kerby, R.L.; Zhang, Q.; Pradhan, M.; Mehrabian, M.; Lusis, A.J.; Bergström, G.; Bäckhed, F.; Rey, F.E. Gut bacterial metabolism contributes to host global purine homeostasis. *Cell Host Microbe* **2023**, *31*, 1038–1053.e10. [CrossRef]
240. Huynh, T.N.; Stewart, V. Purine catabolism by enterobacteria. *Adv. Microb. Physiol.* **2023**, *82*, 205–266. [CrossRef] [PubMed]
241. Wang, H.; Xie, L.; Song, X.; Wang, J.; Li, X.; Lin, Z.; Su, T.; Liang, B.; Huang, D. Purine-Induced IFN-γ Promotes Uric Acid Production by Upregulating Xanthine Oxidoreductase Expression. *Front. Immunol.* **2022**, *13*, 773001. [CrossRef]
242. Schoepp-Cothenet, B.; van Lis, R.; Philippot, P.; Magalon, A.; Russell, M.J.; Nitschke, W. The ineluctable requirement for the trans-iron elements molybdenum and/or tungsten in the origin of life. *Sci. Rep.* **2012**, *2*, 263. [CrossRef] [PubMed]
243. Chen, C.; Lü, J.M.; Yao, Q. Hyperuricemia-Related Diseases and Xanthine Oxidoreductase (XOR) Inhibitors: An Overview. *Med. Sci. Monit.* **2016**, *22*, 2501–2512. [CrossRef] [PubMed]
244. Luna, G.; Dolzhenko, A.V.; Mancera, R.L. Inhibitors of Xanthine Oxidase: Scaffold Diversity and Structure-Based Drug Design. *ChemMedChem* **2019**, *14*, 714–743. [CrossRef]
245. Yamaguchi, Y.; Matsumura, T.; Ichida, K.; Okamoto, K.; Nishino, T. Human Xanthine Oxidase Changes its Substrate Specificity to Aldehyde Oxidase Type upon Mutation of Amino Acid Residues in the Active Site: Roles of Active Site Residues in Binding and Activation of Purine Substrate. *J. Biochem.* **2007**, *141*, 513–524. [CrossRef]
246. Agabiti-Rosei, E.; Grassi, G. Beyond gout: Uric acid and cardiovascular diseases. *Curr. Med. Res. Opin.* **2013**, *29* (Suppl. S3), 33–39. [CrossRef]
247. Schuchardt, M.; Herrmann, J.; Tolle, M.; van der Giet, M. Xanthine Oxidase and its Role as Target in Cardiovascular Disease: Cardiovascular Protection by Enzyme Inhibition? *Curr. Pharm. Des.* **2017**, *23*, 3391–3404. [CrossRef]
248. Polito, L.; Bortolotti, M.; Battelli, M.G.; Bolognesi, A. Xanthine oxidoreductase: A leading actor in cardiovascular disease drama. *Redox Biol.* **2021**, *48*, 102195. [CrossRef]
249. Metz, S.; Thiel, W. QM/MM Studies of Xanthine Oxidase: Variations of Cofactor, Substrate, and Active-Site Glu802. *J. Phys. Chem. B* **2010**, *114*, 1506–1517. [CrossRef]
250. Ribeiro, P.M.G.; Fernandes, H.S.; Maia, L.B.; Sousa, S.F.; Moura, J.J.G.; Cerqueira, N.M.F.S.A. The complete catalytic mechanism of xanthine oxidase: A computational study. *Inorg. Chem. Front.* **2021**, *8*, 405–416. [CrossRef]
251. Ishikita, H.; Eger, B.T.; Okamoto, K.; Nishino, T.; Pai, E.F. Protein Conformational Gating of Enzymatic Activity in Xanthine Oxidoreductase. *J. Am. Chem. Soc.* **2012**, *134*, 999–1009. [CrossRef] [PubMed]

252. Garattini, E.; Terao, M. The role of aldehyde oxidase in drug metabolism. *Expert Opin. Drug Metabol. Toxicol.* **2012**, *8*, 487–503. [CrossRef] [PubMed]
253. Pryde, D.C.; Dalvie, D.; Hu, Q.; Jones, P.; Obach, R.S.; Tran, T.-D. Aldehyde Oxidase: An Enzyme of Emerging Importance in Drug Discovery. *J. Med. Chem.* **2010**, *53*, 8441–8460. [CrossRef]
254. Rendić, S.P.; Crouch, R.D.; Guengerich, F.P. Roles of selected non-P450 human oxidoreductase enzymes in protective and toxic effects of chemicals: Review and compilation of reactions. *Arch. Toxicol.* **2022**, *96*, 2145–2246. [CrossRef]
255. Ferreira, P.; Cerqueira, N.M.F.S.A.; Fernandes, P.A.; Romão, M.J.; Ramos, M.J. Catalytic Mechanism of Human Aldehyde Oxidase. *ACS Catal.* **2020**, *10*, 9276–9286. [CrossRef]
256. Montefiori, M.; Jørgensen, F.S.; Olsen, L. Aldehyde Oxidase: Reaction Mechanism and Prediction of Site of Metabolism. *ACS Omega* **2017**, *2*, 4237–4244. [CrossRef]
257. Coelho, C.; Mahro, M.; Trincão, J.; Carvalho, A.T.P.; Ramos, M.J.; Terao, M.; Garattini, E.; Leimkühler, S.; Romão, M.J. The First Mammalian Aldehyde Oxidase Crystal Structure: Inisights into Substrate Specificity. *J. Biol. Chem.* **2012**, *287*, 40690–40702. [CrossRef]
258. Kappler, U.; Dahl, C. Enzymology and molecular biology of prokaryotic sulfite oxidation. *FEMS Microbiol. Lett.* **2001**, *203*, 1–9. [CrossRef]
259. Johannes, L.; Fu, C.-Y.; Schwarz, G. Molybdenum Cofactor Deficiency in Humans. *Molecules* **2022**, *27*, 6896. [CrossRef] [PubMed]
260. Johnson, J.L. Prenatal diagnosis of molybdenum cofactor deficiency and isolated sulfite oxidase deficiency. *Prenat. Diagn.* **2003**, *23*, 6–8. [CrossRef] [PubMed]
261. Dublin, A.B.; Hald, J.K.; Wootton-Gorges, S.L. Isolated sulfite oxidase deficiency: MR imaging features. *Am. J. Neuroradiol.* **2002**, *23*, 484–485. [PubMed]
262. Kohlmeier, M. Chapter 8—Amino Acids and Nitrogen Compounds. In *Nutrient Metabolism*, 2nd ed.; Kohlmeier, M., Ed.; Academic Press: San Diego, CA, USA, 2015; pp. 265–477.
263. Hille, R. Molybdenum enzymes. *Essays Biochem.* **1999**, *34*, 125–137. [CrossRef]
264. Johnson-Winters, K.; Tollin, G.; Enemark, J.H. Elucidating the Catalytic Mechanism of Sulfite Oxidizing Enzymes Using Structural, Spectroscopic, and Kinetic Analyses. *Biochemistry* **2010**, *49*, 7242–7254. [CrossRef]
265. Kisker, C.; Schindelin, H.; Pacheco, A.; Wehbi, W.A.; Garrett, R.M.; Rajagopalan, K.V.; Enemark, J.H.; Rees, D.C. Molecular Basis of Sulfite Oxidase Deficiency from the Structure of Sulfite Oxidase. *Cell* **1997**, *91*, 973–983. [CrossRef]
266. Astashkin, A.V.; Raitsimring, A.M.; Feng, C.; Johnson, J.L.; Rajagopalan, K.V.; Enemark, J.H. Pulsed EPR studies of nonexchangeable protons near the Mo(V) center of sulfite oxidase: Direct detection of the alpha-proton of the coordinated cysteinyl residue and structural implications for the active site. *J. Am. Chem. Soc.* **2002**, *124*, 6109–6118. [CrossRef]
267. Coelho, C.; Romão, M.J. Structural and mechanistic insights on nitrate reductases. *Protein Sci.* **2015**, *24*, 1901–1911. [CrossRef]
268. Moreno-Vivián, C.; Ferguson, S.J. Definition and distinction between assimilatory, dissimilatory and respiratory pathways. *Mol. Microbiol.* **1998**, *29*, 664–666. [CrossRef]
269. Moir, J.W.; Wood, N.J. Nitrate and nitrite transport in bacteria. *Cell. Mol. Life Sci.* **2001**, *58*, 215–224. [CrossRef]
270. Sparacino-Watkins, C.; Stolz, J.F.; Basu, P. Nitrate and periplasmic nitrate reductases. *Chem. Soc. Rev.* **2014**, *43*, 676–706. [CrossRef]
271. Yoneyama, T.; Suzuki, A. Light-Independent Nitrogen Assimilation in Plant Leaves: Nitrate Incorporation into Glutamine, Glutamate, Aspartate, and Asparagine Traced by ^{15}N. *Plants* **2020**, *9*, 1303. [CrossRef]
272. Kaviraj, M.; Kumar, U.; Snigdha, A.; Chatterjee, S. Nitrate reduction to ammonium: A phylogenetic, physiological, and genetic aspects in Prokaryotes and eukaryotes. *Arch. Microbiol.* **2024**, *206*, 297. [CrossRef] [PubMed]
273. Hird, K.; Campeciño, J.O.; Lehnert, N.; Hegg, E.L. Recent mechanistic developments for cytochrome c nitrite reductase, the key enzyme in the dissimilatory nitrate reduction to ammonium pathway. *J. Inorg. Biochem.* **2024**, *256*, 112542. [CrossRef] [PubMed]
274. Ingledew, W.J.; Poole, R.K. The respiratory chains of Escherichia coli. *Microbiol. Rev.* **1984**, *48*, 222–271. [CrossRef] [PubMed]
275. Lin, J.T.; Stewart, V. Nitrate assimilation by bacteria. *Adv. Microb. Physiol.* **1998**, *39*, 379. [CrossRef]
276. Campbell, W.H. Structure and function of eukaryotic NAD(P)H:nitrate reductase. *Cell Mol. Life Sci.* **2001**, *58*, 194–204. [CrossRef]
277. Richardson, D.J.; Berks, B.C.; Russell, D.A.; Spiro, S.; Taylor, C.J. Functional, biochemical and genetic diversity of prokaryotic nitrate reductases. *Cell Mol. Life Sci.* **2001**, *58*, 165–178. [CrossRef]
278. Cole, J.A.; Richardson, D.J. Respiration of Nitrate and Nitrite. *EcoSal Plus* **2008**, *3*, 1–28. [CrossRef]
279. van Spanning, R.J.M.; Richardson, D.J.; Ferguson, S.J. Introduction to the biochemistry and molecular biology of denitrification. In *Biology of the Nitrogen Cycle*; Bothe, H., Ferguson, S.J., Newton, W., Eds.; Elsevier: Amsterdam, The Netherlands, 2007; pp. 3–20.
280. Leung, P.M.; Daebeler, A.; Chiri, E.; Hanchapola, I.; Gillett, D.L.; Schittenhelm, R.B.; Daims, H.; Greening, C. A nitrite-oxidising bacterium constitutively consumes atmospheric hydrogen. *ISME J.* **2022**, *16*, 2213–2219. [CrossRef]
281. Islam, Z.F.; Welsh, C.; Bayly, K.; Grinter, R.; Southam, G.; Gagen, E.J.; Greening, C. A widely distributed hydrogenase oxidises atmospheric H_2 during bacterial growth. *ISME J.* **2020**, *14*, 2649–2658. [CrossRef] [PubMed]

282. Yang, J.; Jung, H.-C.; Oh, H.-M.; Choi, B.G.; Lee, H.S.; Kang, S.G. $NADP^+$ or CO_2 reduction by *frhAGB*-encoded hydrogenase through interaction with formate dehydrogenase 3 in the hyperthermophilic archaeon *Thermococcus onnurineus* NA1. *Appl. Environ. Microbiol.* **2023**, *89*, e01474-01423. [CrossRef] [PubMed]
283. Bird, L.J.; Bonnefoy, V.; Newman, D.K. Bioenergetic challenges of microbial iron metabolisms. *Trends Microbiol.* **2011**, *19*, 330–340. [CrossRef] [PubMed]
284. Kelly, D.P.; Shergill, J.K.; Lu, W.-P.; Wood, A.P. Oxidative metabolism of inorganic sulfur compounds by bacteria. *Antonie Van Leeuwenhoek* **1997**, *71*, 95–107. [CrossRef]
285. Shaikh, Z.; Ali, A. Nitrate assimilation: Cross talk between plants and soil. In *Frontiers in Plant-Soil Interaction*; Aftab, T., Hakeem, K.R., Eds.; Academic Press: New York, NY, USA, 2021; pp. 135–151.
286. Salas, A.; Cabrera, J.J.; Jiménez-Leiva, A.; Mesa, S.; Bedmar, E.J.; Richardson, D.J.; Gates, A.J.; Delgado, M.J. Bacterial nitric oxide metabolism: Recent insights in rhizobia. *Adv. Microb. Physiol.* **2021**, *78*, 259–315. [CrossRef]
287. Singh, S.; Anil, A.G.; Kumar, V.; Kapoor, D.; Subramanian, S.; Singh, J.; Ramamurthy, P.C. Nitrates in the environment: A critical review of their distribution, sensing techniques, ecological effects and remediation. *Chemosphere* **2022**, *287*, 131996. [CrossRef]
288. Rocha, B.S.; Laranjinha, J. Nitrate from diet might fuel gut microbiota metabolism: Minding the gap between redox signaling and inter-kingdom communication. *Free Radic. Biol. Med.* **2020**, *149*, 37–43. [CrossRef]
289. White, S.A.; Christofferson, A.J.; Grainger, A.I.; Day, M.A.; Jarrom, D.; Graziano, A.E.; Searle, P.F.; Hyde, E.I. The 3D-structure, kinetics and dynamics of the *E. coli* nitroreductase NfsA with NADP+ provide glimpses of its catalytic mechanism. *FEBS Lett.* **2022**, *596*, 2425–2440. [CrossRef]
290. Bertero, M.G.; Rothery, R.A.; Palak, M.; Hou, C.; Lim, D.; Blasco, F.; Weiner, J.H.; Strynadka, N.C.J. Insights into the respiratory electron transfer pathway from the structure of nitrate reductase A. *Nat. Struct. Mol. Biol.* **2003**, *10*, 681–687. [CrossRef]
291. Elliott, S.J.; Hoke, K.R.; Heffron, K.; Palak, M.; Rothery, R.A.; Weiner, J.H.; Armstrong, F.A. Voltammetric studies of the catalytic mechanism of the respiratory nitrate reductase from Escherichia coli: How nitrate reduction and inhibition depend on the oxidation state of the active site. *Biochemistry* **2004**, *43*, 799–807. [CrossRef]
292. Cerqueira, N.M.; Gonzalez, P.J.; Brondino, C.D.; Romão, M.J.; Romão, C.C.; Moura, I.; Moura, J.J. The effect of the sixth sulfur ligand in the catalytic mechanism of periplasmic nitrate reductase. *J. Comput. Chem.* **2009**, *30*, 2466–2484. [CrossRef] [PubMed]
293. Maia, L.B.; Moura, I.; Moura, J.J.G. Carbon Dioxide Utilisation—The Formate Route. In *Enzymes for Solving Humankind's Problems: Natural and Artificial Systems in Health, Agriculture, Environment and Energy*; Moura, J.J.G., Moura, I., Maia, L.B., Eds.; Springer: Cham, Switzerland, 2021; pp. 29–81.
294. Leimkühler, S. Metal-Containing Formate Dehydrogenases, a Personal View. *Molecules* **2023**, *28*, 5338. [CrossRef] [PubMed]
295. Kobayashi, A.; Taketa, M.; Sowa, K.; Kano, K.; Higuchi, Y.; Ogata, H. Structure and function relationship of formate dehydrogenases: An overview of recent progress. *IUCrJ* **2023**, *10*, 544–554. [CrossRef] [PubMed]
296. Holden, J.F.; Sistu, H. Formate and hydrogen in hydrothermal vents and their use by extremely thermophilic methanogens and heterotrophs. *Front. Microbiol.* **2023**, *14*, 1093018. [CrossRef]
297. Niks, D.; Hille, R. Molybdenum- and tungsten-containing formate dehydrogenases and formylmethanofuran dehydrogenases: Structure, mechanism, and cofactor insertion. *Protein Sci.* **2019**, *28*, 111–122. [CrossRef]
298. Hartmann, T.; Schwanhold, N.; Leimkühler, S. Assembly and catalysis of molybdenum or tungsten-containing formate dehydrogenases from bacteria. *Biochim. Biophs. Acta* **2015**, *1854*, 1090–1100. [CrossRef]
299. Mishra, A.; Kumar Padhi, S. Harnessing Ruthenium and Copper Catalysts for Formate Dehydrogenase Reactions. *Chem. Rec.* **2024**, *24*, e202400172. [CrossRef]
300. Masson-Delmotte, V.; Zhai, P.; Pörtner, H.-O.; Roberts, D.; Skea, J.; Shukla, P.R.; Pirani, A.; Moufouma-Okia, W.; Péan, C.; Pidcock, R. (Eds.) *Global Warming of 1.5 °C.*; Intergovernmental Panel on Climate Change (IPCC): Cambridge University Press: Cambridge, UK, 2018; p. 616.
301. Johnson, M.K.; Rees, D.C.; Adams, M.W. Tungstoenzymes. *Chem. Rev.* **1996**, *96*, 2817–2840. [CrossRef]
302. Moura, J.J.; Brondino, C.D.; Trincão, J.; Romão, M.J. Mo and W bis-MGD enzymes: Nitrate reductases and formate dehydrogenases. *J. Biol. Inorg. Chem.* **2004**, *9*, 791–799. [CrossRef]
303. Roy, R.; Adams, M.W. Tungsten-dependent aldehyde oxidoreductase: A new family of enzymes containing the pterin cofactor. *Met. Ions Biol. Syst.* **2002**, *39*, 673–697.
304. L'Vov N, P.; Nosikov, A.N.; Antipov, A.N. Tungsten-containing enzymes. *Biochemistry* **2002**, *67*, 196–200. [CrossRef] [PubMed]
305. Das, A.; Das, U.; Das, A.K. Relativistic effects on the chemical bonding properties of the heavier elements and their compounds. *Coord. Chem. Rev.* **2023**, *479*, 215000. [CrossRef]
306. Tenderholt, A.L.; Szilagyi, R.K.; Holm, R.H.; Hodgson, K.O.; Hedman, B.; Solomon, E.I. Sulfur K-edge XAS of $W^{V}O$ vs. $Mo^{V}O$ bis(dithiolene) complexes: Contributions of relativistic effects to electronic structure and reactivity of tungsten enzymes. *J. Inorg. Biochem.* **2007**, *101*, 1594–1600. [CrossRef] [PubMed]
307. Thayer, J.S. Relativistic Effects and the Chemistry of the Heaviest Main-Group Elements. *J. Chem. Ed.* **2005**, *82*, 1721. [CrossRef]
308. Pyykko, P. Relativistic effects in structural chemistry. *Chem. Rev.* **1988**, *88*, 563–594. [CrossRef]

309. Rivas, M.G.; González, P.J.; Brondino, C.D.; Moura, J.J.; Moura, I. EPR characterization of the molybdenum(V) forms of formate dehydrogenase from Desulfovibrio desulfuricans ATCC 27774 upon formate reduction. *J. Inorg. Biochem.* **2007**, *101*, 1617–1622. [CrossRef]
310. Duffus, B.R.; Schrapers, P.; Schuth, N.; Mebs, S.; Dau, H.; Leimkühler, S.; Haumann, M. Anion Binding and Oxidative Modification at the Molybdenum Cofactor of Formate Dehydrogenase from *Rhodobacter capsulatus* Studied by X-ray Absorption Spectroscopy. *Inorg. Chem.* **2020**, *59*, 214–225. [CrossRef]
311. Dong, G.; Ryde, U. Reaction mechanism of formate dehydrogenase studied by computational methods. *J. Biol. Inorg. Chem.* **2018**, *23*, 1243–1254. [CrossRef]
312. Niks, D.; Hille, R. Reductive activation of CO_2 by formate dehydrogenases. *Methods Enzymol.* **2018**, *613*, 277–295. [CrossRef]
313. Reich, H.J.; Hondal, R.J. Why Nature Chose Selenium. *ACS Chem. Biol.* **2016**, *11*, 821–841. [CrossRef]
314. Niks, D.; Hakopian, S.; Canchola, A.; Lin, Y.-H.; Hille, R. Mechanism of Action of Formate Dehydrogenases. *J. Am. Chem. Soc.* **2024**, *146*, 28601–28604. [CrossRef] [PubMed]
315. Kumar, H.; Khosraneh, M.; Bandaru, S.S.M.; Schulzke, C.; Leimkühler, S. The Mechanism of Metal-Containing Formate Dehydrogenases Revisited: The Formation of Bicarbonate as Product Intermediate Provides Evidence for an Oxygen Atom Transfer Mechanism. *Molecules* **2023**, *28*, 1537. [CrossRef] [PubMed]
316. Radon, C.; Mittelstädt, G.; Duffus, B.R.; Bürger, J.; Hartmann, T.; Mielke, T.; Teutloff, C.; Leimkühler, S.; Wendler, P. Cryo-EM structures reveal intricate Fe-S cluster arrangement and charging in Rhodobacter capsulatus formate dehydrogenase. *Nat. Commun.* **2020**, *11*, 1912. [CrossRef] [PubMed]
317. Oliveira, A.R.; Mota, C.; Mourato, C.; Domingos, R.M.; Santos, M.F.A.; Gesto, D.; Guigliarelli, B.; Santos-Silva, T.; Romão, M.J.; Cardoso Pereira, I.A. Toward the Mechanistic Understanding of Enzymatic CO2 Reduction. *ACS Catal.* **2020**, *10*, 3844–3856. [CrossRef]
318. Verhees, C.H.; Kengen, S.W.; Tuininga, J.E.; Schut, G.J.; Adams, M.W.; De Vos, W.M.; Van Der Oost, J. The unique features of glycolytic pathways in Archaea. *Biochem. J.* **2003**, *375*, 231–246. [CrossRef]
319. Roy, R.; Menon, A.L.; Adams, M.W. Aldehyde oxidoreductases from Pyrococcus furiosus. *Methods Enzymol.* **2001**, *331*, 132–144. [CrossRef]
320. Kengen, S.W.M. 'Pyrococcus furiosus, 30 years on'. *Microb. Biotechnol.* **2017**, *10*, 1441–1444. [CrossRef]
321. Bevers, L.E.; Bol, E.; Hagedoorn, P.-L.; Hagen, W.R. WOR5, a Novel Tungsten-Containing Aldehyde Oxidoreductase from *Pyrococcus furiosus* with a Broad Substrate Specificity. *J. Bacteriol.* **2005**, *187*, 7056–7061. [CrossRef]
322. Winiarska, A.; Ramírez-Amador, F.; Hege, D.; Gemmecker, Y.; Prinz, S.; Hochberg, G.; Heider, J.; Szaleniec, M.; Schuller, J.M. A bacterial tungsten-containing aldehyde oxidoreductase forms an enzymatic decorated protein nanowire. *Sci. Adv.* **2023**, *9*, eadg6689. [CrossRef]
323. Rauh, D.; Graentzdoerffer, A.; Granderath, K.; Andreesen, J.R.; Pich, A. Tungsten-containing aldehyde oxidoreductase of Eubacterium acidaminophilum. *Eur. J. Biochem.* **2004**, *271*, 212–219. [CrossRef]
324. Huber, C.; Caldeira, J.; Jongejan, J.A.; Simon, H. Further characterization of two different, reversible aldehyde oxidoreductases from Clostridium formicoaceticum, one containing tungsten and the other molybdenum. *Arch. Microbiol.* **1994**, *162*, 303–309. [CrossRef]
325. Schut, G.J.; Thorgersen, M.P.; Poole, F.L.; Haja, D.K.; Putumbaka, S.; Adams, M.W.W. Tungsten enzymes play a role in detoxifying food and antimicrobial aldehydes in the human gut microbiome. *Proc. Natl. Acad. Sci. USA* **2021**, *118*, e2109008118. [CrossRef] [PubMed]
326. Sevcenco, A.-M.; Bevers, L.E.; Pinkse, M.W.H.; Krijger, G.C.; Wolterbeek, H.T.; Verhaert, P.D.E.M.; Hagen, W.R.; Hagedoorn, P.-L. Molybdenum Incorporation in Tungsten Aldehyde Oxidoreductase Enzymes from *Pyrococcus furiosus*. *J. Bacteriol.* **2010**, *192*, 4143–4152. [CrossRef] [PubMed]
327. Kalimuthu, P.; Hege, D.; Winiarska, A.; Gemmecker, Y.; Szaleniec, M.; Heider, J.; Bernhardt, P.V. Electrocatalytic Aldehyde Oxidation by a Tungsten Dependent Aldehyde Oxidoreductase from *Aromatoleum Aromaticum*. *Chem. Eur. J.* **2023**, *29*, e202203072. [CrossRef]
328. Winiarska, A.; Hege, D.; Gemmecker, Y.; Kryściak-Czerwenka, J.; Seubert, A.; Heider, J.; Szaleniec, M. Tungsten Enzyme Using Hydrogen as an Electron Donor to Reduce Carboxylic Acids and NAD+. *ACS Catal.* **2022**, *12*, 8707–8717. [CrossRef]
329. Hagedoorn, P.-L. Steady-state kinetics of the tungsten containing aldehyde: Ferredoxin oxidoreductases from the hyperthermophilic archaeon *Pyrococcus furiosus*. *J. Biotechnol.* **2019**, *306*, 142–148. [CrossRef]
330. Chan, M.K.; Mukund, S.; Kletzin, A.; Adams, M.W.W.; Rees, D.C. Structure of a Hyperthermophilic Tungstopterin Enzyme, Aldehyde Ferredoxin Oxidoreductase. *Science* **1995**, *267*, 1463–1469. [CrossRef]
331. Arndt, F.; Schmitt, G.; Winiarska, A.; Saft, M.; Seubert, A.; Kahnt, J.; Heider, J. Characterization of an Aldehyde Oxidoreductase From the Mesophilic Bacterium Aromatoleum aromaticum EbN1, a Member of a New Subfamily of Tungsten-Containing Enzymes. *Front. Microbiol.* **2019**, *10*, 71. [CrossRef]

332. ten Brink, F. Living on Acetylene. A Primordial Energy Source. In *The Metal-Driven Biogeochemistry of Gaseous Compounds in the Environment*; Kroneck, P.M.H., Torres, M.E.S., Eds.; Springer: Dordrecht, The Netherlands, 2014; pp. 15–35.
333. Yalkowsky, S.H.; He, Y.; Jain, P. *Handbook of Aqueous Solubility Data*, 2nd ed.; CRC Press: Boca Raton, FL, USA, 2010.
334. Abbasian, F.; Lockington, R.; Megharaj, M.; Naidu, R. A Review on the Genetics of Aliphatic and Aromatic Hydrocarbon Degradation. *Appl. Biochem. Biotechnol.* **2016**, *178*, 224–250. [CrossRef]
335. Stewart, W.D.; Fitzgerald, G.P.; Burris, R.H. In situ studies on N_2 fixation using the acetylene reduction technique. *Proc. Natl. Acad. Sci. USA* **1967**, *58*, 2071–2078. [CrossRef]
336. Oremland, R.S. Got acetylene: A personal research retrospective. *FEMS Microbes* **2021**, *2*, xtab009. [CrossRef] [PubMed]
337. Culbertson, C.W.; Strohmaier, F.E.; Oremland, R.S. Acetylene as a substrate in the development of primordial bacterial communities. *Orig. Life Evol. Biosph.* **1988**, *18*, 397–407. [CrossRef] [PubMed]
338. Rosner, B.M.; Schink, B. Purification and characterization of acetylene hydratase of Pelobacter acetylenicus, a tungsten iron-sulfur protein. *J. Bacteriol.* **1995**, *177*, 5767–5772. [CrossRef] [PubMed]
339. Seiffert, G.B.; Ullmann, G.M.; Messerschmidt, A.; Schink, B.; Kroneck, P.M.H.; Einsle, O. Structure of the non-redox-active tungsten/[4Fe:4S] enzyme acetylene hydratase. *Proc. Natl. Acad. Sci. USA* **2007**, *104*, 3073–3077. [CrossRef]
340. tenBrink, F.; Schink, B.; Kroneck, P.M.H. Exploring the Active Site of the Tungsten, Iron-Sulfur Enzyme Acetylene Hydratase. *J. Bacteriol.* **2011**, *193*, 1229–1236. [CrossRef]
341. Vidovič, C.; Peschel, L.M.; Buchsteiner, M.; Belaj, F.; Mösch-Zanetti, N.C. Structural Mimics of Acetylene Hydratase: Tungsten Complexes Capable of Intramolecular Nucleophilic Attack on Acetylene. *Chem. Eur. J.* **2019**, *25*, 14267–14272. [CrossRef]
342. Liao, R.-Z.; Thiel, W. Comparison of QM-Only and QM/MM Models for the Mechanism of Tungsten-Dependent Acetylene Hydratase. *J. Chem. Theory Comp.* **2012**, *8*, 3793–3803. [CrossRef]
343. Liu, Y.-F.; Liao, R.-Z.; Ding, W.-J.; Yu, J.-G.; Liu, R.-Z. Theoretical investigation of the first-shell mechanism of acetylene hydration catalyzed by a biomimetic tungsten complex. *J. Biol. Inorg. Chem.* **2011**, *16*, 745–752. [CrossRef]
344. Vorholt, J.A.; Thauer, R.K. The active species of 'CO_2' utilized by formylmethanofuran dehydrogenase from methanogenic Archaea. *Eur. J. Biochem.* **1997**, *248*, 919–924. [CrossRef]
345. Lemaire, O.N.; Wagner, T. All-in-One CO_2 Capture and Transformation: Lessons from Formylmethanofuran Dehydrogenases. *Acc. Chem. Res.* **2024**, *57*, 3512–3523. [CrossRef]
346. Sahin, S.; Lemaire, O.N.; Belhamri, M.; Kurth, J.M.; Welte, C.U.; Wagner, T.; Milton, R.D. Bioelectrocatalytic CO_2 Reduction by Mo-Dependent Formylmethanofuran Dehydrogenase. *Angew. Chem. Int. Ed. Engl.* **2023**, *62*, e202311981. [CrossRef] [PubMed]
347. Mand, T.D.; Metcalf, W.W. Energy Conservation and Hydrogenase Function in Methanogenic Archaea, in Particular the Genus Methanosarcina. *Microbiol. Mol. Bio.L Rev.* **2019**, *83*, e00020-19. [CrossRef]
348. Appel, A.M.; Bercaw, J.E.; Bocarsly, A.B.; Dobbek, H.; DuBois, D.L.; Dupuis, M.; Ferry, J.G.; Fujita, E.; Hille, R.; Kenis, P.J.A.; et al. Frontiers, Opportunities, and Challenges in Biochemical and Chemical Catalysis of CO_2 Fixation. *Chem. Rev.* **2013**, *113*, 6621–6658. [CrossRef] [PubMed]
349. Lane, T.W.; Morel, F.M.M. A biological function for cadmium in marine diatoms. *Proc. Natl. Acad. Sci. USA* **2000**, *97*, 4627–4631. [CrossRef] [PubMed]
350. Lane, T.W.; Saito, M.A.; George, G.N.; Pickering, I.J.; Prince, R.C.; Morel, F.M.M. A cadmium enzyme from a marine diatom. *Nature* **2005**, *435*, 42. [CrossRef]
351. Xu, Y.; Feng, L.; Jeffrey, P.D.; Shi, Y.; Morel, F.M.M. Structure and metal exchange in the cadmium carbonic anhydrase of marine diatoms. *Nature* **2008**, *452*, 56–61. [CrossRef]
352. Steenhoudt, O.; Vanderleyden, J. *Azospirillum*, a free-living nitrogen-fixing bacterium closely associated with grasses: Genetic, biochemical and ecological aspects. *FEMS Microbiol. Rev.* **2000**, *24*, 487–506. [CrossRef]
353. Aasfar, A.; Bargaz, A.; Yaakoubi, K.; Hilali, A.; Bennis, I.; Zeroual, Y.; Meftah Kadmiri, I. Nitrogen Fixing *Azotobacter* Species as Potential Soil Biological Enhancers for Crop Nutrition and Yield Stability. *Front. Microbiol.* **2021**, *12*, 628379. [CrossRef]
354. Baranu, B.S.; Lawrence, E. Nitrogen Bacteria Associated with Bioremediation Soil and their Ability to Degrade Hydrocarbon. *Int. J. Curr. Microbiol. App. Sci.* **2022**, *11*, 306–314. [CrossRef]
355. Song, X.; Zhang, J.; Li, D.; Peng, C. Nitrogen-fixing cyanobacteria have the potential to improve nitrogen use efficiency through the reduction of ammonia volatilization in red soil paddy fields. *Soil Tillage Res.* **2022**, *217*, 105274. [CrossRef]
356. Coelho, F.C.; Cerchiaro, G.; Araújo, S.E.S.; Daher, J.P.L.; Cardoso, S.A.; Coelho, G.F.; Guimarães, A.G. Is There a Connection between the Metabolism of Copper, Sulfur, and Molybdenum in Alzheimer's Disease? New Insights on Disease Etiology. *Int. J. Mol. Sci.* **2022**, *23*, 7935. [CrossRef] [PubMed]
357. Ghasemzadeh, N.; Karimi-Nazari, E.; Yaghoubi, F.; Zarei, S.; Azadmanesh, F.; Reza, J.Z.; Sargazi, S. Molybdenum Cofactor Biology and Disorders Related to Its Deficiency; A Review Study. *J. Nutr. Food Secur.* **2019**, *4*, 206–217. [CrossRef]
358. McGlynn, S.E.; Boyd, E.S.; Peters, J.W.; Orphan, V.J. Classifying the metal dependence of uncharacterized nitrogenases. *Front. Microbiol.* **2013**, *3*, 419. [CrossRef] [PubMed]

359. Eisenstein, M. Freeze frame: Cracking molecular motion. Time-resolved cryo-electron microscopy. *Nature* **2025**, *642*, 827–829. [CrossRef]

Disclaimer/Publisher's Note: The statements, opinions and data contained in all publications are solely those of the individual author(s) and contributor(s) and not of MDPI and/or the editor(s). MDPI and/or the editor(s) disclaim responsibility for any injury to people or property resulting from any ideas, methods, instructions or products referred to in the content.